On the effect of reactive oxidized nitrogen emissions from natural sources on air concentrations and deposition of nitrogen compounds in European coastal areas

Dissertation
zur Erlangung des Doktorgrades der Naturwissenschaften
an der Fakultät für Mathematik, Informatik und Naturwissenschaften
Fachbereich Geowissenschaften
der Universität Hamburg

vorgelegt von
Jan Alexander Arndt
geboren in Schleswig
Deutschland

Hamburg, 2019

Als Dissertation angenommen am Fachbereich Geowissenschaften

Tag des Vollzugs der Promotion: 11.07.2019

Gutachter:
Prof. Dr. Kay-Christian Emeis
Dr. Volker Matthias

Vorsitzender des Fachpromotionsausschusses Geowissenschaften:
Prof. Dr. Dirk Gajewski

Dekan der Fakultät MIN:
Prof. Dr. Heinrich Graener

Abstract

Reactive nitrogen emissions are part of the nitrogen cycle. Human activities alter this cycle, while natural emissions remain as background emissions. This thesis investigates the influence of natural reactive oxidized nitrogen emissions in Europe on air concentrations and nitrogen deposition. Europe is the continent with the second highest share of coastline relative to its area; thus, it is dominated by coastal zones that are fragile habitats and ecosystems. It is highly populated and therefore an area of high interest regarding possible ecosystem status changes.
Natural oxidized nitrogen emissions are mainly nitrogen monoxide emissions, originating from microbes, lightning and vegetation fires.

In this thesis, the years 2010-2012 are used to determine the influence of natural oxidized nitrogen emissions on air concentrations and nitrogen deposition. Including all processes, the share of natural emissions of the total reactive oxidized nitrogen emissions is approximately 10% for Europe. The total annual emission of reactive oxidized nitrogen in Europe is 7.2 Tg N, with 6.5 Tg N originating from anthropogenic sources. Soil has the greatest share in the total natural emissions, with 0.37 Tg N (5.3% of total emissions), followed by lightning 0.30 Tg N (4.4%). Wildfires are of minor relevance, with 0.02 Tg (0.3%) for the total budget of reactive oxidized nitrogen, but they are essential for temporally and spatially limited investigations. Primary emission flux reduction by vegetation, called canopy reduction, reduces the amount emitted by soil significantly from 0.43 Tg N to 0.37 Tg N (reduction of 14%). Reduced nitrogen emissions in Europe are 5.8 Tg N in total. Livestock, manure and mineral fertilizers are responsible for the majority of such emissions, and wildfires, industries and traffic are only responsible for approximately 10%. The total emissions of reactive nitrogen to the European air are 13 Tg N per year according to the model calculations.
By assuming the maximum technically feasible reduction scenario for 2040, the emissions reduction based on 2010 emissions is calculated and compared to natural emissions. Under the assumption of unchanged natural emissions, they doubled their relative contribution to the total budget of reactive oxidized nitrogen. This is clearly visible in summer with a contribution of about 20% in the base case to 40% in the scenario calculations. The use of chemistry transport models reveals nonlinear responses to emission changes in single regions. Dry deposition and wet deposition, which are sensitive to the particle formation reactions, decrease regionally when nat-

ural emissions of nitrogen and organic compounds from biogenic sources are added. The deposition decrease reaches over 30% regionally.
The calculations were performed with the COSMO-CLM, SMOKE for Europe and CMAQ model chain. For the calculation of canopy reduction and lightning emissions, preprocessors were built, and models were developed. The canopy reduction was implemented as in the GEOS-Chem model through a big-leaf approach depending on stomatal activity. Lightning was calculated with a fitting approach based on model simulations of convective precipitation and satellite observation climatologies of flash densities. Both techniques, in combination with an evaluation for the European model domain, are published in peer-reviewed scientific journals and have added significant new findings to the knowledge base.

Zusammenfassung

Reaktive Stickstoffemissionen sind Teil des Stickstoffkreislaufs. Der Mensch verändert diesen Kreislauf, während die natürliche Emissionen einen festen Emissionshintergrund darstellen. Diese Dissertation untersucht den Einfluss natürlicher reaktiver oxidierter Stickstoffemissionen auf Luftkonzentration und Deposition von Stickstoff in Europa. Europa ist der Kontinent mit dem zweithöchsten Küstenanteil im Verhältnis zu seiner Fläche. Daher wird Europa von Küstenzonen dominiert, die fragile Lebensräume und Ökosysteme sind. Europa ist stark besiedelt und daher hinsichtlich möglicher Statusänderungen des Ökosystems von großem Interesse.
Natürliche oxidierte Stickstoffemissionen sind hauptsächlich Stickstoffmonoxidemissionen. Stickstoffmonoxid wird von Bakterien, Gewitter und Vegetationsbrände emittiert.

In dieser Arbeit werden die Jahre 2010-2012 betrachtet, um den Einfluss der Emissionen von oxidiertem Stickstoff auf Luftkonzentration und Deposition von Stickstoff zu bestimmen. Der Anteil der natürlichen Emissionen an den gesamten reaktiven oxidierten Stickstoffemissionen für Europa beträgt etwa 10%. Die Gesamtemission von reaktivem oxidiertem Stickstoff in Europa beträgt 7,2 Tg N, wobei 6,5 Tg N aus anthropogenen Quellen stammen. Der Boden hat mit 0,37 Tg N (5,3% der absoulten Emission) den größten Anteil an den gesamten natürlichen Emissionen, gefolgt von Blitzen mit 0,30 Tg N (4,4%). Vegetationsbrände sind mit 0,02 Tg (0,3%) für das Gesamtbudget von reaktivem oxidiertem Stickstoff von untergeordneter Bedeutung,

sie sind jedoch für zeitlich und räumlich begrenzte Untersuchungen unerlässlich. Die Verringerung des primären Emissionsflusses durch die Vegetation, auch als „Canopy Reduction“ bezeichnet, reduziert die aus Böden emittierte Menge Stickstoffmonoxid signifikant von 0,43 Tg N auf 0,37 Tg N (das entspricht einer Reduktion um 14%). Die Emissionen reduzierter Stickstoffverbindungen in Europa betragen insgesamt 5,8 Tg N. Viehhaltung, Gülle und Mineraldünger sind für den Großteil dieser Emissionen verantwortlich, Waldbrände, Industrie und Verkehr nur für etwa 10%. Die Gesamtemission von reaktivem Stickstoff in die europäische Luft beträgt Modellrechnungen nach 13 Tg N pro Jahr.

Unter der Annahme eines maximal technisch realisierbaren Emissions-Reduktionsszenarios für 2040 wurde die Reduktion anthopogener Emissionen basierend auf den Emissionen von 2010 berechnet. Vorausgesetzt, dass sich die natürlichen Emissionen bis 2040 nicht verändern, verdoppelten sie ihren relativen Beitrag zum Gesamtbudget von reaktivem oxidiertem Stickstoff. Dies sieht man besonders im Sommer, wo der Anteil natürlicher Emissionen im Basifall etwa 20% beträgt, im Szenarienfall hingegen bis zu 40%. Die Verwendung von Chemietransportmodellen zeigt zudem ein nicht-lineares Verhalten in einzelnen Modellregionen. Trockene Deposition und Nassdeposition, welche stark von der vorherigen Partikelbildung abhängen, reagieren regional mit einer Abnahme bei Zunahme der natürlichen Emissionen, die aus Stickstoffmonoxid und organischen Verbindungen aus biogenen Quellen bestehen. Die Depositionsabnahme erreicht regional Werte bis zu 30%.

Die Berechnungen wurden mit der Modellkette COSMO-CLM, SMOKE for Europe und CMAQ durchgeführt. Für die Berechnungen der Canopy Reduction und der Blitzemissionen wurden Preprozessoren erstellt und Rechenmodelle entwickelt. Die Canopy Reduction wurde wie im GEOS-CHEM-Modell durch einen Big-Leaf-Ansatz in Abhängigkeit der Aktivität der Stomata implementiert. Die Blitzemissionen wurden mit einem linearen Regressionsansatz berechnet, der auf Modellsimulationen von konvektivem Niederschlag und Satellitenbeobachtungsklimatologien von Blitzdichten basiert. Beide Techniken wurden, in Kombination mit einer Auswertung für eine europäische Modelldomäne, in wissenschaftlichen Zeitschriften veröffentlicht und haben zum Grundlagenverständins und der Modellierung natürlicher Emissionen bedeutende neue Erkenntnisse beigetragen.

Contents

Acronym list

All acronyms are explained within the text either. Single used abbreviations, chemical substances and acronyms in common scientific use are not listed here.

Acronym	*Explanation*
BEIS	Biogenic Emission Inventory System
CB05tucl AE6	carbon bond 5 chemistry mechanism with ISORROPIA AE6 aerosol mechanism
CLC2000	Corine Land Cover dataset
CMAS	Community Modeling and Analysis System
CMAQ	Community Multi-scale Air Quality Model
COSMO-CLM	Consortium for small scale modeling - Climate limited-area modelling-community
CTM	Chemistry Transport Model
CRF	Canopy Reduction Factor
DWD	Deutscher Wetterdienst
ECLIPSE	Evaluating the Climate and Air Quality Impacts of Short-Lived Pollutants, *research project*
ECMWF	European Centre for Medium-Range Weather Forecasts
EMEP	European Monitoring and Evaluation program
FINN	Fire Inventory from NCAR
GEIA	Global Emissions InitiAtive
GEOS-CHEM	Goddard Earth Observing System Chemistry transport model
GFED	Global Fire Emissions Database
GHG	Green House Gases
GLC2000	Global Land Cover dataset
HGF	Helmholtz-Gemeinschaft Deutscher Forschungszentren e. V.
HTAP	Hemispheric Transport of Air Pollution
HZG	Helmholtz-Zentrum Geesthacht
IIASA	International Institute for Applied Systems Analysis
IPCC	Intergovernmental Panel on Climate Change
LAI	Leaf Area Index
LIS/OTD	Lightning Imaging Sensor / Optical transient detector

Acronym	*Explanation*
MCIP	Meteorological Preprocessor for CMAQ
MEGAN	Model of Emissions of Gases and Aerosols from Nature
MODIS	Moderate Resolution Imaging Spectroradiometer
NASA	National Aeronautics and Space Administration
OMI	Ozone Measurement Instrument
PACES 2	Polar regions And Coasts in the changing Earth System, *research program*
PBL	Planetary boundary layer
PM	Particulate Matter
RCP	Representative Concentration Pathway
SMOKE-EU	Sparse Matrix Operator Kernel Emissions for Europe
STEAM	Ship Traffic Emission Assessment Model
TRMM	Tropical Rainfall Measuring Mission
UTC	Universal Time Code
VHF	Very High Frequency
VOC	Volatile Organic Compound

Statistic metrics

Acronym	*Explanation*
BIAS	difference of means
corr	linear Correlation coefficient
FB	Fractional BIAS
IOA	Index of Agreement
NMB	Normalized mean bias
RMSEP	Root mean square error of prediction

1 Introduction

1.1 Forms and sources of nitrogen

Nitrogen has long been known to humankind as a useful substance. Nitrogen was even known in old China and ancient Egypt (Weyer, 2018), although not in its chemical form but rather as a substance usable for different applications, such as fertilization and textile processing.
Nitrogen is a key element for life. Proteins and enzymes, as well as the genetic information in deoxyribonucleic acid (DNA), are based on nitrogen compounds. Thus, nitrogen is involved in the metabolism of plants, animals and humans and is an important nutrient for organic matter (Butterbach-Bahl et al., 2011; Fowler et al., 2013).
Nitrogen can basically be present in three states: inert as N_2 molecules, which are chemically nonreactive, and in two reactive forms, oxidized or reduced. Although the Earth's atmosphere is composed of 78% inert nitrogen, the reactive forms are trace gases with a proportion on the magnitude of 10^{-4}% (Seinfeld and Pandis, 1998).
Inert nitrogen does not participate in chemical reactions or act as a nutrient, unless it is fixed by biotic (nitrogen-fixing bacteria) or abiotic (lightning and combustion) processes.
The reactive forms of nitrogen in the atmosphere originate from different processes. Oxidized nitrogen is primarily emitted from combustion processes and microbial activities. Reduced nitrogen in the atmosphere is mainly emitted from manure (Butterbach-Bahl et al., 2011; Seinfeld and Pandis, 1998; Yienger and Levy, 1995; Williams and Fehsenfeld, 1991; Crutzen, 1979; Martin et al., 2003; Hertel et al., 2011; Rostami et al., 2015).

With the invention of the Haber-Bosch process in 1909 (Birch, 2016), ammonia has been technically producible from nitrogen in the air. This invention was a revolution

in the industrial production of fertilizers. The worldwide demand and production of industrially produced nitrogen fertilizer in 2010 was approximately 150 Tg N (teragram nitrogen), with 200 Tg N predicted for 2020 (Heffer and Prudhomme, 2010, 2016). Emissions to the atmosphere from industrial nitrogen fertilizers are generally lower than emissions from manure (Hertel et al., 2011; Rostami et al., 2015). Global emissions of reduced reactive nitrogen are estimated to be 69 Tg N, with 40 Tg being anthropogenic related, 20 Tg N from natural terrestrial emissions and 9 Tg N from the oceans (Fowler et al., 2013).
Reduced reactive nitrogen is an important precursor and a source of secondary aerosols. Reduced nitrogen is not only a problem for air quality but is also a problem for ground water due to ground water nitrification (Sutton et al., 2011a).

Oxidized nitrogen compounds, especially nitrogen monoxide, originate from combustion and microbial processes. Combustion includes anthropogenic and natural high-temperature processes, such as lightning and vegetation fires. Nitrogen oxides play a major role in tropospheric chemistry (Crutzen, 1979). They control the ozone cycle and are involved in the acidification of rainwater due to the formation of nitric acid in cloud droplets (Seinfeld and Pandis, 1998). Moreover, nitrogen dioxide is a toxic gas. Humans and animals exposed to nitrogen dioxide have an increased risk for pulmonary diseases, specifically pulmonary edema (von Nieding and Wagner, 1979), which might lead over longer periods to lung cancer (Hamra et al., 2015). Furthermore, nitrogen oxides also have an influence over the formation of fine particulate matter, which are also harmful to the respiratory system.
The natural emission of nitrogen monoxide from soil and lightning strikes oxidizing inert nitrogen close the nitrogen cycle and make inert nitrogen available for plants and bacteria (Sutton et al., 2011b).
The total global emissions of reactive oxidized nitrogen is estimated to be 45 - 50 Tg N, with approximately 30 Tg N emitted by anthropogenic processes and 15- 17 Tg N by fires, soil and lightning, with approximately 5-7 Tg N each (Fowler et al., 2013; Martin et al., 2003). Vegetation fires count as natural emissions, but in 80% of the cases, the fires are caused by anthropogenic reasons.

1.2 The nitrogen cycle and reaction pathways in the atmosphere

All three types of nitrogen are involved in microbial activities in the soil. The inert nitrogen will only be used by a few nitrogen-fixing bacteria. Reduced nitrogen, especially ammonium (NH_4^+), will be used by plants via nitrogen assimilation at the roots(Sorgoná et al., 2011). Ammonia (NH_3) will be used by bacteria in the process of nitrification (Eq. 1.1), where ammonia is converted into nitrate (NO_3^-) with intermediate steps of hydroxylamine (NH_2OH) and nitrite (NO_2^-). Nitrate is also available to plants through nitrogen assimilation. After assimilation, it will be converted to ammonium by nitrate reduction (Tischner, 2000).

$$NH_3 \rightarrow NH_2OH \rightarrow NO_2^- \rightarrow NO_3^- \tag{1.1}$$

In addition to manure and chemical fertilizers, atmospheric deposition will serve as a source for ammonia and ammonium. Oxidized nitrogen is directly available as nitrate and does not need to participate in the nitrification process. After dilution and dissociation in water, nitrogen oxides are already nitrate ions that will infiltrate the soil. This is accomplished by washout from deposited matter and from atmospheric washout of nitrogen oxides (as nitric acid, HNO_3). Another source is plant residue that is depolymerized and made available in the step of ammonification.

Following nitrification, there are several pathways for the further processing of nitrate. The nitrate could be leeched to the ground water or be retransformed to ammonia by the dissimilatory nitrate reduction to ammonium (DNRA) (Butterbach-Bahl et al., 2011), which is more related to aquatic systems. Some bacteria can use the nitrate as the final electron acceptor and are responsible for the process of denitrification (Eq. 1.2). Denitrification forms new inert nitrogen (N_2) that is emitted from the soil to the atmosphere.

$$NO_3^- \rightarrow NO_2^- \rightarrow NO \rightarrow N_2O \rightarrow N_2 \tag{1.2}$$

This closes the nitrogen cycle (Fig 1.1). In addition to denitrification, the anaerobic ammonia oxidation (Anammox) process is able to form N_2 directly in the soil. Anammox is a topic of recent research and is identified as a very important process in coastal aquatic systems (Holtappels et al., 2009). Denitrification has some further

steps that lead to the direct emission of nitrous oxide (N_2O) and nitrogen monoxide (NO) from the soil (Butterbach-Bahl et al., 2011).

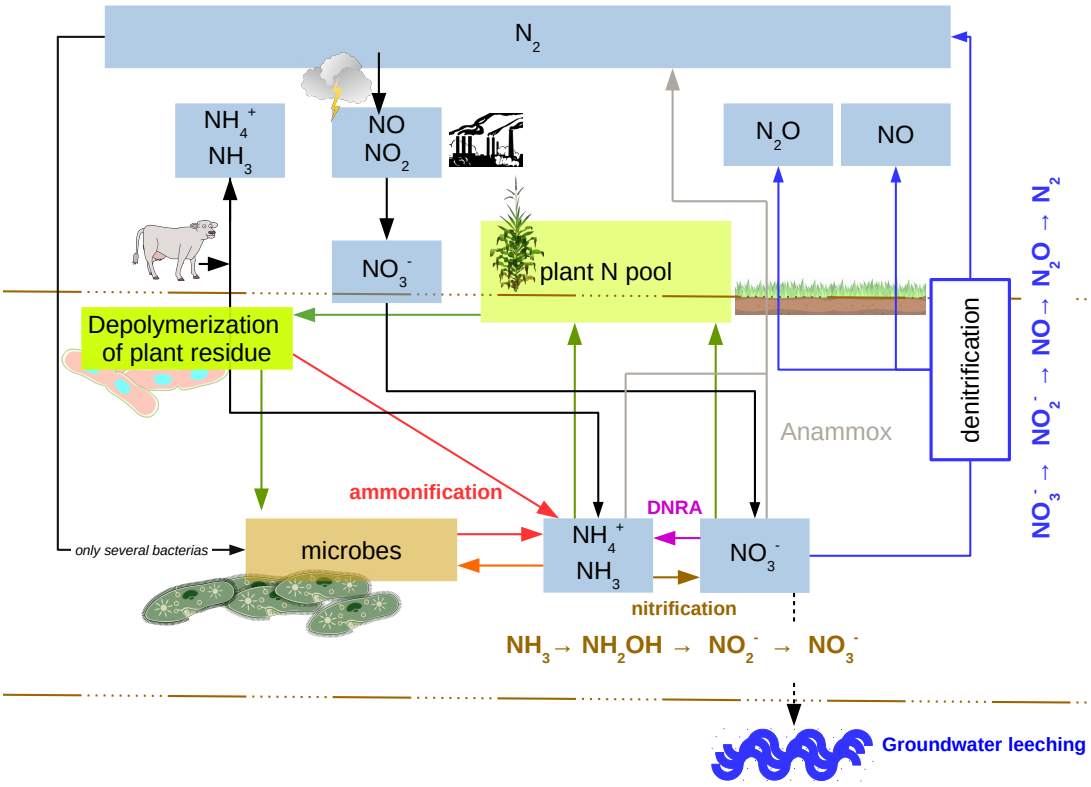

Figure 1.1: A simplified scheme of the nitrogen cycle through the compartments of soil, vegetation and atmosphere. Black arrows indicate migration pathways from the atmosphere to the soil. Green indicates plant-related processes, and brown indicates processes related to the soil and nitrification. Red is related to the ammonification processes. Light blue are the nitrogen compounds, and blue are processes related to denitrification. Grey is the anammox reaction, and purple is the DNRA reaction. Modified and merged from (Butterbach-Bahl et al., 2011; Schimel and Bennett, 2004).

Despite the nitrogen cycle combining the compartments of soil, vegetation and atmosphere, there are several atmospheric reaction pathways of nitrogen. The overview given here references Hertel et al. (2011) and Seinfeld and Pandis (1998). The relevant atmospheric reaction pathways are shown in Figure 1.2.
Atmospheric reactive nitrogen develops from two sides: reduced and oxidized. Ammonia is the primary emission of reduced nitrogen. The oxidized nitrogen starts

with the primary emission of nitrogen monoxide. Nitrogen monoxide quickly reacts to nitrogen dioxide (NO_2) by ozone (O_3) (Eq. 1.3).

$$NO + O_3 \rightarrow NO_2 + O_2 \tag{1.3}$$

This reaction depends on the available ozone and occurs with and without sunlight. It makes nitrogen monoxide available for further reactions in the atmosphere by oxidation. In daytime with the influence of UV light (as $h\nu$), it can be converted back through a photolytic reaction (Eq. 1.4).

$$NO_2 + O_2 + h\nu \rightarrow NO + O_3 \tag{1.4}$$

The reactions 1.3 and 1.4 are called the tropospheric ozone cycle. The ozone cycle consists of the most important reaction pathways in the troposphere regarding oxidized nitrogen. It makes the less reactive nitrogen monoxide available to many other compounds and allows it to participate in many more reactions by conversion to nitrogen dioxide. The other way to form nitrogen dioxide from nitrogen monoxide is through nitrous acid and the OH radical.
From NO_2, reactions into organic nitrates like peroxyacyl nitrate (PAN) and isopropyl nitrate,n-propyl nitrate, isoprene nitrates and isobutyl nitrate (NTR) and inorganic peroxynitric acid (PNA) as reservoir molecules are possible. Furthermore, the nitrate radical and dinitrogen pentoxide (N_2O_5) are formed. These species act more like reactive intermediate species, leading to the formation of nitric acid (HNO_3).
The direct reaction to form nitric acid is the reaction of the OH radical with NO_2 (Eq. 1.5).

$$NO_2 + OH\cdot \rightarrow HNO_3 \tag{1.5}$$

Nitric acid forms together with ammonia the ammonium nitrate aerosol, which combines the emission and complex reaction pathways of oxidized nitrogen with the emission of ammonia.
This thesis analyzes the total budgets of reactive nitrogen, either reduced or oxidized. All reactive oxidized nitrogen compounds are denoted as NO_y and include NO, NO_2, NO_3,NO_3^-, N_2O_5, HONO, HO_2NO_2, HNO_3 organic and inorganic nitrates (PAN, NTR and PNA), while NO_x are only NO and NO_2. Reduced reactive nitrogen is denoted NH_x and consists of NH_3 and NH_4^+.

Reaction partners are several species. As already mentioned, UV light as $h\nu$, ozone as O_3 and OH· as peroxyradical are the most important. Other partners are Δ (energy), O (oxygen), RO_2 (alkyl peroxy radical), H_2O (water), RH (hydrocarbons) and ROO_2 (peroxyradicals). They have several formation mechanisms, but these are beyond the scope of this thesis.
Another group of substances that influence the nitrogen cycle in the atmosphere are volatile organic compounds (VOCs). These are mainly hydrocarbons that contribute to the carbon cycle (Stavrakou et al., 2009). VOCs also consume nitrogen dioxide by chemical transformation to organic nitrates (NTR). Organic nitrates can be as important as 5% of the total NO_y (Shepson, 2007). VOCs are emitted by anthropogenic combusion processes (e.g., alkenes, aromatic compounds, ketones and aldehydes) and biogenic evaporation and processes by plants (e.g., isoprene, terpenes, ketones and aldehydes) (Ng et al., 2017; Kesselmeier and Staudt, 1999).

Chemical species in the atmosphere are transported, react and are deposited. Deposition describes the removal of species from the air by gravitational settling or washout. The settling process is referred to as dry deposition. The removal by washout in fog and rain is designated as wet deposition (Finlayson-Pitts and Pitts, 2000; Hemond and Fechner, 2015; Seinfeld and Pandis, 1998).
Dry deposition works by the gravitation force that draws matter to the Earth's surface. This force is opposed by friction forces. Wesely (1989) describes the most common model for describing dry deposition processes. Dry deposition is modeled as an electrical current through a network of resistances. The current describes the deposition by gravitation, while the resistors are all opposing forces. The current reaching the end points at the leaves or the surface is the resulting dry deposition. Essentially, the resistor network is split into three parts, describing the aerodynamic resistance, the boundary layer resistance and the resistance by the up-taking processes. It is utilized in the majority of common chemistry transport models (Byun and Schere, 2006; Wang et al., 1998; Schlünzen et al., 2012).
Wet deposition scavenges chemical substances by dissolution or by coagulation processes by cloud, fog and rain droplets. There are different approaches that all need to take Henry's law and the coagulation efficiency into account for the correct representation of wet deposition. For details on the parameters, see, e.g., Fountoukis and Nenes (2007). The captured chemicals are then bound to the rain, cloud or fog water. In solution, they participate in wet-phase chemistry. The amount of cloud

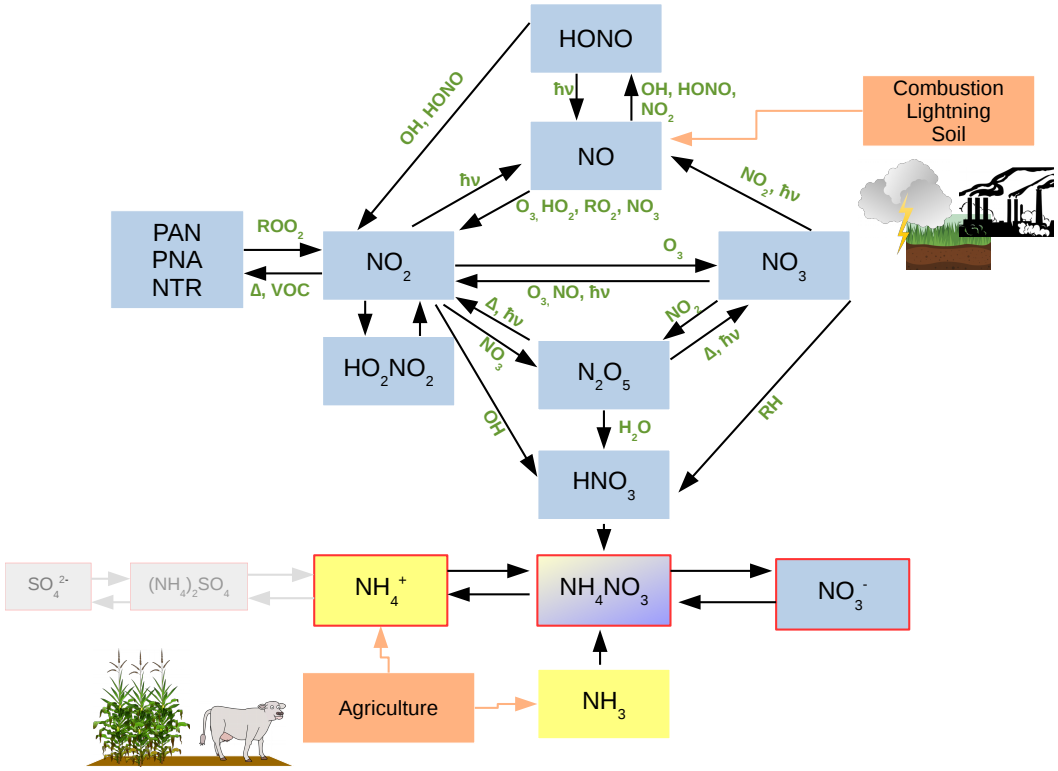

Figure 1.2: A simplified scheme of the chemical nitrogen conversions in the atmosphere. Green substances are reaction partners for the blue boxes (oxidized nitrogen) and the yellow boxes (reduced nitrogen). Red lines around boxes indicate aerosol particles. Main emissions sources are displayed as orange boxes. Following Hertel et al. (2011).

water that is converted into precipitation and the part of fog that settles deposit the contained chemical compounds to the Earth's surface (Hemond and Fechner, 2015). Because gas molecules are sufficiently compact, they are less influenced by the aerodynamic resistance than particles. Particles are instead better capturable by coagulation than gases by dissolution in cloud water. This leads to preferred deposition pathways by the phase state of the chemical compounds. Particles are more affected by wet deposition, while gasses are more affected by dry deposition (Finlayson-Pitts and Pitts, 2000; Hemond and Fechner, 2015; Kulshrestha, 2017; Seinfeld and Pandis, 1998).

1.3 Problems arising from nitrogen

Nitrogen is not only a nutrient and driver of living matter but may also act as a poison. Atmospheric emissions of reduced nitrogen are precursors of secondary aerosols. Fine particles cause serious health problems, such as cardiovascular diseases and pulmonary disease, and they may cause premature death of people already suffering from cardiovascular and pulmonary diseases (Pope III et al., 2002). Nitrogen depositions to different ecosystems are acting as a seminatural fertilizer, but over fertilization has negative implications for ecosystem status and diversity (Sala et al., 2000; Ærtebjerg et al., 2001; Durand et al., 2011). In addition to atmospheric pollution, nitrate, which is exceedingly leeching from manure, is a challenging problem of the 21st century. Nitrate is very mobile in soils, and leeching to the groundwater leads to groundwater pollution. Under certain conditions, nitrate is converted into nitrite. Nitrite is highly poisonous because it oxidizes the iron in the blood and blocks oxygen transport in the body. Nitrite concentrations in drinking water that are too high lead to blue baby syndrome, which is a medical condition that can be fatal to infants (Ward et al., 2005). This is even true for regions that are not associated with severe pollution problems, such as regions in lower Saxony of Germany (Fuest, 2000).

Oxidized nitrogen, which is mainly emitted from anthropogenic combustion processes, is another challenge for the ecosystem and human health. In addition to forming precursor substances for ammonium nitrate aerosols and the problems linked with particles described above, nitrogen oxides are leading to a series of problems.

Nitrogen oxides have a serious impact on the oxidation capacity of the atmosphere, are responsible for the acidification of rain water and are influencing the near-ground ozone levels, leading to smog and immediate health problems (Crutzen, 1979; Townsend et al., 2003; Benton et al., 2000). On longer time scales and for longer exposure, studies indicate that there are serious health problems caused by nitrogen dioxide. Already existing health problems become worse, such as COPD or asthmatic diseases (Khaniabadi et al., 2018; Strand et al., 1998), and new pulmonary diseases can occur. These are inflammatory diseases, such as pulmonary edema, and may lead in extreme cases to lung cancer (von Nieding and Wagner, 1979; Hamra et al., 2015).

Nitrogen emissions and reactive nitrogen in the atmosphere are not unusual. Different natural emissions sources create a background of nitrogen that will be in a natural balanced state that is not harmful to living matter and the ecosystem status. Consequently, understanding the natural processes that cause nitrogen emissions is highly relevant to understanding those sources that are in agreement with human health. Singular events, such as volcanic activities or massive biomass burning, may alter this background in specific cases and be harmful. However, in general, this natural background creates a stable state of the nitrogen cycle.

1.4 Coastal zones as fragile habitats

Coastal zones are the transition zones between the main compartments of the Earth's ecosystem. Aquatic, terrestrial and atmospheric effects are linked very closely in this region; thus, individual effects have the largest impact on the other compartments in coastal areas. Ocean dynamics will be highly influenced by the form of coastal areas and the meteorology, thereby influencing ocean dynamics, which in turn influence atmospheric dynamics (Ortiz-Suslow et al., 2016).

In terms of chemical interactions, oceanic processes are highly sensitive in this area because nutrient and pollutant transport by runoff, deposition and estuarine systems are the highest in coastal areas, and dilution is small in coastal areas compared to the open ocean. Thus, the sensitivity of the coastal zone to any natural or human-caused change is very high and directly impacts ecosystem health, biodiversity and the quality of life of its inhabitants (Durand et al., 2011).

In terms of nitrogen load, the flux to aquatic coastal ecosystems is dominated by riverine transport and atmospheric deposition processes (Voss et al., 2011). Depending on the geographical location, either atmospheric deposition or riverine input is a more important source of nitrogen. For example, the Mediterranean Sea is more influenced by atmospheric deposition than by riverine input. In northern Europe, estuarine and shelf areas of the North and Baltic Seas are more influenced by riverine input than by atmospheric deposition (Voss et al., 2011). The atmospheric nitrogen deposition to the North Sea is approximately one third of the riverine input to the North Sea, while the atmospheric deposition to the Baltic Sea is one fifth of the riverine input for the Baltic Sea. The exceeding input of nitrogen to coastal waters leads to critical levels of algae bloom and microorganism fertilization (Durand et al., 2011). This impacts oxygen and light availability, leading to increased death rates or mass deaths of species and therefore a changing composition of marine species (see Fig. 1.3). Although oceanic ecosystems are large enough to compensate for a certain amount of extra nutrient input, coastal areas are the areas with the highest nutrient concentrations due to their small extent and are much more sensitive. An-

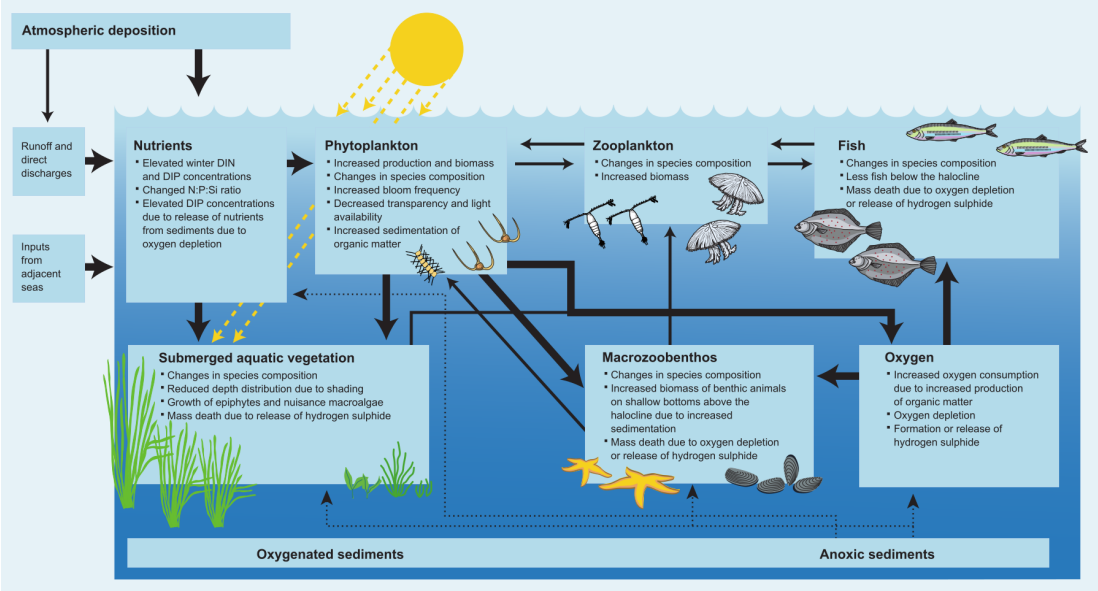

Figure 1.3: Chain of processes leading to ecosystem failure in aquatic, especially coastal, zones. From (Durand et al., 2011).

thropogenic and natural nitrogen oxides in the atmosphere are washed out within rain and fog. Washout, dilution and dissociation lead to an acidification of the rainwater. Larger systems such as oceans are less sensitive to this, and the pH value is mainly controlled by carbon dioxide. Coastal systems are more vulnerable to an

acidification of the water bodies by nitrogen oxide deposition (Doney et al., 2007). The onshore coastal ecosystem status also reacts to the acidification of rainwater by a loss of biodiversity (Remke et al., 2009).

1.5 Policies regarding reactive nitrogen

There are several national and multinational agreements, policies and legislative approaches regarding the reduction of reactive nitrogen in the environment. However, there is no joint reactive nitrogen legislation approach regulating reactive nitrogen as an interdisciplinary problem (Oenema et al., 2011). This is related to the partitioning of nitrogen research and the related economic and legislative fields that are independent of each other regarding the sources of nitrogen. The nitrogen oxides mainly emitted by traffic and industry are concerns of other interest and economic sectors than the reduced nitrogen that is emitted from agriculture. However, there are basic approaches for reducing the nitrogen load to the environment. For instance, thresholds for nitrogen dioxide concentrations at measurement stations are implemented on a multinational basis (threshold values of the European Union for NO_x, for example) or emission guidelines and restrictions related to car exhaust emissions, such as the EURO 0 to 6 classes. For a review of the legislation, see Nesbit et al. (2016). For agriculture, manure insertion techniques and times are defined that specifically regulate atmospheric emissions (Backes et al., 2016c,b).
Legislative approaches are in the conflicting fields of human welfare, ecosystem health and economic interest and strength. With respect to economical projections and legislation approaches, the calculation of emission scenarios is possible.
Natural emissions do not underlie legislation or could be controlled by human activities like combustion emissions could. The strength of natural emissions may also be altered by climate change, land use change and the seminatural fertilization by enhanced nitrogen deposition, but they form the background level that will interact with and influence the concentration and deposition patterns of nitrogen independently of human activities.

1.6 Natural nitrogen emissions

Natural emissions are often considered by the descriptions and problems above. The key point regarding natural emissions to the atmosphere is that they are a natural

background that will not disappear. Another key fact is that they are responsible for closing the gap in the nitrogen cycle. In particular, the reactive nitrogen emissions from the soil and the nitrogen oxidation by lightning are responsible for this closure. These emissions are influenced by meteorological conditions and the state of the soil. Under changing environmental conditions, these emissions might drastically change. However, even under unchanged physical conditions, natural emissions might become more important because of changes in the chemical composition of the atmosphere. Anthropogenic nitrogen oxide emissions are declining and expected to decline more in the future (Amann et al., 2012). This will make natural emissions more important and a significant source of air pollutants, even in anthropogenically utilized regions such as Europe or North America.

Actual emissions of reactive oxidized nitrogen by soil, lightning and vegetation fires (with the assumption that these fires are natural) globally are approximately 17 Tg N (Martin et al., 2003; Fowler et al., 2013; Galloway et al., 2004), which is approximately 40% of the total global emissions of reactive oxidized nitrogen. The three sources are almost equally responsible for the 17 Tg N, with the highest emissions by lightning with 6.2 Tg N.

Europe has a share of 17% (Martin et al., 2003) to the global emissions of reactive oxidized nitrogen. The sum of emissions from natural sources in Europe of reactive oxidized nitrogen are in a wide range, with 0.66 Tg N by Galloway et al. (2004) and a range between 0.14 and 1.5 Tg N by Simpson et al. (1999). This opens a span of natural emissions contribution from 2.3% to 25%.

Natural emissions of reactive reduced nitrogen in Europa are estimated to be 0.07 Tg N to 0.7 Tg N (Simpson et al., 1999; Galloway et al., 2004) with anthropogenic emissions being approximately 4-5 Tg N (Backes et al., 2016c; Galloway et al., 2004). This is a share of 1.4% to 18% depending on the emission estimates.

1.7 Scientific questions

As stated above, natural emissions of reactive nitrogen lead to a concentration and deposition background that will not disappear. However, how intense is this background, what is naturally caused and where are the hot spots of natural reactive nitrogen emissions?

As most atmospheric chemistry processes are nonlinear, so are the physical processes related to the chemical species in the atmosphere. Chemical transformation will create aerosols that have a completely different deposition behavior than gaseous substances. As shown in Aulinger et al. (2016) and Backes et al. (2016a), shipping emissions and agricultural emissions form vast amounts of nitrogen aerosols when reacting in coastal zones. How do natural emissions interact with anthropogenic emissions? Do they contribute to secondary pollutants and aerosols in the atmosphere, and to what extent? Which areas will be influenced the most by deposition and how much would be anthropogenicly not disturbed? Additionally, as natural emissions concerning nitrogen are organic compounds, how do these emissions interact with other compounds in the atmosphere?
Another important part is the quantification of natural sinks. As soil, vegetation and atmosphere exchange are primarily described by direct emission and dry deposition in common models, how does the vegetation influence the emission of reactive nitrogen to the atmosphere? Which type of vegetation affects emissions the most?
Under the pressure of changing anthropogenic emissions, natural emissions might become more important for specific regions. Which regions will be more influenced in the future by natural emissions, and in which regions will natural emissions dominate the nitrogen budget?

Continental Europe covers approximately 16% of the Earth's surface. It is the continental region with the second highest fraction of coastline relative to its area after America. Approximately half of its coastlines belong to its northern regions. Thus, northern European areas are mainly coastal zones, which are particularly concerned with atmospheric nitrogen input and input change. This makes Europe a suitable investigation area for coastal research. How much do natural emissions influence this fragile habitat in terms of concentration and deposition? Are natural emissions in this region of any importance, or are they negligible?

This thesis asks some of the questions raised above under the following overall question: **How do reactive oxidized nitrogen emissions from natural sources affect air concentrations and the deposition of nitrogen compounds in northern European coastal areas?**

In particular, three questions will be focused on:

- Will the vegetation act as a sink for natural reactive oxidized nitrogen emissions?
- How important are natural sources of reactive nitrogen for the European atmospheric nitrogen budget?
- What role will reactive nitrogen from natural sources play in Europe under largely reduced anthropogenic emissions?

1.8 Structure of the thesis

The first chapter of this thesis is an introduction to nitrogen, atmospheric nitrogen reactions and problems arising from nitrogen. The second chapter is dedicated to the methods used in this thesis for emissions modeling and chemistry transport modeling.

The third chapter is about emissions modeling as a tool for air quality and basic research and a general overview of natural emissions sources. It is an extraction of parts from the review paper „Modeling emissions for three-dimensional atmospheric chemistry transport models“ by Volker Matthias, Jan A. Arndt, Armin Aulinger, Johannes Bieser, Hugo Denier van der Gon, Richard Kranenburg, Jeroen Kuenen, Daniel Neumann, George Pouliot and Markus Quante published in Taylor & Francis: Journal of the Air & Waste Management Association, Vol 68, 2018, p. 763-800.

The fourth Chapter will evaluate vegetation as an important impact factor on the primary emissions of natural oxidized nitrogen to determine whether the vegetation acts as a sink for natural reactive nitrogen emissions. This chapter is from the research paper „Implementation of different big-leaf canopy reduction functions in the Biogenic Emission Inventory System (BEIS) and their impact on concentrations of oxidized nitrogen species in northern Europe“ by Jan A. Arndt, Armin Aulinger and Volker Matthias published in Elsevier Journal: Atmospheric Environment Vol. 191, October 2018, p. 302-311. Preliminary results were presented at the 17th CMAS Conference in 2017 in Chapel Hill, North Carolina, United States of America, and at the GEIA Emission Modeling Conference 2017 in Hamburg, Germany.

The fifth chapter is about lightning as an atmospheric natural nitrogen source. It will evaluate the importance of lightning as a natural source of reactive nitrogen for the European atmospheric nitrogen budget. This chapter is the research paper „Quantification of lightning-induced nitrogen oxide emissions over Europe“ by Jan A. Arndt, Armin Aulinger and Volker Matthias published in Published in Elsevier Journal: Atmospheric Environment Vol. 202, April 2019, p. 128-141.

The sixth chapter combines the different natural impact factors on nitrogen oxide emissions and presents them in the context of decreasing anthropogenic nitrogen emissions in the future. Based on an emissions scenario, it will estimate what role reactive nitrogen from natural sources will play in Europe under largely changing emissions conditions. It is a manuscript in a draft state written by Jan A. Arndt, Armin Aulinger and Volker Matthias. It is submitted as a conference presentation and abstract for the 37th International Technical Meeting on Air Pollution Modelling and its Application 2019 Conference in Hamburg, Germany. It is also planned to be published in a peer-reviewed journal in 2019.

The last chapter is an overarching conclusion summarizing the findings of the research articles and chapters. The scientific questions asked will be answered there, and an outlook for further activities in the field of natural nitrogen emissions will be given.

2 Approach and procedure

2.1 Meteorological, Emissions and Chemistry Transport Models

Different types of models are used to describe the changes in atmospheric physical and chemical parameters. Although there are simple models that are very computationally efficient, these models do not use nonlinear reaction pathways, consider all relevant species, feature depositional loss calculations or are spatially resolved. Rather, three types of spatially resolved numerical models are used in this thesis. These models are time-integrating models that allow studying the effects of chemical composition changes with a justifiable effort: wet-primitive equation solving meteorological models, time and space resolving emissions models and numerical chemical transport models. Because most parts described in this chapter are basic atmospheric science knowledge, this material references the common textbooks (Seinfeld and Pandis, 1998; Etling, 1996; Jacobson, 1999; Sokhi et al., 2018).

Wet-primitive equation solving meteorological models are state-of-the-art in weather forecasting models that are also applied in climate research. They solve the primitive equations of momentum, energy and mass conservation with respect to water and phase change of water. Greenhouse gas concentrations (such as CO_2), radiation, precipitation and other subscale parameters are parameterized in the models such that they can cover the full spectrum of atmospheric physical and chemical states. Some models are even able to consider reactive chemical compounds that form aerosols in their cloud physics through physicochemical exchange and therefore to include the first and second direct and indirect aerosol effects in their computations. These coupled models consume an extreme amount of computational power. They have a high nonlinearity to differentiate between the effect directly caused by emissions change and side effects, e.g., higher rain rates, which is difficult. Thus, this thesis does not use these coupled models to reduce the complexity of the experiments. Rather,

a regional weather forecasting model in climate mode, the Consortium for small scale modeling - Climate limited-area modelling-community model (COSMO-CLM) (Rockel et al., 2008), was used.

Emissions models are the basis for numerical chemical compound modeling. Emissions models compute the amount, location and time of chemical compounds that are released into the atmosphere based on bottom-up and top-down approaches. Bottom-up means that spatial surrogates and related activity data are used with an emissions factor to calculate the emissions. A good example is road traffic, where roads and corresponding traffic data are used with an emissions factor of chemical species, which results in emissions per street kilometer. Top-down is based on an emissions estimate already known that is afterwards distributed with a spatial surrogate. A typical example is agricultural emissions calculation, where an annual total emissions estimate from an emissions register is used in conjunction with land use data to calculate the emissions in specific agricultural areas. After the spatial separation, time profiles are assumed for each emissions sector and applied to the emissions. This creates the amount, location and time of chemical compounds that are released.
Emissions models are toolboxes combining different tools and techniques to create an emissions dataset rather than a closed model, such as the meteorological model. This is due to the different types of input data that an emissions model must handle to create a total emissions dataset. This work uses the emissions model Sparse Matrix Operator Kernel Emissions for Europe (SMOKE for Europe) (Bieser et al., 2011a).

Chemistry transport models calculate the transport and transformation of reactive chemical compounds in the atmosphere. These models also describe depositional loss by gravity and washout. The model used to describe the chemical changes in this work is comparable to a meteorological model. Chemistry transport models are basically a representation of the transport equation with source and sink terms, where there is a mathematical formulation for every term and an equation system for every source and sink portion.

$$\frac{\partial C_i}{\partial t} = -\overrightarrow{v}\nabla C_i + D\nabla^2 C_i + \Sigma r_{source} - \Sigma r_{sink} + \Sigma r_{chem.prod} - \Sigma r_{chem.loss} \quad (2.1)$$

Equation 2.1 shows the transport equation, with C_i as species concentration, $\overrightarrow{v}$ as wind vector, D as diffusion coefficient, and r representing production and loss rates due to emission, deposition and chemical transformation, respectively. The processes described in Equation 2.1 are the local concentration change with time equals the advection, diffusion, emission, deposition and the chemical transformation of species. Additionally, the chemical transport model solves an equation system for every Σr term specifically for the reaction pathways of the respective species C_i. In this thesis, the Community Multi-scale Air Quality (CMAQ) model is used (Byun and Ching, 1999; Byun and Schere, 2006). This model features a gas-phase, water-phase and aerosol chemistry based on the carbon bond 5 gas reactions (Kelly et al., 2010) and the aero6 aerosol mechanism and is therefore highly suitable for the purposes of this study. The three models are summarized in the COSMO-CLM SMOKE-EU CMAQ chemistry transport model framework (see Fig. 2.1)

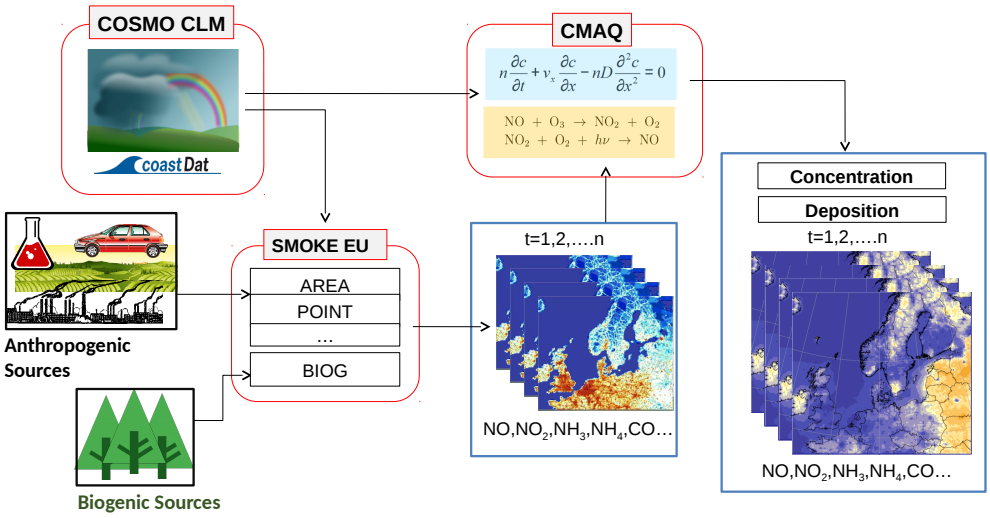

Figure 2.1: Model chain as used for the simulations in this thesis. COSMO-CLM meteorological data from the coastDat 2 and 3 project are used, together with emissions processed with the SMOKE-EU model. Dispersion, deposition and chemical reactions are calculated by CMAQ.

2.2 Technical basics of spatially resolved time integrating models

Models are descriptions of reality with reduced complexity. Although there are various types of models, e.g., conceptual or deterministic analytical mathematical models, numerical simulation models are mathematical models that solve equation systems with numerical methods. The formulations of these models are coupled partial differential equation systems that have no analytic solution and that need to be solved with numerical iterative methods.

Because the models used are spatially resolved models, there is a need to distinguish between global and limited area models. Although global models cover the entire Earth, limited area models are regional models applied to a limited region, the so-called model domain. Both types use equidistantly spaced boxes to represent the chemical and physical conditions of the Earth and its atmosphere for each box representatively. The created grid is used to discretize the partial differential equations of transport and chemical transformation for numerical solving.
Limited area models need the information of inflow and outflow of substances at their lateral boundaries to correctly reproduce the actual concentration fields in a global context. The boundary condition is sliced out from coarser global models and provided along with the emissions data. This is called 1-way nesting. This technique is often used to increase the resolution of the target model domain without losing the information at the boundaries.

Solving the equation systems requires considerable computational power. Numerical models that are time integrating models have two critical sizes defining the required computational power. One is the typical scale of movement, and the other is the spatial resolution. They are linked by the conservation law of physics and must fulfill the Courant–Friedrichs–Lewy condition. This condition requires the integrating time step to be adjusted by the spatial resolution. Models with high spatial resolution will need a shorter integration time step than those with larger resolution by a comparable typical process velocity. Shorter time steps in higher-resolution models significantly increase the required computational power and time. Notably, this makes the resolution of the model used a critical value, and it must be adopted to the scientific question asked.

Thus, 1-way nesting reduces the computational power needed by calculating on a global grid with coarse resolution and limits the computational power needed for the high-resolution calculation by choosing only a small domain. This favors the usage of nested models because they have a high resolution by saving computational power using a smaller model domain.
There is a limitation of downscaling between two grids by a factor of 4 to retain the stability of the model. This may need multiple nestings to achieve the target resolution by a given global resolution. Meanwhile, 1-way nesting does not support feedback of the increased resolution on the coarser grid by design. This means that there might be a difference and therefore high gradients at the boundaries between the coarse and the high-resolution grids.

2.3 Model evaluation procedures and statistics

To prove that a model performs well, model output data are statistically analyzed. This often means that the output data are compared against observational data with statistical measures, such as differences of means (expressed as the bias), normalized mean bias (NMB) and mean normalized bias (MNB), root mean square error of prediction (RMSEP) or correlation (corr), which are the most important time series analysis tools. With A and B as the time series to be compared, with $\overline{A}$ and $\overline{B}$ being the averages of A and B, respectively, the statistical measures are defined as follows:

$$BIAS = \overline{A} - \overline{B} \tag{2.2}$$

$$MNB = \frac{1}{N}\sum_{i=1}^{N}\left(\frac{A_i - B_i}{B_i}\right) \tag{2.3}$$

$$NMB = \frac{\overline{A} - \overline{B}}{\overline{B}} \tag{2.4}$$

$$RMSEP = \sqrt{\frac{1}{N}\sum_{i=1}^{N}(A_i - B_i)} \tag{2.5}$$

As we need the standard deviation as a statistical parameter and also for the correlation coefficient, it is defined as follows:

$$\sigma_A = \sqrt{\frac{1}{N}\sum_{i=1}^{N}(A_i - \overline{A})^2} \tag{2.6}$$

With the linear (Pearson) correlation coefficient defined as follows:

$$corr = \frac{\frac{1}{N}\sum_{i=1}^{N}(B_i - \overline{B})(A_i - \overline{A})}{\sigma_A \sigma_B} \tag{2.7}$$

according to Schlünzen and Sokhi (2008).

All the above metrics (Eq. 2.2 to 2.7) require normally distributed values. Concentration data are mostly not normally distributed. To use metrics and tests for normally distributed values, transformations are needed. The transformations used in this thesis are logarithmic transformation and Fisher-z transformation for correlation values.

To determine whether a difference between the modeled and observed time series or a change in the statistical parameters is significant, tests are performed. The most used tests are the t-test of means and the Fisher-z-transformed correlation coefficients. Depending on the setup of the experiment, the test is performed as a paired or unpaired t-test.

In the case of air quality and chemical compounds in the atmosphere, this comparison might be performed by air quality measurement station or satellite observations. Although a station measurement has high individual quality, temporal resolution and small uncertainty, it represents only a very limited spatial footprint of chemical conditions. Observation stations are scattered over the research region and do not cover regions completely. Satellite observations, however, have a high spatial representativeness and worldwide coverage, but they only have limited temporal resolution, and the individual observation has a considerable random uncertainty. In contrast to ground measurements, satellites often only retrieve column data, rely on various models and assumptions and are only available for very few chemical species. Nevertheless, both observations can be very useful, particularly in combination and

depending on the scientific question being asked.

This standard technique could be of limited use, especially when changes in the data or model should be evaluated. There might be a model improvement in the manner of better representation of processes in the model or emissions, even when the comparison of values will indicate deterioration. This is the problem of „right for the wrong reason “. To clarify this effect, a simple example is constructed: Let us assume that the modeled concentrations were in good agreement with the observations in the first experiment. In the second experiment, emissions were added to the inventory that were previously missing. The second experiment shows concentrations that are higher than before, and from the perspective of analysis metrics, the model is now less correct than before. However, overall, the model or the inventory was incorrect in the first experiment with an error that led to good model performance, even if the inventory was incomplete. This must be kept in mind and mentioned in the analysis of model performance with statistical measures.

3 Emission models and natural emissions

Modeling emissions for three-dimensional atmospheric chemistry transport models

Volker Matthias, Jan A. Arndt, Armin Aulinger, Johannes Bieser, Hugo Denier van der Gon, Richard Kranenburg, Jeroen Kuenen, Daniel Neumann, George Pouliot, Markus Quante

Published in: Taylor & Francis: Journal of the Air & Waste Management Association, Vol 68, 2018, p. 763-800

Abstract

Poor air quality is still a threat for human health in many parts of the world. In order to assess measures for emission reductions and improved air quality, three-dimensional atmospheric chemistry transport modeling systems are used in numerous research institutions and public authorities. These models need accurate emission data in appropriate spatial and temporal resolution as input. This paper reviews the most widely used emission inventories on global and regional scales and looks into the methods used to make the inventory data model ready. Shortcomings of using standard temporal profiles for each emission sector are discussed, and new methods to improve the spatiotemporal distribution of the emissions are presented. These methods are often neither top-down nor bottom-up approaches but can be seen as hybrid methods that use detailed information about the emission process to derive spatially varying temporal emission profiles. These profiles are subsequently used to distribute bulk emissions such as national totals on appropriate grids. The wide area of natural emissions is also summarized, and the calculation methods are described. Almost all types of natural emissions depend on meteorological information, which is why they are highly variable in time and space and frequently calculated within the chemistry transport models themselves. The paper closes with an outlook for new ways to improve model ready emission data, for example, by using external databases about road traffic flow or satellite data to determine actual land use or leaf area. In a world where emission patterns change rapidly, it seems appropriate to use new types of statistical and observational data to create detailed emission data sets and keep emission inventories up-to-date.

This chapter consists of the manuscript published as declared above. It was published by me as co-author. Major parts of the manuscript are omitted. Those parts, regardless of the authorship, that are useful to give a brief overview over emission modeling in general remained in the emission modelling part of the manuscript. The section about natural emissions has been wholly taken over. Substantial contributions are made by Jan A. Arndt to the subsections of emissions from soil and the emissions by lighting.

Here a part of the original manuscript has been omitted.

3.1 Emission Models

Atmospheric chemistry transport models are used to better understand the relationship between emissions from different sources – like natural and anthropogenic emissions – and concentration levels of harmful substances as well as their spatial and temporal distribution. In order to deliver the best possible description of the fate of air pollutants in the atmosphere, these models need accurate information about chemical reactions, the physical state of the atmosphere and about the flux of certain trace gases and particles into the atmosphere. This flux is typically called 'emission'. Many studies have emphasized that a profound knowledge about how, where and when substances are released ('emitted') into the atmosphere is crucial for the reliability of air quality predictions because transport and chemical transformation heavily depends on meteorological variables that also vary in space and time (Frost et al., 2013; Fuzzi et al., 2015; Bergström et al., 2012; Denier van der Gon et al., 2015; Fountoukis et al., 2014; Im et al., 2018; Kühlwein et al., 2002; Vedrenne et al., 2016). In addition, chemical reactions, adsorption, desorption and coagulation processes depend on the presence of possible reaction or collision partners.
Emission data for anthropogenic emissions are provided in the form of emission inventories, which typically contain annual national totals for certain emission sectors, like industry, transportation and households, sometimes on predefined grids. A temporal distribution of the emissions is typically not given. However, in 3D chemistry transport models (CTMs), the emission information needs to be available with sufficiently high temporal resolution and on the same spatial grid used by the CTM. This paper reviews the models and methods that are used around the world in order to transform the information given in global and regional emission inventories into temporally and spatially resolved data that can directly be used in 3D CTMs.
Emissions from natural sources like sea spray, desert dust or biogenic particles and volatile organics depend to a large extent on meteorological conditions, in particular on wind speed (for sea spray and desert dust), temperature (biogenic particles and semivolatile species) and radiation (volatile organics). Therefore they are often not part of inventories but computed inline within the CTMs using adequate parameterizations. Typically meteorological data as well as land use data are used in these

parameterizations.

Here a part of the original manuscript has been omitted.

3.2 Emission Inventories

Emission inventories are collections of emission data from many sources combined into one integrated data set. They usually contain annual total emissions of certain substances in a specified region, e.g. per country. The collection of the emission data is often done in a very detailed way for a high number of individual sources such as power plants, industrial plants or motor vehicles. Each individual facility is categorized into so called emission sectors and sometimes split into subsectors. The methods of emission compilation vary from region to region and from country to country. Often, the data collection starts on the level of rather small political units like counties in the US and is then progressively aggregated to larger political units. In Europe, for example, every country reports annual total emissions per emission sector to the European Monitoring and Evaluation Program (EMEP). When brought onto a map, the data may be given as the sum of all sources in a certain sector of this country. Because this is hardly usable in three dimensional emission models, many emission inventories are, in addition to country totals, also given on a grid. This gridding is done with methods described in one of the following sections. Often it needs to be repeated in order to map the emissions onto the specific grid needed for a certain model application. This may cause specific problems like emissions being placed into regions without sources or the reduction of emission gradients.

Here a part of the original manuscript has been omitted.

3.2.1 Emitted substances

The substances included in emission inventories can be divided into the 'classical' pollutants, greenhouse gases (GHG), and toxic substances. The 'classical' pollutants are SO_2, NO_x, CO, NMVOC, NH_3 and PM. These species have to be considered by

every comprehensive CTM for two reasons. Firstly, they are the so called criteria pollutants or their precursors. Criteria pollutants are substances that can harm human health and the environment and cause damage to buildings. For these substances (O_3, NO_2, CO, SO_2, PM) air quality standards and concentration limits are enforced in all developed countries. Secondly, the 'classical' pollutants are necessary to determine the oxidative state of the atmosphere and the particle number, mass, and surface area available for physico-chemical interactions. Thus they induce a direct feedback on the lifetime and transport patterns of most air pollutants. Greenhouse gases are sometimes reported together with the classical pollutants in the same inventory (e.g. in the RCPs and in EDGAR).

Here a part of the original manuscript has been omitted.

Furthermore, some emission species are actually mixtures of substances and need to be split into components for the use in CTMs. NO_x includes NO and NO_2 and almost all sources of nitrogen oxides contain both compounds. An emission split has to be prescribed.

Here a part of the original manuscript has been omitted.

3.2.2 Global and continental inventories

A number of global and regional emission inventories exist. Most of them contain mainly anthropogenic emissions and emissions from biomass burning. Others are dedicated to single sources, like vegetation fires, desert dust or biogenic emissions. They cover very different timescales, ranging from single years to more than a century. An overview of many of the available inventories can be found at the ECCAD (Emissions of atmospheric Compounds & Compilation of Ancillary Data) home page (ECCAD, 2017).

Here a part of the original manuscript has been omitted.

The IIASA developed the GAINS model which includes a bottom-up methodology to calculate national emissions by source sector and fuel type (Amann et al., 2013, 2012, 2011). Moreover, a number of worldwide emission scenarios for most

of the relevant greenhouse gases and air pollutants, including, the IPCC RCP 8.5 scenario are developed at IIASA (Riahi et al., 2007). The GAINS model explores cost-effective emission control strategies that simultaneously tackle local air quality and greenhouse gases so as to maximize benefits at all scales. GAINS is now implemented for the whole world, distinguishing 165 regions including 48 European countries and 46 provinces/states in China and India. However, as it focusses on policy support and (costs of) control technologies no gridded data are prepared. Within the European ECLIPSE project, global emission fields for the past as well as for the future have been constructed. Three different scenarios for the future exist, which are a baseline scenario, a mitigation scenario and a "no further control" scenario. One set of monthly varying emission patterns is given but there is no further information on modified temporal patterns available for the scenarios. More details can be found in Klimont et al. (2017) and Stohl et al. (2015).

Here a part of the original manuscript has been omitted.

For shipping and aircraft emissions, global inventories exist that treat just these sectors.

Here a part of the original manuscript has been omitted.

Global emissions from aircraft have been published by Lee et al. (2009) for the year 2005. They also summarize other inventories, e g. from Sausen and Schumann (2000) and Kim et al. (2007), but they do not provide any spatial maps. A key aspect of aviation emission inventories is emission height. For regional air quality studies the emissions during Landing and Take-off (LTO) are most relevant. LTO includes all emissions below 1 km (3000 feet). For global atmospheric composition and climate applications, aircraft cruise emissions are also relevant.Wilkerson et al. (2010) published gridded data for the years 2004 and 2006 on 0.5° x 0.5° horizontal and 0.5 km vertical resolution. More recently Wasiuk et al. (2016) published spatially resolved global inventories for the years 2005-2011, extending the time series for 2000 – 2005 from Kim et al. (2007).

Here a part of the original manuscript has been omitted.

3.3 Natural Emissions

Natural emissions can be responsible for a large fraction of the total emissions of certain substances, e.g. for VOCs and PM. They need to be included in chemistry transport model calculations, not only because of their share in the emission totals but also because of their interaction with anthropogenic emissions. Consequently, the correct spatial and temporal distribution is of similar importance as it is for anthropogenic emissions. Natural emissions typically depend on meteorological conditions and on land use. Often, special models exist for biogenic and dust emissions.

3.3.1 Biogenic emissions

Biogenic VOCs (BVOCs) are an important atmospheric constituent significantly affecting atmospheric chemistry. They contribute to both gas phase chemistry (Atkinson and Arey, 2003) and heterogeneous chemistry of aerosols and clouds (Hallquist et al., 2009) in the troposphere. BVOCs strongly influence ozone and secondary aerosol formation, both of which ultimately influence air quality and radiative forcing (Andreae and Crutzen, 1997; Arneth et al., 2010; Kanakidou et al., 2005). In the boreal forest, 70-90% of the water-soluble organic aerosol can be attributed to secondary products of BVOC oxidation (Cavalli et al., 2006). CH2O and O3 are among important secondary products in the gas phase (Curci et al., 2009). Terrestrial vegetation is the dominant source of all VOCs in the atmosphere accounting for about 90% of the total emission, and isoprene and monoterpenes are the most abundant species among the biogenic VOCs (Sindelarova et al., 2014). In the marine environment, isoprene is produced by both phytoplankton and seaweed. The total global oceanic emissions of isoprene are estimated to be in the range 0.27-1.7 TgC/yr (Arnold et al., 2009) which is at maximum 0.4 % of the estimated global terrestrial isoprene source of 400-750 TgC/yr (Müller et al., 2008; Guenther et al., 2006). In the urban environment BVOCS are usually less important than anthropogenic VOCs, but they might influence urban NO_x and O_3 budgets under specific conditions (Lee et al., 1997; Churkina et al., 2017). Quantitative estimates of BVOC emissions are needed to effectively model air quality. These estimations are challenging due to the large number of compounds and biological sources involved. The implementation of BVOC emission inventories in atmospheric CTMs is further complicated by the high complexity of in-canopy processes such as chemical reaction, aerosol formation,

deposition and turbulent exchange. Due to their high reactivity, BVOC emitted from foliar biomass are partially converted to secondary gas-phase products and particulate products before actually entering the lower atmosphere. The vertical resolution of 3-D atmospheric chemistry models is usually too coarse (20-40 m) to fully capture the vertical variation in the production of secondary aerosol precursor species (Saylor, 2013). BVOC emissions and their biological and chemical diversity are comprehensively reviewed by Guenther (2013). The overview also offers strategies for improving BVOC emission modeling approaches by focusing on better representations of the underlying diversity. Quantitative emission models also need to account for all the processes that lead to and control the variability of emissions. In order to quantify the terrestrial biogenic emission of isoprene on regional but also on the global scale and with high spatial resolution (1 km) the Model of Emissions of Gases and Aerosols from Nature (MEGAN) was compiled (Guenther et al., 2006). Via several steps this modelling system was extended and more compounds and processes have been considered. MEGAN 2.1 is now able to account for 149 known compounds (Guenther et al., 2012; Guenther, 2013). MEGAN is driven by land cover, weather, and atmospheric chemical composition but it does not consider secondary gas phase and aerosol products that are formed before they enter the lower atmosphere. MEGAN 2.1 components are shown in Figure 3.1.

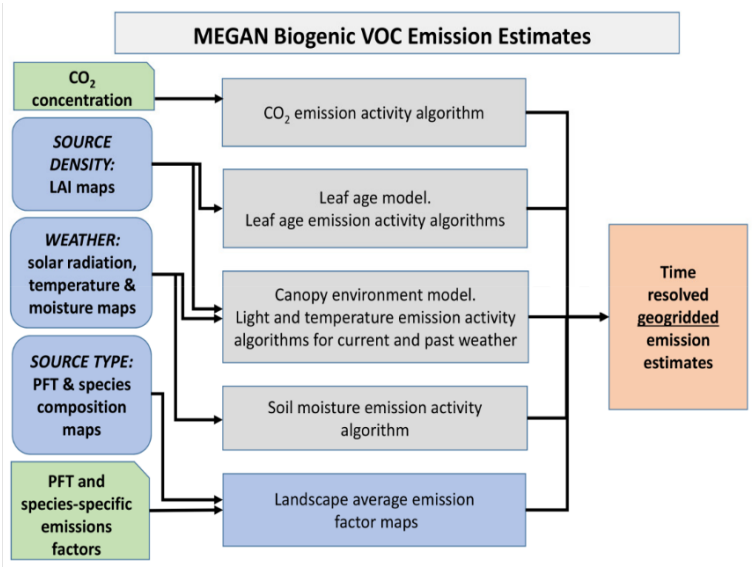

Figure 3.1: MEGAN2.1 schematic diagram. LAI: Leaf Area Index. PFT: Plant Functional Type. Diagram adapted fromSakulyanontvittaya et al. (2012)

MEGAN can either run stand-alone for generating emission inventories or can be incorporated as an on-line component of chemistry transport models (prepared for CAMx and CMAQ, WRFchem) (Pouliot and Pierce, 2009), Zhao et al. (2016). A 30-year global BVOC emission dataset based on MEGAN 2.1 is presented by Sindelarova et al. (2014). The BEIS system, which has been a component of the CMAQ (Byun and Schere, 2006; Byun and Ching, 1999) modelling system for a long time Pierce and Waldruff (1991); Pierce et al. (2002); Byun and Schere (2006); Appel et al. (2017) has been further developed. All BEIS-3 versions (Vukovich and Pierce, 2002; Schwede et al., 2005) are designed for use with the SMOKE system of CMAS. Bash et al. (2016) describe the latest version (BEIS3.6.5) and discuss a thorough evaluation of the system using BEIS emissions in CMAQ v5.02 for a Californian case study. MEGAN and BEIS both estimate BVOC emissions following the empirical algorithm initially developed by Guenther et al. (2006). The emission factors between MEGAN and BEIS differ as MEGAN uses emission factors for 16 different global plant functional types (Guenther et al., 2012) while BEIS uses species- or species-group-specific emission factors where available and MODIS plant function types where no species-specific data are available (Bash et al. 2016). The variability in BEIS emission rates is greater than in MEGAN 2.1 (Guenther et al., 2012) due to the more detailed representation of vegetation species.
GloBEIS is a biogenic emissions modeling system based on the BEIS emission factors and algorithms but with an easier-to-use interface and compatibility with a wider range of input data sources and enhanced algorithms including canopy environment, leaf age, variable LAI, and the influence of antecedent temperature conditions (Yarwood et al., 1999, 2010). GloBEIS was developed to allow users to estimate biogenic emissions of volatile organic compounds, carbon monoxide, and soil NOx emissions for any time scale and domain. Some reserachers select GloBEIS because it uses vegetation species specific emissions factors, requires minimal inputs and can be run on a desktop computer. The emission factors used in GloBEIS are the same as those reported by Guenther et al. (1995) and the MEGAN model, but expressed at the leaf level and not the canopy level (Drewniak et al., 2014). A detailed description of the differences in model approaches of GloBEIS, BEIS and MEGAN and results of an emission comparison in the US are provided by Sakulyanontvittaya et al. (2012). The model results varied considerably for the various species, depending on model version, time and location. In an earlier study, Sakulyanontvittaya et al. (2010) found that isoprene emissions between GloBEIS and MEGAN were

comparable.
The first comprehensive regional BVOC emission inventory for Europe has been set up by Simpson et al. (1999) and implemented in the EMEP MSC-W chemical transport model. Simpson et al. (1999) established a national estimate of species distribution of 32 vegetation types in Europe by using statistical inputs at the national scale for 37 countries. More recently the BVOC emission inventory in the EMEP model has been updated (Simpson et al., 2012), using BVOC emission factors for forests created from the map of forest species generated by Köble and Seufert (2001). This work provided maps for 115 tree species in 30 European countries, based upon a compilation of data from the ICP-forest network (FORESTS, 2017). ICP tree maps were also used together with additional land use information on agriculture and other vegetation, to develop a BVOC emission inventory for Europe. This has been done with special regard to the plant-specific land use data for the use in chemistry transport models. The inventory and its evaluation as well as comparison with other inventories is described by Karl et al. (2009). Another BVOC emission inventory for Europe aiming for an improved seasonality and land-cover component was developed by Oderbolz et al. (2013). Further sensitivity experiments show that land surface schemes do influence the simulated BVOCs, but the impact is much smaller than that of vegetation distributions (Zhao et al., 2016). Most atmospheric chemistry schemes include at most only a few BVOCs and may lump these together with other compounds which limits the advantages of a detailed emissions chemical speciation. The increased number of compounds is a disadvantage as there might be a significant increase in the computational resources associated with emissions parameterization, processing inputs, and emission calculations. Performance depends partly also on the region of interest, in which certain processes are more relevant than other or than BVOC categories used.

Here a part of the original manuscript has been omitted.

3.3.2 Emissions from soil

Soil is not only a source of dust particles but also of oxidized nitrogen compounds. Nitrification and denitrification of reactive nitrogen in soil by microorganisms leads to formation of nitrogen monoxide (NO) and nitrous oxide (N2O). They are emitted to the atmosphere and are responsible for up to 21 Tg N NO (Davidson and Kinger-

lee, 1997) and 6.6 Tg N N_2O (Syakila and Kroeze, 2011) annual global emissions. This accounts for about 15% of the NO and 37% of the N2O total emissions. N_2O is an important GHG but because of its low reactivity, N_2O is often neglected in chemistry transport modeling.
Two main approaches exist in soil emission modeling. One approach is a simple parameterization based on macroscale variables like land use classification and temperature such as presented by Yienger and Levy (1995) and implemented in standard emission models like BEIS. Yienger and Levy presented an emission function that is an exponential function of temperature fitted to the results of chamber soil emission measurements with biome-specific parameters. It can be described by temporally resolved model variables such as temperature and land use classification and may be altered and modified with functions for rain-pulsing emissions, fertilization, fire-fertilization and canopy reduction.
The other approach is a more sophisticated nutrient load simulation model that calculates nitrification- and denitrification rates and resulting gaseous nitrogen emissions. Examples for those models are EPIC and DNDC (Li et al., 1992). They are used as separate preprocessors for emission inventories and calculate the emission rates based on temporally resolved information such as meteorological conditions, runoff, fertilizer application, growing- and harvesting times as well as stationary information such as crop type, plant type, root depth and soil properties.
Depending on the data available, NO emissions from soil can be calculated in a preprocessor or inline in the chemical transport model during runtime.

3.3.3 Vegetation fires

Wildfires around the world have increasingly affected human values, assets and ecosystem services, among which air quality is of common interest (Moritz et al., 2014). These vegetation fires are an important source of pollutants, gases and aerosol particles (Langmann et al., 2009). Globally, fire emissions are responsible for 5 to 8% of the annual premature deaths from poor air quality, and across much of the tropics fire is the primary cause of elevated mortality from air pollution (Lelieveld et al., 2015). Thus, for many regions emissions from vegetation fires should be considered in air quality studies.
The methods for calculating emissions from vegetation fires or biomass burning are comparable to the bottom-up methods for generating emissions from combustion

engines. Necessary parameters are the mass of fuel burned per unit of time and area and the type of fuel, i.e. the vegetation types that determine the emission factors for the different pollutants. Seiler and Crutzen (1980) proposed a basic formula:

$$E_i \;=\; A(x,t) \;\times B(x) \;\times\; FB \;\times\; ef_i \tag{3.1}$$

This describes the emissions E_i of substance i as the product of the area burnt A at time t and location x, the fuel load B, i.e. the biomass per area, at location x, the fraction of the biomass that is actually combusted by the fire FB and the emission factor efi for substance i. While the area burnt is usually derived from satellite observations, the fuel loads and the fraction burned is derived from land use and vegetation type maps, which are also mostly taken from satellite observations. In order to create emissions in high temporal resolutions many authors recommend the usage of burnt area in combination with active fire detection products (Liousse et al., 2004; Michel et al., 2005; Hoelzemann et al., 2004; van der Werf et al., 2006; Mieville et al., 2010; Ichoku and Kaufman, 2005). An example is the MODIS Thermal Anomalies Product (Giglio et al., 2003) used by Wiedinmyer et al. (2006, 2011) to create a global inventory with daily emission estimates in 1 km2 resolution, the Fire Inventory from NCAR (FINN). It is available for download at http://bai.acom.ucar.edu/Data/fire/. A large collection of emission factors for all relevant gaseous and particulate species distinguished by vegetation types that can be found in literature is also provided (Yokelson et al., 2013; Stockwell et al., 2014, 2015).

Sofiev et al. (2009) presented an alternative method for calculating emissions of particulate matter from satellite products. They established a direct relation between the 4 μm Brightness temperature anomaly (TA) and fire radiative power (FRP) and empirical emission factors for PM2.5 and PM10, respectively. The emission factors are calibrated by using the fire emissions in a dispersion model (SILAM), comparing the thus calculated concentrations to observations and adapting the emission factors so that the deviations between observed and modelled pollutant concentrations are minimized (Soares and Sofiev, 2014). Emissions of other compounds in the particulate and gaseous phase were calculated using scaling factors for different vegetation types (Andreae and Merlet, 2001). Annual fire emission inventories produced with this method for the years 2000 – 2015 are available on the internet (Andreae and Merlet, 2001).

Another recently updated source for emissions from vegetation fires is the Global Fire Emissions Database (GFED), which is now available in its 4th version (GFED, 2017; Randerson et al., 2015). The database allows one to quantify global fire emissions patterns during 1997 to 2016. The Carnegie–Ames–Stanford Approach (CASA) biogeochemical model was used for its creation, input datasets are largely based on satellite products. The GFED dataset provides global estimates of monthly burned area, monthly emissions and fractional contributions of different fire types. Daily or 3-hourly fields are provided to allow for scaling monthly emissions to higher temporal resolutions. The data on all typical fire emission compounds are given at 0.25-degree latitude by 0.25-degree longitude spatial resolution and are available from June 1995 through 2016 as yearly totals by region, globally, and by fire source for each region (van der Werf et al., 2017). Emission estimates for C, CO2, CO, CH4, H2, N2O, NOx, NMHC, OC, BC, PM2.5, TPM, SO2, and dry matter (DM), were derived by combining burned area data with results of the revised version of the biogeochemical model CASA-GFED, that estimates fuel loads and combustion completeness for each monthly time step (van der Werf et al., 2010, 2017). Daily and 3-hourly time series were derived by the disaggregation of the monthly MODIS data, mean diurnal cycles were constructed from Geostationary Operational Environmental Satellite (GOES) Wildfire Automated Biomass Burning Algorithm (WF_ABBA) active fire observations (Mu et al., 2011). GFEDv4 vegetation fire emissions from 1995 through 2016 are available online (GFED, 2017).

A system which allows for near real time use of emission from vegetation fires is described by Kaiser et al. (2012). The Global Fire Assimilation System (GFAS) calculates biomass burning emissions by assimilating Fire Radiative Power (FRP) observations from the MODIS instruments onboard the Terra and Aqua satellites. GFAS makes use of the quantitative information on the combustion rate that is contained in the FRP observations from the satellites, and it detects fires in real time at high spatial and temporal resolution. Daily fire emissions for 40 gas-phase and aerosol trace species are compiled on a global 0.5×0.5 grid from 2003 to the present. For an improvement of the assimilation system see Di Giuseppe et al. (2017).

An additional challenge related to the creation of model ready fire emissions is the determination of the effective injection height. Depending on the heat content of the fire plume relative to the ambient air masses and the local weather conditions fire emissions could enter the model in the ground layer or far above the planetary boundary layer. Freitas et al. (2006, 2011) proposed a mechanism to determine the

effective injection height of fire emissions using a plume buoyancy approach. They calculated the plume rise with a 1-dimensional cloud resolving model for every model grid cell where a fire occurs.

3.3.4 Volcanoes

Volcanoes are important natural sources of ash particles and a number of reactive gases including sulfur dioxide and halogens. They have the potential for huge impacts on the local and regional environment but this depends very much on the location of the volcano and the weather conditions during its eruption. Volcanic emissions are highly intermittent and almost impossible to forecast. Similar to dust emissions, the size spectrum of the emitted particles is subject to large variations, depending on details during the eruption process (Sparks et al., 1997). The amount of transportable particles is typically just a few percent of the total emitted mass (see e.g. Langmann et al. (2012) about the eruption of the Eyjafjallajökull in 2010) and it is hard to determine during the eruption how big this fraction really is and its size distribution. Observations combined with model simulations are needed for a reliable estimate of the ash concentrations and their regional distribution (Stohl et al., 2011; Matthias et al., 2012). In the future, online monitoring networks such as the Network for Observation of Volcanic and Atmospheric Change (NOVAC) (Galle et al., 2010) will help representing volcanic emissions in emission data sets.

Because volcanic emissions consider only one large source of aerosol particles that do not interact with other pollutants in the atmosphere, they are usually treated with Lagrangian models (Stohl et al., 2011; Mastin et al., 2009) and emissions from other sources are not considered. Therefore they are in most cases not included in emission data sets used for air quality simulations. In some regions, volcanoes are permanent sources of SO2 and it might therefore be recommendable to consider these emissions. Neely and Schmidt (2016) compiled an emission data base for SO_2 emissions from volcanoes for the time period from 1850 until today. However, it focuses on explosive emissions during which SO_2 enters the stratosphere. There, it might remain for a long time and contribute to the formation of small sulfuric acid droplets.

3.3.5 Lightning

Von Liebig proposed already in 1827 that lightning might be a natural influence factor for the production of nitrogen oxides. The ionic lightning channel heats up to several thousand degrees Celsius. At these temperatures, molecular nitrogen and oxygen from ambient air react to form nitrogen oxides. The range of emission estimates on the global scale varies from 1 Tg to 20 Tg (Schumann and Huntrieser, 2007; Zhang et al., 2003; Lee et al., 1997). This is mainly because the emission estimate per flash varies. Following Intergovernmental Panel on Climate Change (2001) lightning NO_x contributes about 5 Tg N to the global annual emissions, which is about 10%. Because the highest lightning density occurs in the Inter Tropical Convergence (ITC) zone, most emissions are located around the equator.
Emissions are usually calculated based on the flash counts. Three approaches how they can be derived are common: A parameterizations based on meteorological model data that predicts thunderstorms and consequently lightning activity. Alternatively, lightning detection network measurements like the National Lightning Detection Network (NLDN) in the US and optical satellite images like the Lightning Imaging Sensor (LIS) and the Optical Transient Detector (OTD) satellite instruments can be used to retrieve the number of flashes at a certain location. Usually the flash counts are converted into flash densities and then multiplied with an emission factor to derive the NO emissions. These emission factors are derived from field experiments and satellite data (Ott et al., 2010; Allen et al., 2012) and can be constant or based on flash data like flash energy and length. Such data is used to constrain models that calculate flash densities based on cloud top height, e.g. Murray et al. (2012) for GEOS-Chem and Wang et al. (2013) for CMAQ.
Some parameterizations distinguish between the in-cloud flashes and the cloud-to-ground flashes. The emissions are distributed according to the vertical lightning energy distribution. Assuming a fixed ratio between the in-cloud and cloud-to-ground flashes (Fehr et al., 2004), the NO emissions are uniformly distributed between the ground and the cloud top. Depending on which of the methods described above is used, lightning NO_x can be calculated in a preprocessor or inline in the chemical transport model itself.

Here a part of the original manuscript has been omitted.

3.4 Summary and Outlook

Detailed emissions data are critical for accurately predicting concentrations of atmospheric air pollutants through chemistry transport modeling. For three dimensional chemistry transport model systems, emission amounts as well as their spatial and temporal distribution need to be provided for a number of anthropogenically and naturally emitted pollutants. Over recent years greater emphasis has been devoted to this fact, partly due to the better source specific availability of emission data. Nowadays a number of emission inventories exist for the global and the regional scale and for time periods of several years up to decades.

Here a part of the original manuscript has been omitted.

Biogenic and most types of natural emissions, e.g. dust, sea spray and soil emissions depend on meteorological conditions, which means that they are highly variable in space and time. While their temporal variation can be calculated using the best available meteorological data, the total amount of emitted gas or particles are still connected with large uncertainties. This holds in particular for the size distribution of dust or sea salt particles and here for the fraction of small particles that can be transported over large distances. Sea spray may contain significant amounts of organic aerosol in times of high biological productivity in the oceans. This is seldom or only rudimentary considered in emission models.
Although there is still much space for the improvement of emission data that is used in 3D chemistry transport model systems, it should also be born in mind that more details being considered in the emission models does not necessarily improve the data. When processes are taken into account that could have large effects but are not well known, this could introduce high uncertainties and in the end worsen the emission data.

In summary, emission data is arguably the most important input for chemistry transport model systems and it needs to be prepared and checked carefully. It needs to be well adapted to the purpose of the model exercise and to the scientific question being asked. The smaller the model domain and the shorter the modelled time period, the more detail is necessary. A number of improvements have been achieved in recent years concerning more sophisticated temporal and spatial allocation of

emissions. With the upcoming availability of huge data sets gathered through the use of information technologies in almost all areas of daily life, emission inventories can be further improved.

Here a part of the original manuscript has been omitted.

4 The vegetation as nitrogen sink

Implementation of different big-leaf canopy reduction functions in the Biogenic Emission Inventory System (BEIS) and their impact on concentrations of oxidized nitrogen species in northern Europe

Jan A. Arndt, Armin Aulinger, Volker Matthias

Published in: Elsevier Journal: Atmospheric Environment Vol 191, October 2018, p. 302-311

Abstract

Canopy reduction describes NO_2 flux reduction at leaf stomata. We implemented the big-leaf reduction approaches of Wang et al. (1998) and Yienger and Levy (1995) in the Biogenic Emission Inventory System (BEIS) and compared them with the BEIS standard approach. The different reduction functions lead to a reduction of 17 Gg N or 27 Gg N respectively of nitrogen emission in comparison to the standard approach which reduces the nitrogen flux by about 1 Gg N in the three summer months of 2012. These are significant differences to the standard approach. The concentration reduction of oxidised reactive nitrogen in the model area shows also a significant reduction. While concentration reduction in central Europe is low, in more rural regions of europe, concentration changes are considerably higher. The calculated concentrations of NO_2 show a significant improvement of the model performance when compared to EMEP observations in central europe. This study favors the implementation and use of canopy reduction factors, especially the parameterization of Wang et al. (1998), for regional and global emission models for reasons of model physical correctness and improved model results.

Acknowledgments

This work has been funded by the HGF through the PACES 2 project.
US EPA is gratefully acknowledged for the use of BEIS and SMOKE. We thank Dr. Beate Geyer from HZG department KSR for meteorological data and Dr. Johannes Bieser for the generation and processing of land based emission data.

This chapter consists of the manuscript published as declared before. It was published by me as corresponding and lead author for the purpose of this thesis. Major parts of the manuscript were written from me, with annotations and corrections made by Armin Aulinger and Volker Matthias. Analysis and Discussion of the Results were conducted by the supervision of Armin Aulinger and Volker Matthias. The manuscript was peer-reviewed by two anonymous referees with one revision under editorial supervision of Prof. James Schauer.
In order to avoid multiple introductions with very coherent content, the introduction of this manuscript was omitted for the purpose of this thesis.
Minor changes were made in comparison to the published version, regarding equation enumeration, table justification and figure labeling.

4.1 Biogenic Emissions and Canopy Reduction

4.1.1 Biogenic NO emission from soil in BEIS 3.14

Microorganisms in soil utilize nitrogen as a main nutrient for their metabolic processes. The processes of denitrification (equation 4.2) and nitrification (equation 4.1) occure in this metabolic processes and release gaseous nitrogen monoxide. This nitrogen monoxide exhausts from the soil surface to the atmosphere.

$$NH_3 \rightarrow NH_2OH \rightarrow NO_2^- \rightarrow NO_3^- \tag{4.1}$$

$$NO_3^- \rightarrow NO_2^- \rightarrow \mathbf{NO} \rightarrow N_2O \rightarrow N_2 \tag{4.2}$$

Microbial activity is highly related to the soil temperature and soil moisture. Yienger and Levy (1995) describes, based on Williams and Fehsenfeld (1991), a temperature-, soil moisture-, time- and landuse-dependend soil NO flux parameterization. This parameterization is used in the BEIS model. In the model it is splitted in an landuse-dependend emission factor and a correction factor. The correction factor is constructed following the equations 1, 7b and 9a in Yienger and Levy (1995). After rain events, soil moisture is increased and microbial activity is gained. This is called pulsing. In BEIS the pulsing of NO emissions after rain events is parameterized following equations 4, 5 and 6 of Yienger and Levy (1995). Fertilization effect is simply parameterized by a declining function, where the fertilization effect leads to no emission reduction in the first 30 days of the growing season and after day 30 for the remaining 184 a decline from 0% reduction to 100% reduction of the NO emission of agricultural used soils.
Nitrogen Oxides are absorbed and reemitted by the stomatal openings of leafs, depending of the ambient air concentration. This is called bi-directional flux. BEIS does not include a bi-directional flux scheme, only absorbtion is parameterized (see 4.2.1).

4.1.2 General Canopy Reduction Process

Canopy Reduction describes the uptake of nitrogen dioxide gas at the stomatal opening of leafs and the resulting reduction of nitrogen dioxide flux through the canopy (Yienger and Levy, 1995; Wang et al., 1998; Ganzeveld et al., 2002; Rasool

et al., 2016). The gaseous nitrogen dioxide dissolves in the water belonging to the stomata and gets incorporated by the plant (Rogers et al., 1979). This reduces the flux of nitrogen oxides from the soil to the atmosphere. The worldwide reduction of nitrogen dioxide emissions resulting from canopy reduction is in the order of 20%. Local amounts of reduction can be as large as 70% (e.g. in the tropic rain-forest region) (Wang et al., 1998).

It is important to keep this in mind that despite the fact that biogenic emissions are mainly nitrogen monoxide emissions, it is the flux of nitrogen dioxide to the atmosphere which is reduced. Nitrogen dioxide is about ten times more water soluble than nitrogen monoxide. This makes nitrogen dioxide flux reduction on leafs considerably more efficient. Because nitrogen monoxide is highly reactive, it is assumed that a certain amount of nitrogen monoxide is already oxidized to nitrogen dioxide when it reaches the canopy (Bakwin et al., 1990; Jacob and Bakwin, 1991; Yienger and Levy, 1995). Canopy reduction models use typically a fixed fraction to calculate the reduction amount in terms of primary emitted nitrogen monoxide. A typical NO_2 to NO_x split in the canopy is 0.5 to 0.9 (Jacob and Bakwin, 1991), with 0.7 as used in Wang et al. (1998).

All three tested parameterizations are big-leaf approaches. This means that only one big leaf is assumed as canopy. In contrast, multi-layer approaches consider multiple leaf layers in more complex vegetation-atmosphere exchange models. For the polluted region of Europe big-leaf approaches are suitable (Ganzeveld et al., 2002) and technically most efficient because of their simplicity in implementation. In more complex soil models, big-leaf approaches are also used. Implemented, but not fully tested and evaluated was the Wang et al. (1998) parameterization in Rasool et al. (2016) as a part of an updated soil NO emission model BDSNP for the CMAQ model system.

It should be noted that canopy reduction does not only affect natural emissions from soil. Anthropogenic emissions in rural areas might flow through the canopy first by horizontal advection and afterwards by mixing with higher atmospheric layers. Thus, anthropogenic emissions may also be affected, but there is no previous research and literature about this effect.

4.2 Different Canopy Reduction Schemes used in this study

4.2.1 Current implementation in emission model BEIS 3.14: Vukovich and Pierce (2002)

The Biogenic Emission Inventory System (BEIS) (Vukovich and Pierce, 2002) models biogenic emissions of nitrogen oxide with a soil temperature dependent function and a classification of agricultural, non-agricultural and growing-season or non-growing-season of the underlying land use class. For the "agricultural growing season" case, there is a vegetation adjustment factor (a model-internal synonymous for the (1-CRF) canopy reduction factor formulation) that scales between 1 and 0.5, depending on the day of the growing season. Furthermore, the vegetation adjustment factor is only applied to one of three posibble cases. The first possible case is frozen soil, where no NO is emitted. The second is the calculation of gassland emissions with no adjustments for vegetation, rain or fertilization. The third one is the plant specific emission with adjustment for vegetation, rain and fertilizer. The vegetation adjustment is only used, when the soil is not frozen and the pure grassland emission is lower than the plant specific emission. This is an incomplete approximation. In particular, it neglects the reduction of non-agricultural emissions in more natural landscapes.

The original decription of the BEIS model in the SMOKE framework does not include the vegetation adjustment, the parameterization with the vegetation factor is mentioned in Pouliot and Pierce (2009) and according to the CMAS model history implemented directly in the model version described in Vukovich and Pierce (2002). Therefore, the original implementation of the parameterization is denoted here as **VP02**.

4.2.2 Parameterization of Yienger and Levy (1995)

Yienger and Levy (1995) describe different influence factors for nitrogen oxide emissions from soil. Their aim is an emission estimate for global annual nitrogen oxide from soil. They use gridded geographic and geoscientific information like the land use class and temperature as input. One of the influence factors for the emission

estimate is the canopy reduction for which they developed a parameterization. It is based on the leaf area index (LAI) and the stomatal area index (SAI). Both are parameterized through the gridded land use class.

$$CRF = \frac{exp(-k_s \times SAI) + exp(-k_c \times LAI)}{2} \tag{4.3}$$

with CRF as Canopy Reduction Factor, $k_s = 8.75\ m^2\ m^{-2}$ and $k_c = 0.24\ m^2\ m^{-2}$ as absorbtion coefficients.

Model limitation and adaption measures

The model is a gray absorber model and has some limitations. The vertical transfer and therefore the canopy residence time is not taken into account. The model does not contain a stomata resistance model either. As described above, the emissions and influence factor formulations are intended for global annual emissions. Daily or hourly profiles are not implemented. As a first order approximation a fixed annual profile for leaf cover progression as well as a daily profile for stomatal resistance is implemented. This adapts the annual formulations for modelling of hourly emissions.
As a general driver of this parameterization the specified land use classes of the Yienger and Levy (1995) parameterization are remapped to the CMAQ 24 USGS land use categories.
The suggested NO to NO_2 split by Yienger and Levy (1995) is adapted through using the proposed absorption coefficients for stomatal and cuticular activity.
The implementation of the parameterization of Yienger and Levy (1995) is denoted as **YL95**.

4.2.3 Parameterization of Wang et al. (1998)

Wang et al. (1998) developed a canopy reduction function explicitly for usage in chemistry transport models. It is currently implemented in the GEOS-Chem chemistry transport model in the soil NO_x emission routine. They expressed the canopy reduction as a fraction of ventilation and deposition flux through the canopy following the formulation of Jacob and Bakwin (1991). The ventilation fluxes are calculated based on the canopy surface resistance, canopy depth, above-canopy windspeed and leaf area index (Eq. 4.4 to 4.6).

$$CRF = \frac{k_d}{l_d + k_\nu} \tag{4.4}$$

$$kd = \frac{1}{R_c \, \Delta Z} \tag{4.5}$$

$$k\nu = \frac{\alpha \, \min\left(\frac{V}{\gamma\sqrt{LAI}}, V\right)}{\Delta Z} \tag{4.6}$$

with canopy surface resistance R_c, canopy depth ΔZ, above-canopy windspeed V, canopy ventilation time coefficient α that is at day = 0.01 and at night = 0.0002 and in-canopy windspeed extinction coefficient γ calculated from the land-use classification as described in Wang et al. (1998).

Model limitation and adaption measures

The work of Wang et al. (1998) is based on Jacob and Bakwin (1991) 's canopy reduction mechanism for the Amazon Forest and canopy of higher trees. This might lead to an inadequate formulation for mid-latitude ecosystems, especially for vegetation near the ground.
The formulation is applied to the soil NO emission and includes the part of the chemical transformation to NO_2 with the assumption of an 0.7 concentration ratio between NO_2 and NO inside the canopy. We adapted the canopy reduction function, here in form of the in-canopy windspeed extinction coefficient γ by remapping the CMAQ 24 USGS land use categories to the land use classes and their respective coefficients of the GEOS-Chem soil NO_x routine.
We denote our implementation of the parameterization of Wang et al. (1998) as **WA98**.

4.3 Model and emission data setup

4.3.1 CMAQ

The CMAQ model (Byun and Ching, 1999; Byun and Schere, 2006) was used in its version 5.0.1 (US EPA Office of Research and Development, 2012) with the CB05 photo-chemical mechanism (CB05tucl) (Kelly et al., 2010) in the so-called AE6

aerosol mechanism. The model was run for the three summer month with a spin-up time of 2 weeks to avoid influence of initial conditions on the modeled atmospheric concentrations. The model was setup on a 64 x 64km^2 gridcellsize grid for entire Europe and subsequently on a nested 16 x 16km^2 gridcellsize grid for northern Europe (see Fig. 4.1). Chemical boundary conditions for the outer model domain were taken from the hemispheric 0.5° x 0.5° grid resolution chemistry transport model simulation of SILAM and were provided by the Finish Meteorological Institute (FMI). Boundary conditions for the nested grid were calculated from the outer coarse grid. The vertical model extent contains 30 layers up to 100 hPa. Twenty of these layers are below approximately 2000m, the lowest layer extending to approximately 36m above ground.

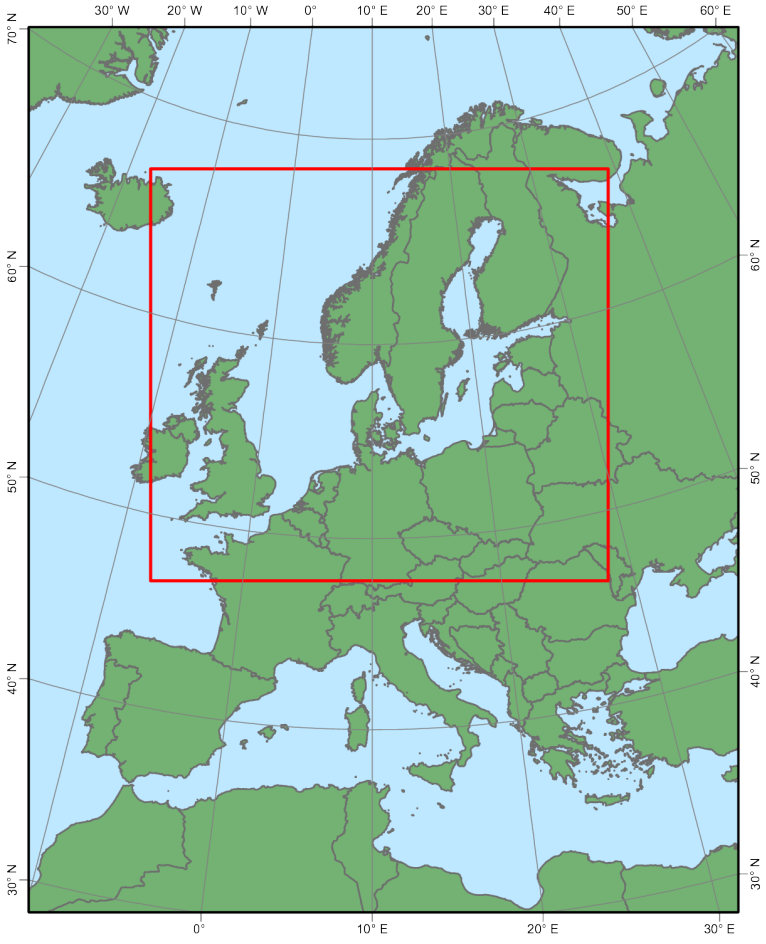

Figure 4.1: Overview of the modeling domain. The whole graphic shows the extent of the 64x64km^2 gridcellsize mother grid, the red lined box shows the extent of the 16x16km^2 gridcellsize nested grid.

4.3.2 COSMO-CLM

The meteorological fields that drive the chemistry transport model were simulated with the COSMO-CLM (Rockel et al., 2008) mesoscale meteorological model (version 5.0) for the year 2012 using ERA-Interim forcing data (Dee et al., 2011). This year was chosen because it does not contain very unusual meteorological conditions in Europe and can therefore be used to represent typical weather conditions in Europe.
COSMO-CLM is the climate version of the numerical weather prediction model COSMO (Schaettler et al., 2008), originally developed by Deutscher Wetterdienst (DWD) Steppeler et al. (2003); Schaettler et al. (2008). It was run on a 0.11° x 0.11° grid using 40 vertical layers up to 20 hPa for entire Europe. The meteorological fields were afterwards processed to match the CMAQ grid with the Model-3 MCIP preprocessor. The impact of the meteorological fields on the output of the chemistry transport model was investigated in detail in the articles by Matthias et al. (2009) and Bieser et al. (2011a).

4.3.3 Emissions

The model runs were performed with emissions from biogenic sources, agriculture, anthropogenic point, area and road traffic sources in the model domain. Land based emissions in hourly temporal resolution were produced with SMOKE-EU (Bieser et al., 2011a) for the year 2012. They are based on officially reported EMEP emissions which are distributed in time and space using appropriate surrogates like population density, street maps or land use. Point sources were considered as far as information from the European point source emission register was available. The vertical distribution of the emissions was calculated online with the SMOKE model, the results are given by Bieser et al. (2011b).
Shipping emissions for the Baltic Sea and North Sea with high spatial and temporal resolution for this study were obtained from the Ship Traffic Emission Assessment Model (STEAM) (Jalkanen et al., 2009, 2012; Johansson et al., 2013, 2017).
Canopy reduction is applied by a separate preprocessor for biogenic emissions and recombined with the rest of the emission data before the model run is started. Therefore canopy reduction is only applied to biogenic emissions.

4.3.4 Reference Case

In order to estimate the effect of canopy reduction at all, a reference case is calculated. This is an emission dataset with anthropogenic (see 4.3.3) and and biogenic emissions (see 4.1.1) without any canopy reduction effect. It is used as a measure, how much the canopy reduction influences the nitrogen budget.

4.4 Results and discussion

The greatest effect is observable in the summer months June, July and August when LAI is highest (see fig. 4.2). This time span has therefore been chosen for the in-depth investigation of canopy reduction effects.

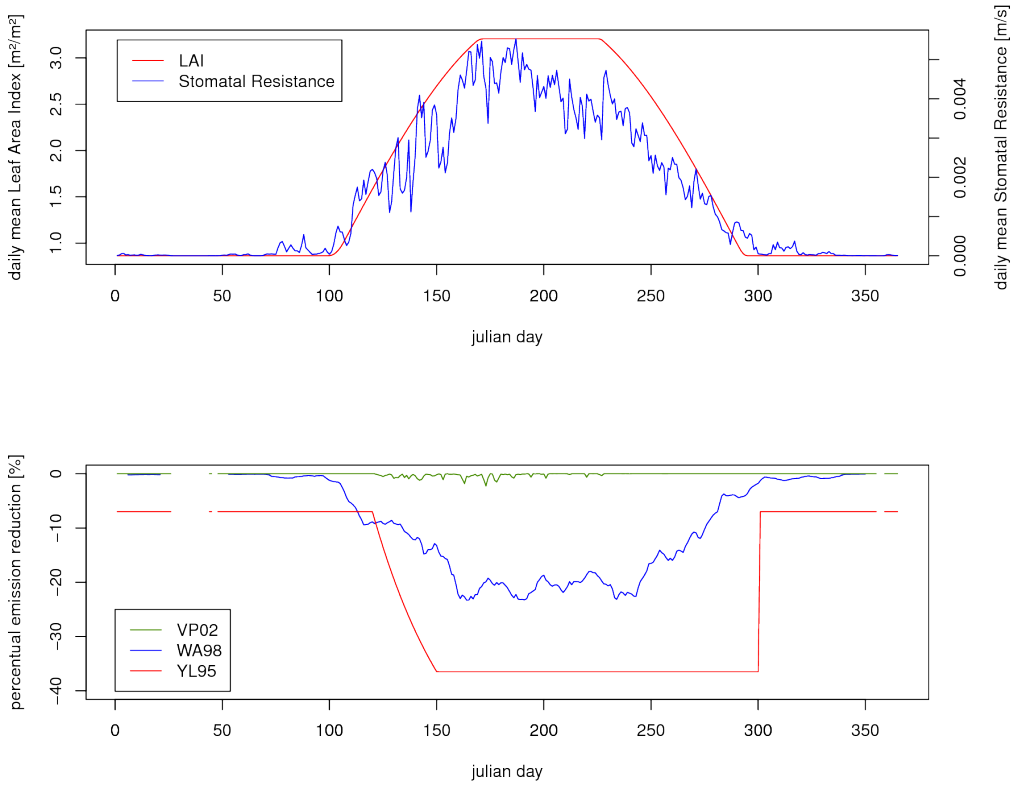

Figure 4.2: Main drivers of Canopy Reduction and the canopy reduction over the year, here as a area mean for predominantly natural region over parts of Lithuania, Kaliningrad Oblast, Poland and Belarus. Shown are the Leaf Area Index (LAI) and the Stomatal Resistance (R_S) (upper graph), Canopy Reduction influenced emission profiles for the same area(lower graph). The graphs show that canopy reduction effect is highest in summer, roughly between day 150 and day 250 of the year 2012, then LAI and stomatal resistance are highest.

4.4.1 Emission

Using VP02 the total emission of NO_x is reduced by 1.13 Gg N over the whole domain. This is a reduction of 1.5% of biogenic emissions and 0.27% of total NO_x

total emissions (see Fig. 4.3, upper right graphic). With WA98, NO_x is reduced by 17.97 Gg N over the whole domain, which is a reduction of 24.4% of biogenic emissions and 4.1% of total NO_x emissions (see Fig.4.3, lower left graphic). The total emission of NO_x using YL95 is reduced by 27.87 Gg N over the whole domain, which is a reduction of 37.9% of biogenic emissions and 6.8% of total NO_x emissions (see Fig. 4.3, lower right graphic). Total emissions can be seen in Table 4.1.

Table 4.1: Model Results for the reference case Ref VP02, WA98 and YL95. Emission values are sums for June, July and August of 2012.

	NO_x Emission		Reduction
	Biogenic Gg N	Total Gg N	
Ref	73.51	417.16	-
VP02	72.38	416.03	-0.27%
WA98	55.55	399.67	-4.19%
YL95	45.65	388.77	-6.80%

While VP02 is mainly based on the land-use category of agriculturally used gridcells and is only taken into account in a few cases depending on the emission magnitude, WA98 and YL95 have reduction factors for all land-use categories independent of the emission magnitude. This leads to a spatially more distributed effect that also influences grasslands and forests. Especially in forest-dominated gridcells the emission is strikingly decreased in terms of relative change, whereas absolute emission change is highest in the grassland and crop areas of central and eastern Europe. This discrepancy can be explained by the influence of anthropogenic emissions in central and parts of eastern Europe, that dominate the oxidized nitrogen emissions and therefore cause small relative changes of oxidized nitrogen emissions in this area.

All three parameterizations were tested with a paired t-test. For this the grid, i.e. the 2-dimensional matrix of annual emissions was reshaped to a vector of cells, resulting in 23345 pairs. All parameterizations are highly significant different from the reference case. In order to classify the effect caused by the canopy reduction on the biogenic emission von NO, three other parameters were tested: A meteorology change, a land use change from the GLC2000 (Bartholomé and Belward, 2005) to the CLC2000 (Buttner et al., 2004) classification and a NO_2 to NO_x split change form 0.7 as assumed by Wang et al. (1998) to 0.8. The meteorology change was

Table 4.2: Changes in the sensitivity study as described in 4.3.3 for meteorology change, land use change and NO_2 to NO_x split.

	Meteorology		Land use		Split (for WA98)	
	2012	2010	GLC2000	CLC2000	0.7	0.8
total ch.	73.51 GgN	74.18 GgN	73.51 GgN	87.41 GgN	55.54 GgN	53.07 GgN
mean rel. ch.		+ 1%		+19%		-14%
local rel. ch.		+23%		+ >1000%		-14%

a simulation year change from 2010 to 2012. The mean temperature difference for JJA is 0.39 K with higher temperatures in 2010. Localy this is a temperature rise of up to 0.7%. This leads to 0.67 Gg NO-N higher emissions from soil in 2010, which is locally up to 23% more NO-N emission.

The land use change from the GLC2000 to the CLC2000 classification will enhance the soil NO production so that 13.95 Gg more NO-N are produced than in the GLC2000 case. This is in relation to local changes, especially in north-eastern europe, over 1000%. This is due to the fact that there is a massive landuse change from the GLC2000 to the CLC20000. In the northeastern model region there is in the GLC2000 much less drycrop in the dataset than in the CLC2000 dataset, which has a very high impact on the emission. The differencres in emission are shown in figure 4.4.

Changing the split of the WA98 canopy reduction function leads to a reduction increase of 14% of the canopy reduction factor. Regarding the split experiment it is important to notice that the considered NO_2 to NO split variation is highly uncertain. The considered change is just applied in a stochiometric way, not considering a change in the stomatal conductance or other related parameters. All changes are listed in table 4.2.

A variation of anthropogenic emission parameters may lead to significantly different chemical composition and conditions in the atmosphere, the O3 budget and therefore the NO_2 to NO split under the canopy. Summarizing, the effect of canopy reduction on the biogenic emission is, depending on the uncertainty of the meteorology, in a comparable size as the effect of meteorological parameter variation. Land use changes have a significantly higher impact on the emission of biogenic NO than the canopy reduction. The split consideration has a minor impact on the total reduction factor. Anthropogenic emission variation may have the considerably largest impact and bring the highest uncertainty to the estimation of the canopy reduction impact.

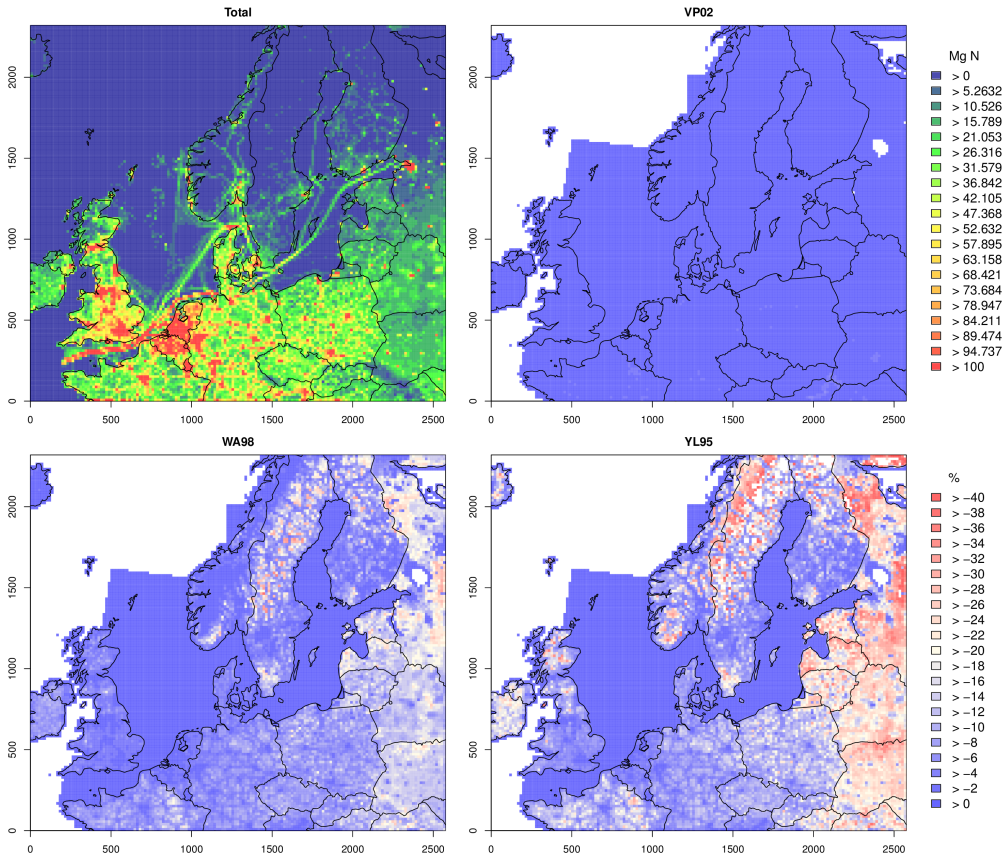

Figure 4.3: Total NO_y Emission of anthopogenic and biogenic sources in the Reference case (upper left) and the relative differences with respect to the reference case and the original BEIS parameterization (VP02, upper right), the Wang et al. (1998) implementation (WA98, lower left) and the Yienger and Levy (1995) implementation (YL95, lower right). The unit is emission of NO_y in Mg N per grid cell and 3 month summer period.

4.4.2 Concentrations and Evaluation

To evaluate whether or not the parameterization improves the model performance, a chemistry transport model simulation was done for each case (see Fig. 4.5). The resulting concentration fields were compared with in-situ measurements form the EMEP station network (Tørseth et al., 2012). Because NO has, in comparison to NO_2, only a short lifetime in the atmosphere, the NO_2 air concentration measurements were used for the evaluation.

36 measurement sites are used for the evaluation. The EMEP stations with less than $< 25\%$ data coverage were excluded in favor of higher statistical reliability. Two more stations have a correlation in the reference case with less then 0.175.

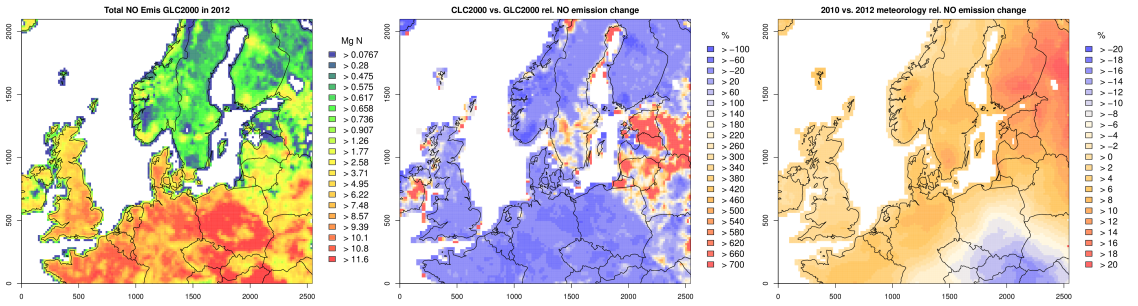

Figure 4.4: Total NO Emission of biogenic sources in the Reference case (left) and the relative differences with respect to the reference case for the land use change (middle) and the meteorology change (right) as used in the sensitivity study described in the text.

These stations are not significantly different from $r = 0$. The tests used in this study are one-sided paired t-tests. Because the applied paramaterizations in the calculated cases lift one of them above this level of uncertainty to a significant different correlation from 0, it was decided to leave these stations in the observation sample.

As measures of model performance, the linear correlation (corr), Fractional Bias (FB), Index of Agreement (IOA), Root Mean Square Error of Prediction (RMSEP) and Mean Normalized Bias (MNB) were calculated (Bossioli et al., 2008) . In order to asses the average performance against all measurements, the averaged statistical values over all evaluation stations for the respective cases were used. For the comparison and evaluation of improved or decreased model performance between the cases, the computed average statistical values for each case were compared and tested against each other.
The reference case has concentrations between 0.14 and 3.72 μg N m^{-3} with a mean of 1.39 μg N m^{-3} at the corresponding measurment stations which have between 0.06 and 4.09 μg N m^{-3} with a mean concentration of 1.08 μg N m^{-3}. The mean linear correlation over all stations is 0.5223, the FB 0.0387, IOA 0.5563, RMSEP 0.8505 μg N m^{-3} and MNB of 0.56. These model results indicate a slight overprediction of NO_2 at the measurement stations. The mean correlation of about 0.5 is low in comparion to other models and seasons (Solazzo et al., 2017), but 8 stations out of the 36 show a correlation higher than 0.7, which is classified as good agreement (Aulinger et al., 2016). In comparison to Solazzo et al. (2017) the other model parameters also

indicate a good representation of the atmospheric chemistry in the model run used here. The model in this configuration is suitable for air quality studies, but still a considerable uncertainty is measurable. This brings some uncertainty in the model evaluation of smaller effects like the canopy reduction.

With regard to the three canopy reduction model cases, most stations show a slightly higher linear correlation (see Table 4.3 and 4.4), with better match to the station measurement of the canopy reduction cases than to the reference. Since the data has a high variance in the time series, correlation differences of about 0.3 are needed to show significant differences at the stations themselves. Because the correlation is raised by only a few percent, significant differences in correlation at the stations and therefore a detectable improvement could not be shown. Using a fisher-z-transformation and the averaged statistic values over all evaluation stations, a significant improvement ($p < 0.05$) of the WA98 case over all stations in average could be shown. The other cases do not show significant improvements in the linear correlation. The mean correlation in the reference case is 0.5223, VP02 is 0.5221, WA98 0.5248 and YL95 0.5233.
The FB is 0.0387 in the reference case, 0.0386 in VP02, 0.0291 in WA98 and 0.026 in YL95. All differences are highly significant ($p < 0.01$) and show an improvement of the averaged statistical parameters. The IOA is 0.5563, 0.5563, 0.5605 and 0.5599 for the four cases and the differences are not significantly different.
The mean RMSEP of the reference case is 0.8505, the VP02 is 0.8503. WA98 and YL95 are 0.829 and 0.8302 respectively and are highly significant different improvement in contrast to the reference case. The MNB is 0.56 in the reference case, highly significant better with 0.5047 and 0.4954 for the VP02, WA98 and YL95 cases respectively.

Because in Europe the concentration level of oxidised nitrogen is highly influenced by anthropogenic sources, the model results are very sensitive to emission changes from the anthopogenic sector. This makes the evaluation results of this natural effect with respect to the anthropogenic emissions highly uncertain. A model test with emissions that does not include shipping emission in the North and Baltic sea showed no significant improvement of the canopy reduction functions. In that experiment, only 17 stations have correlations higher than 0.175 in the reference case

and a general underestimation of the NO_2 concentration in the model domain.

In synopsis this evaluation indicates that canopy reduction parameterizations, especially the parameterization proposed by Wang et al. (1998), could improve the model performance.

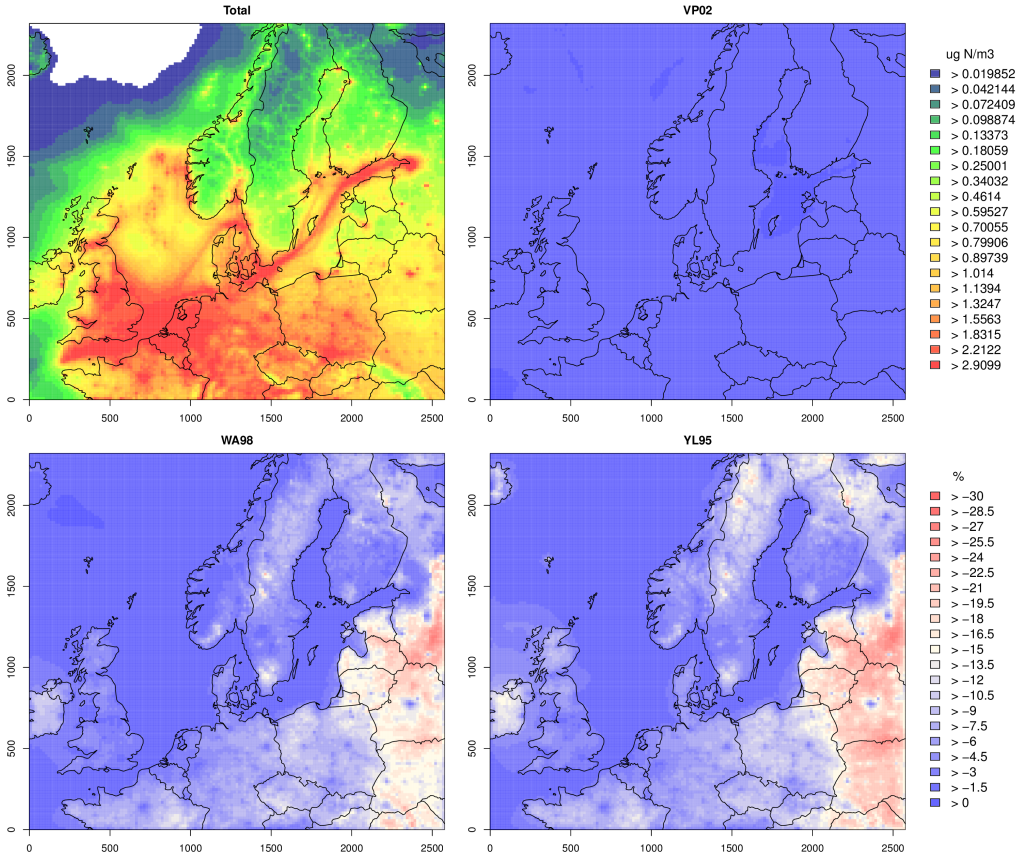

Figure 4.5: Mean NO_y concentration of the Reference case (upper left) and the relative differences with respect to the reference case and the original BEIS parameterization (VP02, upper right), the Wang et al. (1998) implementation (WA98, lower left) and the Yienger and Levy (1995) implementation (YL95, lower right). The values are grid cell representative air concentration of NO_y in μg N per m^3 averaged over the 3 month summer period.

Table 4.3: Selection of EMEP station evaluation for NO_2 against the cases Reference, VP02, WA98 and YL95.

	corr			
Station	Ref	VP02	WA98	YL95
Vezin	0.747	0.738	0.749	0.738
Waldhof	0.552	0.543	0.560	0.544
Neuglobsow	0.666	0.671	0.664	0.672
Keldsnor	0.699	0.701	0.699	0.701
Lahemaa	0.557	0.558	0.557	0.558
Virolahti II	0.710	0.710	0.710	0.710
Preila	0.469	0.483	0.471	0.483
Rucava	0.184	0.174	0.202	0.174
Vredepeel	0.791	0.794	0.793	0.794
De Zilk	0.751	0.752	0.752	0.752
Birkenes II	0.545	0.539	0.545	0.539
Hurdal	0.426	0.424	0.427	0.424
Leba	0.572	0.573	0.576	0.573
Diabla Gora	0.182	0.158	0.181	0.159
Vavihill	0.568	0.563	0.571	0.563
Mean (all 37 st.)	0.522	0.522	5.525	0.523

Table 4.4: Selection of EMEP station evaluation for NO_2 against the cases Reference, VP02, WA98 and YL95, continuation of table 4.3.

	RMSEP				MNB			
Station	Ref	VP02	WA98	YL95	Ref	VP02	WA98	YL95
Vezin	1.234	1.336	1.228	1.337	0.390	0.446	0.395	0.447
Waldhof	0.621	0.611	0.613	0.610	-0.129	-0.059	-0.124	-0.057
Neuglobsow	0.466	0.420	0.470	0.419	-0.257	-0.195	-0.261	-0.194
Keldsnor	1.191	1.199	1.193	1.199	0.078	0.091	0.083	0.092
Lahemaa	1.140	1.163	1.152	1.163	1.196	1.321	1.244	1.321
Virolahti II	0.551	0.556	0.555	0.556	-0.004	0.023	0.005	0.023
Preila	0.398	0.392	0.395	0.392	-0.256	-0.210	-0.243	-0.210
Rucava	0.355	0.443	0.342	0.443	0.485	0.739	0.480	0.740
Vredepeel	1.036	1.020	1.029	1.020	-0.026	0.005	-0.022	0.005
De Zilk	3.810	3.863	3.817	3.865	3.627	3.665	3.634	3.666
Birkenes II	0.401	0.413	0.402	0.413	1.212	1.284	1.220	1.285
Hurdal	0.528	0.540	0.528	0.540	1.066	1.106	1.068	1.106
Leba	0.442	0.440	0.439	0.440	-0.146	-0.111	-0.143	-0.110
Diabla Gora	0.352	0.414	0.355	0.414	0.381	0.615	0.390	0.615
Vavihill	0.598	0.666	0.590	0.667	0.369	0.470	0.367	0.471
Mean (all 37 st.)	0.851	0.850	0.829	0.830	0.560	0.559	0.505	0.495

4.4.3 Deposition

The dry and wet deposition also remove nitrogen oxides from the atmosphere. In total, 29.9 Gg NO_x-N are removed via settling in the reference case. 0.03 Gg NO_x-N less were removed in the VP02 case, 1.57 Gg NO_x-N less were removed dry in the WA98 case and in the YL95 case the dry deposition is lowered by 1.87 Gg NO_x-N.

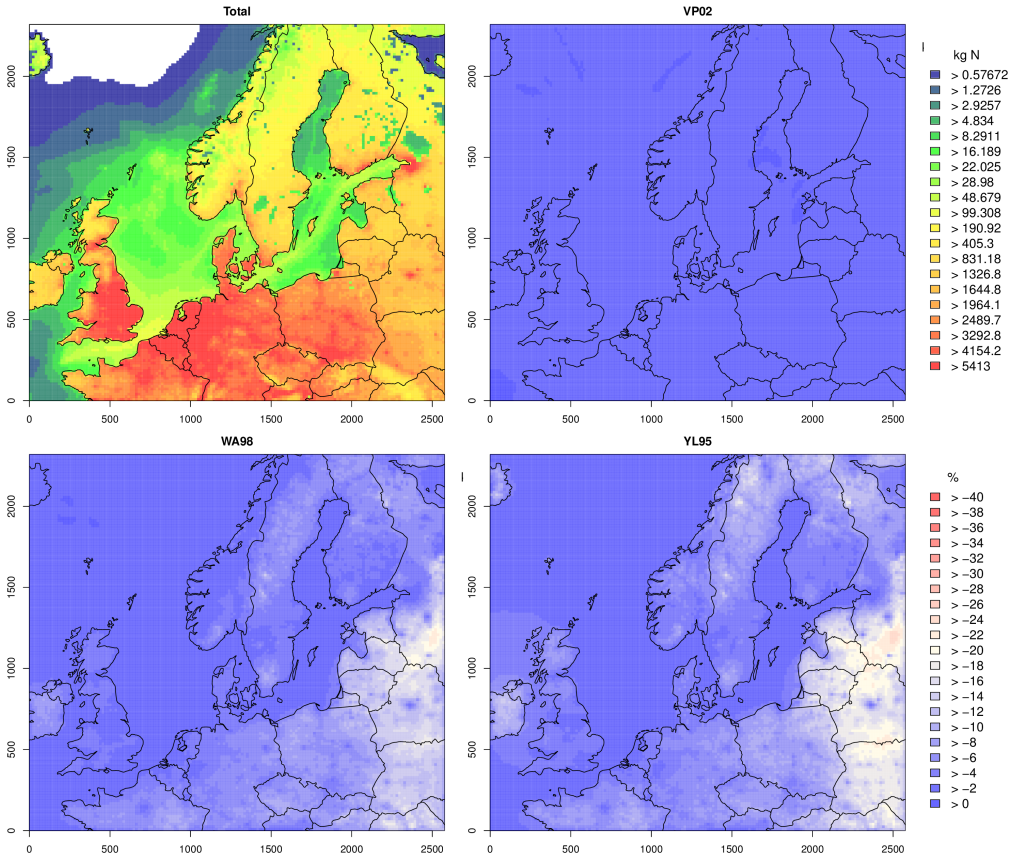

Figure 4.6: Summarized NO_x dry deposition of the Reference case (upper left) and the relative differences with respect to the reference case and the original BEIS parameterization (VP02, upper right), the Wang et al. (1998) implementation (WA98, lower left) and the Yienger and Levy (1995) implementation(YL95, lower right). The unit is total dry deposition of NO_y in kg N per grid cell and 3 month summer period.

Because dry deposition (Fig. 4.6) is mainly due to settling and stomatal absorbance of leaves, such as the canopy reduction for the primary emission flux, the total deposition to the biosphere is 1.16 Gg NO_x-N for VP02, 19.06 Gg NO_x-N for WA98 and 30.25 Gg NO_x-N for YL95. This is 39, 11 and 15 times the VP02, WA98 and YL95 canopy reduction, respectively. This shows that the reduction potential

by the leaves is higher than that by dry deposition of nitrogen.

The wet deposition, due to the low solubility of NO_x in rain water, is extremely low with 51 kg NO_x-N and 0.06 kg NO_x-N, 0.89 kg NO_x-N and 1.45 kg NO_x-N for VP02, WA98 and YL95, respectively.

4.5 Conclusions

This study investigates the effects of different realizations of canopy reduction parameterizations in the SMOKE-CMAQ model system for Europe. Different realizations of canopy reduction parameterizations were implemented in the BEIS model and tested in the SMOKE-CMAQ model system context. The canopy reduction parameterizations are structured following Wang et al. (1998) and Yienger and Levy (1995) and compared against the base case with no canopy reduction and against the basic parameterization of Vukovich and Pierce (2002) which is used in the BEIS model by default.
It was shown that canopy reduction has an impact on NO_y emissions and concentrations in northern Europe and that canopy reduction is a natural sink for oxidised nitrogen compounds.

It is evident that VP02 has a different behavior than WA98 and YL95 and that YL95 has a spatially comparable effect albeit with a larger magnitude than WA98. All three parameterizations lead to statistically significant differences between the reference case without canopy reduction and the three runs with parameterizations. The impact of other model parameters in comparison to canopy reduction effects was evaluated by a varying the meteorological data, a land use classification change and a simplified NO_2 to NO_x split change for the canopy reduction function of the parameterization by Wang et al. (1998). It was shown that a land use change could drastically influence the canopy reduction by changing the soil NO emission budged localy by over 1000%. Meteorological and split changes are of minor effect on the emission budget.
After chemical transport modelling with CMAQ the air concentrations of nitrogen dioxide were compared to EMEP measurement stations. The evaluation of the model at the measurment stations reveals an overestimation of NO_2 at most of the stations with a MNB averaged of 0.56 and an averaged RMSEP of 0.85 μg N m^{-3}. Canopy

reduction reduces the model overestimation and leads to NO_2 concentration levels that are significantly closer to the observations. With the parameterization of Wang et al. (1998) a significantly better correlation averaged over all evaluation sites was achieved. However, this study favors the implementation of the canopy reduction by Wang et al. (1998) in emission and chemical transport models to improve the model perormance.

To gain knowledge about natural processes, it is recomended to install observation stations in more natural and less anthopogoenically influenced regions from an air chemical perspective. Not only to foster further research about natural processes, but also for more long time trend studys under semi-natural conditions.

5 Natural emissions from lightning

Quantification of lightning-induced nitrogen oxide emissions over Europe

Jan A. Arndt, Armin Aulinger, Volker Matthias

Published in: Elsevier Journal: Atmospheric Environment Vol. 202, April 2019, p. 128-141

Abstract

In this study, the importance of lightning-generated NO over Europe in the year 2010 is assessed with the COSMO-CCLM - SMOKE-EU - CMAQ chemistry transport modeling system. Lightning data from TRMM satellite flash density data climatologies are taken and linearly fitted to convective precipitation climatologies. With the resulting linear model, lightning activity in 2010 is calculated based on the convective precipitation rate from model data. This approach combines the globally available satellite observations with the simplicity of linear convective rain parameterizations. It provides a new method for fitting lightning data for linear flash density parameterizations. Compared to other linear flash rate approaches or the very common cloud top height parameterization, the data for 2010 derived by the climatologies and actual 2010 precipitation data better matches the TRMM observation data. Lightning was found to be the second most important natural source after nitrogen monoxide emission from soil, with an annual average amount of 0.295 Tg N per year and an amount in 2010 of 0.278 Tg N. While it is less important for near-surface concentrations, it has a considerable effect on the nitrogen deposition in southern and eastern Europe and a large effect on the NO_2 concentration in higher model layers. The effect in higher atmospheric layers over eastern Europe is 6 times larger than the effect of aircrafts on the air concentration of NO_2 in the mid- and high altitudes. Comparisons with NO_2 observations from the OMI satellite revealed that lightning NO emissions have an observable impact on the NO_2 column density over Europe.

Acknowledgments

This work has been funded by the HGF through the PACES 2 project. We thank our colleagues from IUP for their valuable comments concerning the comparison with satellite data, especially Dr. Andreas Richter for his comments and advice on the comparison routines.

US EPA is gratefully acknowledged for the use of CMAQ, BEIS and SMOKE. We thank Dr. Beate Geyer from HZG department KSR for meteorological data and Dr. Johannes Bieser for the generation and processing of anthropogenic emission data.

This chapter consists of the manuscript published as declared before. It was published by me as corresponding and lead author for the purporse of this thesis. Major parts of the manuscript were written by me, with annotations and corrections made by Armin Aulinger and Volker Matthias. Analysis and Discussion of the Results were made by the supervision of Armin Aulinger and Volker Matthias. The manuscript was peer-reviewed by two anonymous referees with two revisions under editorial supervision of Prof. Chak K Chan.
To avoid multiple introductions with very coherent content, the introduction of this manuscript was omitted.

Acronyms in this manuscript are explained in a acronyms list in the original publication on behave of a reviewer revision. For consistency in this thesis style explanations from the acronyms list are included in the text. Minor other changes, regarding the figure and equation references placing and the table justification has been made.

5.1 Lightning estimates, parameterizations and model data

5.1.1 Emission estimates globally and for Europe

There are several studies estimating the global annual emissions of nitrogen oxide by lightning. The estimations are done by satellite observations or satellite derived variables, online-parameterizations of chemistry transport models or Very High Frequency (VHF) network observations. They are listed in Peterson and Beasley (2011), and the estimates range from 2 Tg to 40 Tg. Peterson and Beasley (2011) calculated global mean emissions of 5 Tg N per year with an uncertainty of 3 Tg N.

Estimates for Europe are rare. Three considerably different values are known. Huntrieser et al. (2000) estimated 0.03 Tg N, Blakeslee et al. (2014) 0.1 Tg and Vinken et al. (2014) 0.5 Tg N. Huntrieser et al. (2000) used a global flash density share of 1% for Europe, the share in Blakeslee et al. (2014) is approximately 3.5%, and in Vinken et al. (2014) the estimate is approximately 10% of the global emission based on Sauvage et al. (2007).

5.1.2 Nonlinear Lightning Parameterizations for Chemistry Transport Models

The parameterization described in Price and Rind (1992) uses the cloud top height as a proxy for the updraft velocity, which is an estimate of the thunderstorm intensity. The authors found two different relationships for continental (Eq. 5.1) and maritime (Eq. 5.2) flash rates.

$$F_{continental} \;=\; 3.44\ 10^{-5}\mathrm{CTH}^{4.90} \tag{5.1}$$

and

$$F_{maritime} \;=\; 6.40\ 10^{-4}\mathrm{CTH}^{1.73} \tag{5.2}$$

where CTH is the model cloud top height in km and F represents the flash rate in flashes per minute. For clouds with less than 5 km vertical extent, the flash rate is set to zero. The CTH-Parameterization is used, as in the Goddard Earth Observing System Chemistry transport (GEOS-CHEM) model (Wang et al., 1998).

5.1.3 Linear Lightning Parameterizations for Chemistry Transport Models

This parameterization is found in Meijer et al. (2001). It represents a linear fit (Eq. 5.3) between the modeled mean ECMWF (European Centre for Medium-Range Weather Forecasts) convective precipitation and the flash frequency as measured with the Lightning Position And Tracking System during the The European Lightning Nitrogen Oxides Project (EULINOX) Experiment over central continental Europe in summer 1998.

$$\overline{F} \;=\; 14700\; CP + 1.7 \tag{5.3}$$

$\overline{F}$ denotes the mean number of flashes per precipitation mass. CP is the convective precipitation in m. Because the parameterization is computed with cloud-ground flashes, it has to be corrected for the total flash rate (Eq. 5.4). This is done with the approach described in Price and Rind (1993) Eqs. 1 and 2

$$p \;=\; \frac{1}{64.09 - 36.54H_0 \;+\; 7.493H_0^2 \;-\; 0.648H_0^3 \;+\; 0.021H_0^4} \tag{5.4}$$

Here, H_0 is calculated as formulated in Price and Rind (1993) Eq. 3 and describes the cloud height above the freezing level. It is set to a minimum at 5.5 km. p is the dimensionless correction factor for intra-cloud and cloud-to-ground flashes.

This linear parameterization has been used in the CMAQ modeling system until version 5.1. It is adopted in the form of Eq. 5.5

$$F \;=\; 147\; CP \frac{\Delta x}{36000\; m} \frac{\Delta y}{36000\; m}\; 4 \tag{5.5}$$

where F denotes the number of flashes, CP is the convective precipitation in cm, and the grid resolution in the x and y directions is Δx and Δy, respectively. The factor 4 accounts for the cloud-to-ground and intra-cloud ratio and is a strong simplification of Equation 5.4. The 36000 m in the parameterization refers to the standard grid cell size of earlier CMAQ versions and scales the result to the actual grid cell size.

Because the experiment where this parametrization is based took place in a certain region over a short time period, the results may not be representative for all model regions and all time scales. Especially over ocean areas, the parameterization overestimates the flash rate by approximately ten times (Boersma et al., 2005).

In the latest model versions of CMAQ, a linear fit between the convective precipitation and the National Lightning Detection Network (NLDN) results in a slope and an intercept value for every grid cell (Eq. 5.6). These values are used in conjunction with the convective precipitation rate to calculate the flash rate even for other temporal scales.

$$F = Slope_{NLDN/CP}\, CP + Intercept_{NLDN/CP} \tag{5.6}$$

Other spatial information, such as land-sea distribution, is optionally usable to correct the flash rate. It is described in Kang et al. (2018). This approach is applied in this study.

5.1.4 LIS/OTD Satellite Data

The LIS and OTD instruments (Lightning Imaging Sensor / Optical transient detector) are mounted on the Tropical Rainfall Measuring Mission (TRMM) satellite. Both sensors monitor the 777.4 nm atomic oxygen multiplet emission line. They are configured to detect pulses of illumination at this wavelength that originate from lightning. The OTD was in operation from 1995 to 2000 and the LIS from 1998 until now. While the LIS has a coverage of approximately 38° North and South around the Equator, the OTD instrument covers nearly the entire globe. The detection efficiencies are approximately 50% for the OTD and 90% for the LIS. Cecil et al. (2014) describes different climatologies that are created with the dataset provided by the OTD and LIS instruments. Because the instrument orbits over the area, different regions have different view-times. This may lead to an underestimation of flash numbers in certain areas. In this study, the High-Resolution Monthly Climatology (HRMC) with a global resolution of 0.5° was used. It contains, binned to 0.5° degree grid cells, the mean flash density for every grid cell from 1995 to 2012. A study of Anderson and Klugmann (2014) showed that VHF network observations and the satellite climatology by Cecil et al. (2014) used in this study are in good agreement.

5.1.5 Meteorology Data from COSMO-CLM

The meteorological fields were simulated with the Consortium for small scale modeling - Climate limited-area modelling-community mesoscale meteorological model

(COSMO, version 5.0, citetRockel2008) for the year 2010 using ERA-Interim forcing data (Dee et al., 2011). COSMO-CLM is the climate version of the numerical weather prediction model COSMO (Schaettler et al., 2008), originally developed by Deutscher Wetterdienst (DWD) Steppeler et al. (2003); Schaettler et al. (2008). It was run on a 0.11° x 0.11° grid using 40 vertical layers up to 20 hPa for all of Europe. COSMO-CLM uses the TERRA-ML land surface model (Schrodin and Heise, 2001), a TKE turbulence closure scheme (Doms and Schättler, 2002; Doms et al., 2011), the Tiedtke scheme (Tiedtke, 1989) for cumulus clouds and a radiation transfer scheme following Ritter and Geleyn (1992).
The meteorological fields were re-gridded to match the CMAQ grid with the Model-3 Meteorological Preprocessor for CMAQ (MCIP) preprocessor.

5.1.6 Emission Data

Anthropogenic emissions at an hourly temporal resolution were produced with the Sparse Matrix Operator Kernel Emissions for Europe (SMOKE-EU) (Bieser et al., 2011a) for the year 2010. A correct representation of anthropogenic emissions is important for studying their interactions with natural nitrogen compounds. Complete sea-, air- and land-based emissions sources in the model domain are used to create the emission dataset. They are based on officially reported European Monitoring and Evaluation program (EMEP) emissions that are distributed in time and space using appropriate proxies, such as population density, street maps or land use. Point sources were considered to the extent that information from the European point source emission register was available. The vertical distribution of the emissions was calculated online with the SMOKE model, and the results are given by Bieser et al. (2011b). Shipping emissions for the Baltic Sea and North Sea with high spatial and temporal resolutions were obtained for this study from the Ship Traffic Emission Assessment Model (STEAM) (Jalkanen et al., 2009, 2012; Johansson et al., 2013, 2017).

5.1.7 CMAQ

The Community Multi-scale Air Quality Model (CMAQ) (Byun and Ching, 1999; Byun and Schere, 2006) version 5.0.1 (US EPA Office of Research and Development, 2012) was used with the carbon bond 5 (CB05) photochemical mechanism

(CB05tucl) (Kelly et al., 2010) and the AE6 aerosol mechanism. The model was run for July 2010 with a spin-up time of 2 weeks to avoid the influence of initial conditions on the modeled atmospheric concentrations. The model was setup on a 24 x 24 km^2 grid cell size grid for entire Europe. Chemical boundary conditions for the outer model domain were taken from the Hemispheric Transport of Air Pollution (HTAP) BASE dataset as described in Im et al. (2018). The vertical model extent comprises 30 layers from the model surface up to the 100 hPa pressure level at the top. Twenty of these layers are below approximately 2000 m, and the lowest layer has a height of approximately 36 m.

5.1.8 Model evaluation data

Air concentrations measured at ground stations are often used as benchmarks for model evaluation. In this study, in situ measurements from the EMEP station network (Tørseth et al., 2012) are used. The data were provided by the EBAS (http://ebas.nilu.no) database. Because NO has only a short lifetime in the atmosphere in comparison to NO_2, NO_2 is used for the evaluation of the model data.

A disadvantage of observation site data is the limited spatial coverage and the limitation to the lowest layer of the planetary boundary layer. Spatially more densely distributed measurement data over broader areas of the model domain are provided by satellite measurements. They are provided as column densities and include information on higher atmospheric layer concentrations as well.
Observations of the Ozone Measurement Instrument (OMI) on the National Aeronautics and Space Administration (NASA) Aura satellite are used in this study. Aura is in a sun-synchronous orbit with an approximately 100 minute period. OMI NO_2 Level 2 data from the Tropospheric Emission Monitoring Internet Service webpage (www.temis.nl) are used in this study (Boersma et al., 2011). Level 2 data are processed satellite data instead of raw radiation sensor data.

A drawback of remote-sensing is its dependence on modeled a priori columns of atmospheric trace gases and radiation transport modeling. Therefore, a direct comparison of model and satellite data is not applicable. To overcome this, the averaging kernel method (Eskes and Boersma, 2003) is used. Here, the averaging kernel of OMI data was applied to the model results, which means the concentrations calculated by the model have been weighted by height in the same manner as has

been done for the original satellite retrieval. This makes the chemistry transport model data and satellite data comparable. To act in a consistent manner of data analysis, it was decided to project the satellite data on the chemistry transport model grid. The necessary spatial interpolation has been done with a moving average with a rectangular three by three grid cell window approach. The single satellite observation has an error in the magnitude of the observation itself. By averaging this data over time, the error was reduced by $\sqrt{n}^{-1}$ with sample size n. To reduce the individual measurement error, the daylight overpass data from 05:00 UTC to 20:00 UTC over the whole month of July 2010 was averaged while including only data with less then 50% cloud cover. This reduces the error of every particular measurement from 100% to approximately 5%. The OMI records the spectral data row-wise. For 2010, the OMI has some row anomalies that lead to invalid values. Therefore, rows 27 - 46 and 54 - 55 have been omitted.

5.2 Fitting Lightning Parameters for Europe

As stated above, this study uses the new CMAQ approach of a linear fit between the convective precipitation and flash density data. Linear approaches are common. They are based on one single linear model (see Eq. 5.3 and 5.5) or are specific for a given region or grid cell as in the new CMAQ approach. Both approaches depend on VHF network observations. If no VHF network observation is available for any reason, it is not possible to use the regional approach. This study tries to close this gap by using freely available satellite datasets.

TRMM LIS/OTD data as HRMC at a resolution of 0.5° was used as lightning data. The convective precipitation data was used as calculated with the COSMO-CLM and processed with MCIP. Because the OTD that covers most of the study area is limited to the years 1995 to 2000, only precipitation data from this time period were used.

The fitting has been calculated for each month individually. As the flash data are given in mean number of flashes per km^2 and day, the monthly mean daily sum of convective rain per m^2 was used. To account for spatial mismatches between lightning data and convective precipitation data, a moving window of 11 × 11 grid cells was applied. The total precipitation inside this window has been used to cal-

culate a linear fit to the flash counts within the same window. The particular linear model is assumed to be valid for the center grid cell of the moving window (Fig. 5.1).

The study area was the extended European domain as seen in Figure 1. For the fitting procedure, multiannual meteorological model data were needed. These data were available at a resolution of approximately 0.5°. We used a grid resolution of 64×64 km^2 and interpolated all relevant information, such as flash densities and precipitation rates, to it because it matches the resolution of the input data well. The linear fitting will be processed on this grid. The following model calculations of the chemistry transport model and the corresponding meteorological driver is on a 24×24 km^2 grid. Therefore the results of the linear fitting process were interpolated with a bilinear interpolation method to the 24×24 km^2 grid.

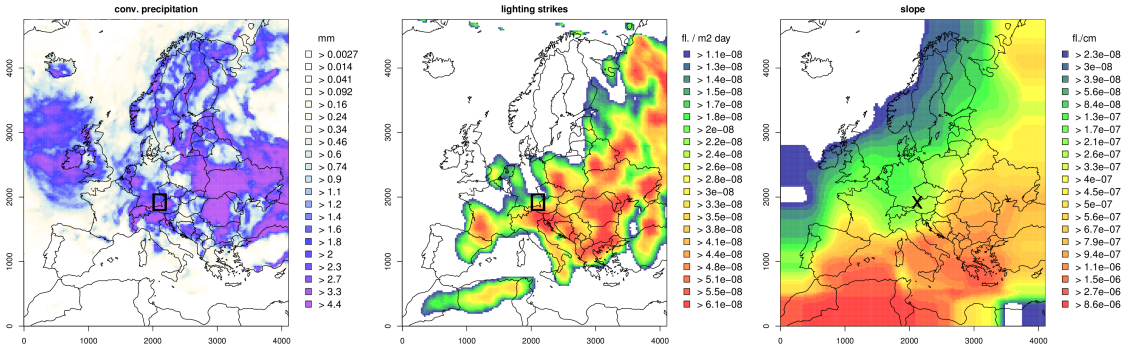

Figure 5.1: The principle of the slope calculation for the linear fit. The plot on the left shows the rain rate, and the middle plot is the flash density. The black boxes show the moving average areas used for the linear fit between flash rate and rain rate. The black cross on the slope plot on the right shows the middle of the red boxes for which the slope is calculated.

5.3 Emission Factors and Global Estimates

Emission factors for lightning emissions are highly uncertain and range from 8 moles NO per flash to more then 4000 moles per flash (Peterson and Beasley, 2011). It is difficult to group these values by observation, laboratory experiment or simulation in order to obtain a smaller range because the large spread of emission factors is found in all three groups. Four different options are possible to choose emission factors for estimating the nitrogen budget in a certain region: a mean emission factor,

two factors and simulations from both ends of the range, a random field of emission factors or to use a commonly used factor. Because the built-in emission calculation in CMAQ is done with an emission factor of 500 moles per flash, this was set as the emission factor for all cases of this study for the reason of better inter-comparability.

With the above described method, global annual emissions were estimated to be approximately 10 Tg N (Fig. 5.2). This is in agreement with the literature values and corresponds to the upper limit of the estimates regarding global lightning emissions. With a mean emission factor of 320 mole per flash, global emissions of approximately 6.4 Tg N were calculated, which is an average value according to the literature.

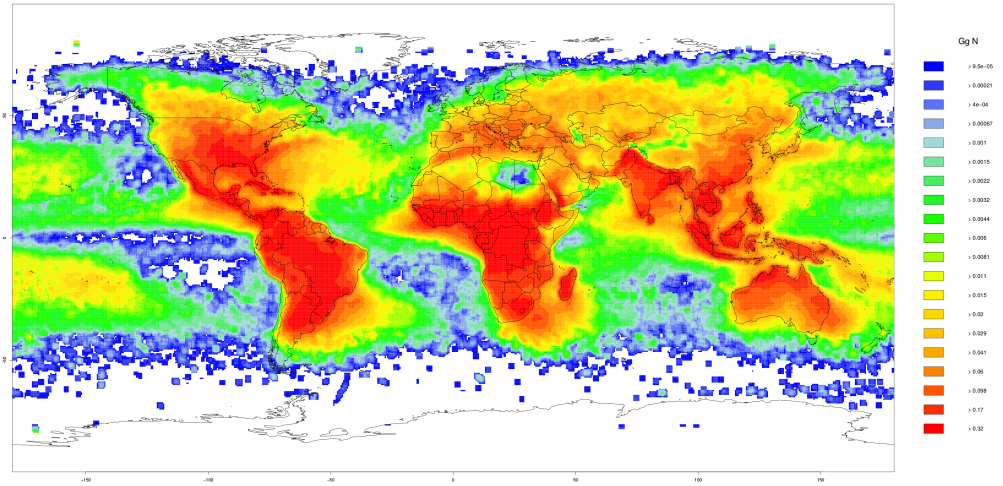

Figure 5.2: Global flash emissions with 500 moles N/flash as the emission factor derived from the 1995 to 2012 TRMM LIS/OTD climatology. The tropics can be clearly identified as a major source of lightning NO, but other regions of the world are also high-emission areas. The unit is emission of NO in Gg N per grid cell and year

5.4 Results and Discussion

In this study, three different parameterizations were tested against the climatology derived from the TRMM LIS/OTD observations.Three cases were distinguished. The observation scenario is denoted as case **SAT**, the parameterization based on convective rain and the TRMM LIS/OTD observation data as **NEW**. The CTH parameterization is denoted with **CTH**, and **OLD** denotes the parameterization used in CMAQ before version 5.2. It is important to notice that NEW and SAT are

not equivalent. SAT represents observations, while NEW uses 2010 precipitation data and proxy data from the climatology to calculate flash rates for 2010.

5.4.1 Lightning NO emissions

All four emission cases show lightning NO emissions over Europe. The values are listed in table 5.1. The annual lightning emissions derived from the TRMM LIS/OTD flash climatologies are approximately 295 Gg N for the year 2012. The old CMAQ parameterization produces 892 Gg N, and the CTH parameterization yields 188 Gg N (Fig. 5.3). The NEW case yields 278 Gg N. While spatial patterns in frame a) and b) are very similar, the pattern in c) shows a clear difference between sea and land masses, and the pattern in d) shows a clear emphasis on the sea areas. The month of July (Fig. 5.4) was used for model-observation evaluation of concentrations (see 5.4.3). The total emissions for July by lightning are 53 Gg N for the TRMM LIS/OTD flash climatology, OLD yields 67 Gg N, the CTH parameterization yields 28 Gg N, and NEW yields 53 Gg N. With a mean emission factor of only 320 moles per flash NO, the emissions are 36% lower than those calculated above.

SAT and NEW have comparable spatial and total emission characteristics. The emissions from CTH are 2 times smaller than the emissions derived in SAT and are more concentrated in the northern parts of Europe. The CTH parameterization is based on the cloud top height of clouds thicker than 5500 m above the freezing level. Because of the higher freezing level, many clouds are not thick enough to produce lightning nitrogen monoxide.

OLD is linearly dependent on the convective rain rate. Convective rain does not necessarily lead to thunderstorms and lightning because separation of charge in the cloud is required and occurs only with certain updraft velocities, instability and cloud heights. Especially over the open ocean, these conditions are not as closely linked to convective precipitation as is assumed. This assumed close dependence explains the high values of nitrogen monoxide emissions over the Atlantic ocean and on the west coast of Norway in the model.

Table 5.1: Emissions from lightning for different time spans, emission factors and parameterizations. Emission factor in mole N per flash (mol/fl.)

	Year 2010 500 mol/fl.	July 2010 500 mol/fl.	Year 2010 320 mol/fl.	July 2010 320 mol/fl.
SAT	295 Gg N	53 Gg N	189 Gg N	34 Gg N
OLD	892 Gg N	67 Gg N	571 Gg N	43 Gg N
CTH	188 Gg N	28 Gg N	120 Gg N	18 Gg N
NEW	278 Gg N	53 Gg N	178 Gg N	34 Gg N

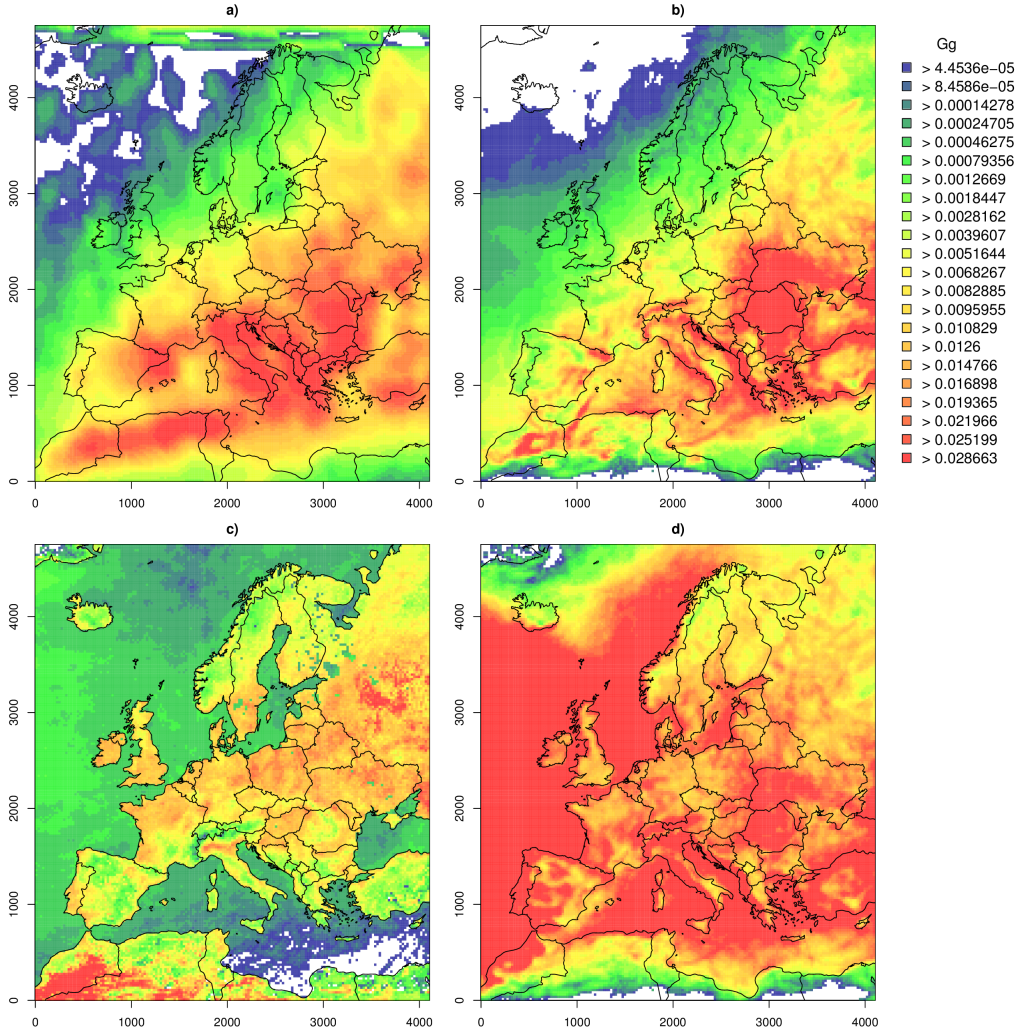

Figure 5.3: Yearly emissions of nitrogen monoxide by lightning in 2010. a) is the TRMM data (SAT), b) is the new NEW parameterization, c) is the CTH parameterization and d) is the OLD parameterization. The unit is emission of NO in Gg N per grid cell and year

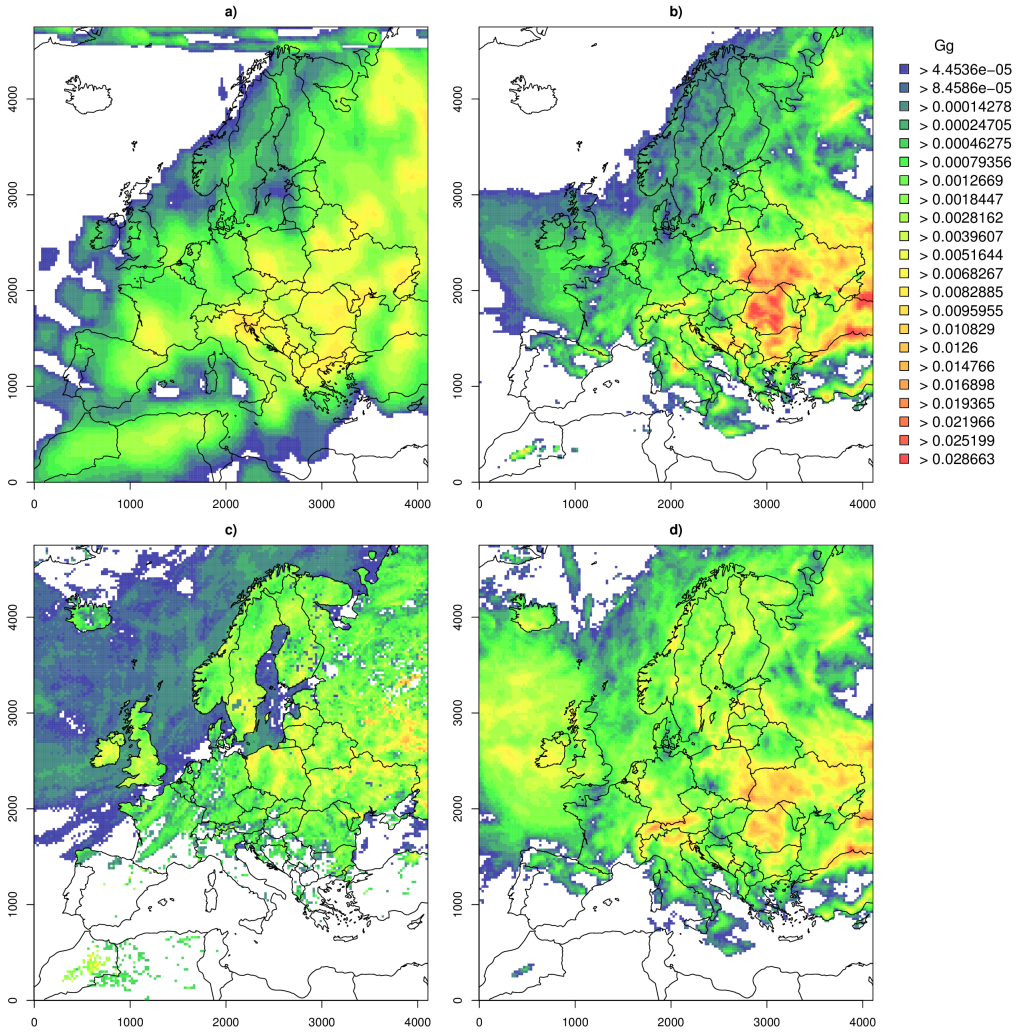

Figure 5.4: Emissions of nitrogen monoxide by lightning in July 2010. The panels are the same as those in figure 5.3. The unit is emission of NO in Gg N per grid cell and month July of 2010

5.4.2 Lightning NO emission sensitivity

To asses the sensitivity of the lightning emissions to the fitting process, five sensitivity experiments for the new parameterization were conducted. In the first two experiments, randomly varying rain amounts were added to the convective precipitation dataset of 2010. Afterwards, the dataset is scaled with a factor so that the sum of the deviated dataset is 10% greater than the original precipitation dataset. In the first experiment, it was added before the fitting process; in the second experiment, it was added after the fitting when calculating the flash rate for a particular rain dataset. The calculation was repeated 20 times in both cases. For the first case, when the noise was added before the fitting had been performed, the impact on the total lightning count was approximately -5%. In the second case, when the noise was added to the precipitation dataset used for lightning calculation, the noise lead to 45% more lightning.
The third and fourth experiments were performed by increasing the precipitation of the original dataset linearly by 10%. The effect on the flash count when adding the increase before the fitting process was -6%. In the second case, when the values were added to the precipitation dataset for the flash count calculation, the impact was +10% more flashes.

The fifth test case was calculated with meteorological data for the year 2012. Because the meteorological parameters rain and cloud extent might differ in different ways, this process can be used to determine the sensitivity of the CTH parameterization to the input variables. The new parameterization emits 48% less, the old 13% less and the CTH 16% less than 2010; the values differ noticeably from those in 2010 (Fig. 5.5). Compared to the sum calculated with the TRMM data of 53 Gg N for July, the old parameterization now represents the conditions best with 58 Gg N. From the perspective of spatial distribution, the old parameterization differs very noticeably from the TRMM data, and in this case, the new parameterization fits best.

Overall, the total emission impact is very sensitive to the meteorology. Only longer time series and climatologies with more than two years of data (as suggested in Finney et al. (2014) and Anderson and Klugmann (2014)) will give a representative overview that is not biased by a dryer or wetter year.

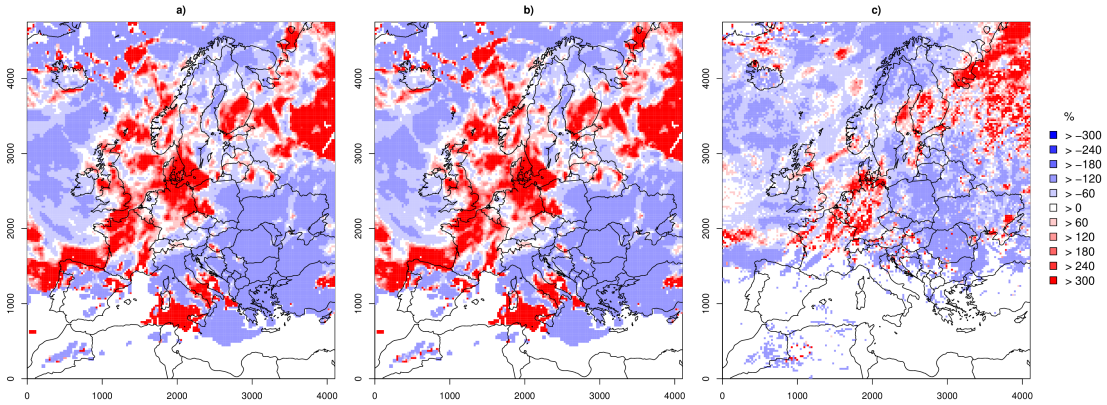

Figure 5.5: Sensitivity to the different meteorological conditions in 2010 and 2012. The relative difference between the both years is shown in a) for NEW, b) for OLD and c) for the CTH parameterization.

5.4.3 Concentration and deposition changes caused by lightning emissions

To investigate the interactions and changes in the summed nitrogen oxides (NO_y) as well as the interaction and changes in reduced nitrogen species (NH_X), chemistry transport model simulations with CMAQ (see 5.1.7) were conducted. The full emission dataset as described in 5.1.6 was used. A base case without lightning emissions and four simulations containing SAT, NEW, OLD and CTH lightning emissions were calculated.

Lower Troposphere

All four cases showed higher concentrations of oxidized nitrogen in the lowest model layer than the base case without lightning emissions (Fig. 5.7). Concentrations of reduced nitrogen were lower in most parts of Europe (Fig. 5.8). This is consistent with higher concentrations of ammonium nitrate aerosols (Fig. 5.9) in the same regions. Higher emissions of nitrogen monoxide cause higher concentrations of HNO_3, which reacts with NH_3 to form particulate ammonium nitrate.
Regional increases in NH_x concentrations are explainable by horizontal and vertical transport of gaseous and particulate nitrogen (for average wind fields in July 2010, see figure 5.6). This was significantly visible in the CTH case. The regions with higher NH_x concentrations in the lowest model layer had lower concentrations summed over the total model column than in the base case. This was caused by

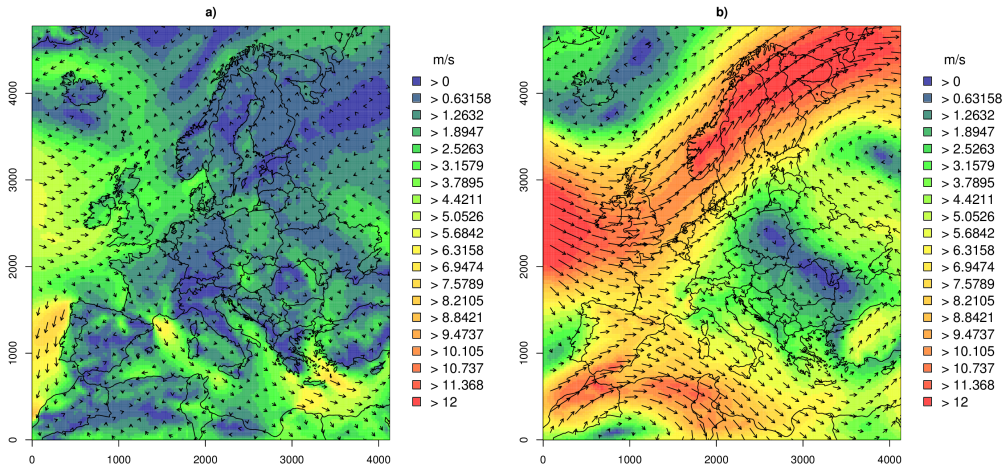

Figure 5.6: Average wind velocity as shading and wind direction as arrows for a) the lowest model layer at a height of approximately 20 m and b) layer 25 representing middle tropospheric wind fields at a height of approximately 5000 m. Averaging time span is one month for July 2010.

greater deposition over the Atlantic ocean, vertical transport to higher layers and horizontal transport to the eastern parts of the model domain.

Because reduced nitrogen is mainly emitted from agriculture, concentration changes in NH_3, which is only a short-range-transport pollutant, is more or less limited to the land surface and will not extend to larger areas in the open sea. This does not apply to the strongly coastally influenced parts of the Mediterranean, as this region is surrounded by agricultural areas.

Sea areas appeared to be influenced more by lightning emissions than surrounding land surface areas when looking at relative concentration changes. On the other hand, the absolute changes were quite low. The reason for this is that anthropogenic emissions over ocean areas are limited to shipping emissions. Both emissions and background concentrations over ocean areas are lower than those on land. Small emission changes like those caused by lightning therefore have a larger impact over ocean areas than on land (Fig. 5.7). This can be best observed in the southern Barents sea.

As only SAT had emissions and increased concentration values of lightning nitrogen monoxide over northwestern Africa (Fig. 5.4 and 5.7), we did not find similar

changes in NEW, OLD and CTH . There are two possible explanations. One of them involves dry thunderstorms for which convective rain parameterizations are not suitable. The other explanation involves thunderstorms with rain that were not simulated correctly by the meteorological model.

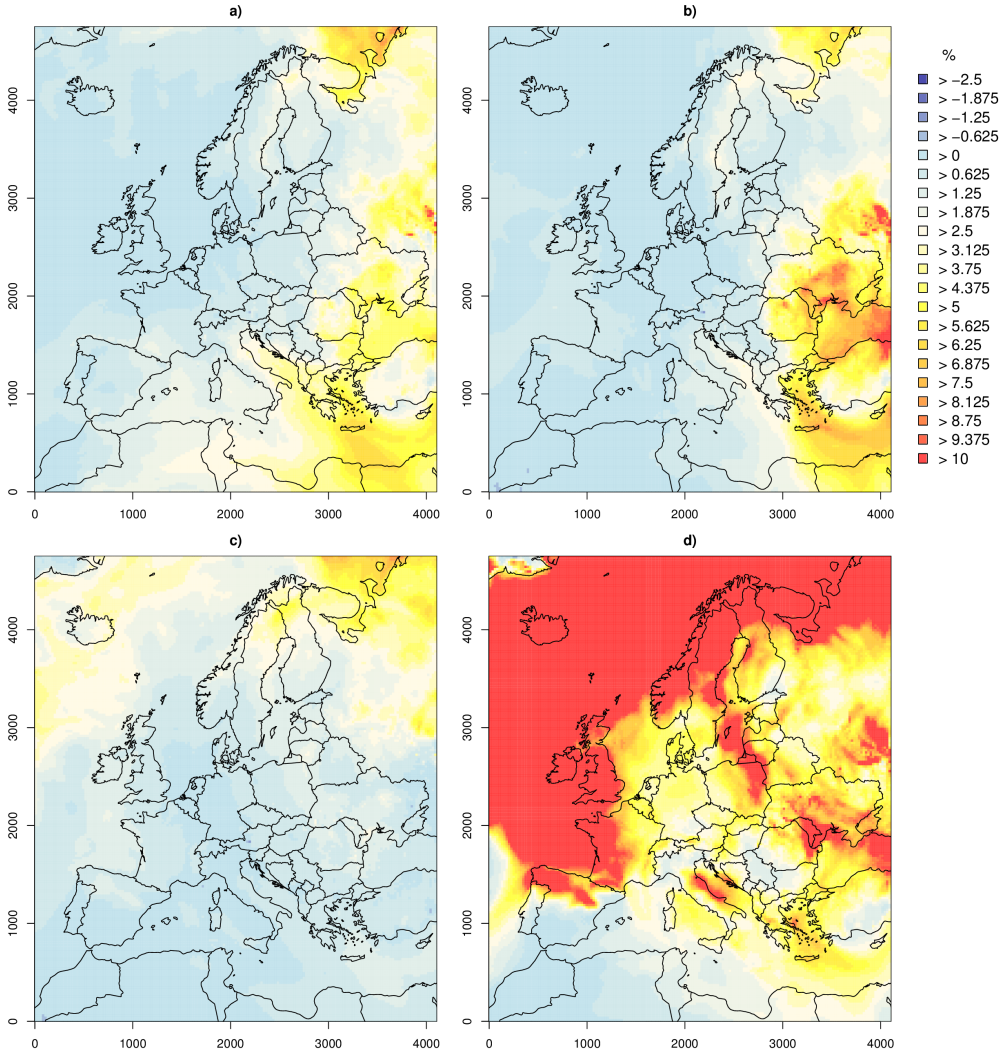

Figure 5.7: Near-ground concentration changes in oxidized nitrogen species for July 2010. a) SAT case, b) NEW, c) CTH and d) old parameterization.

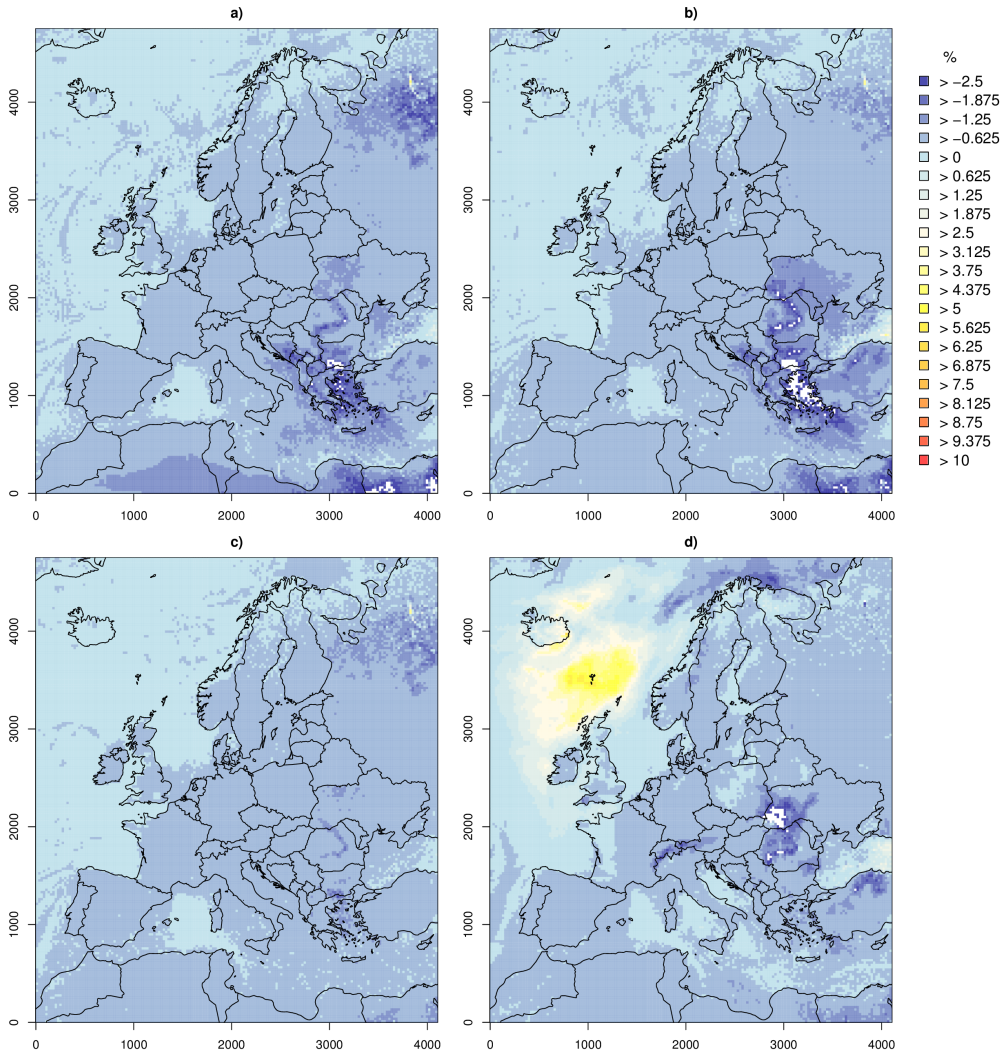

Figure 5.8: Near-ground concentration changes in reduced nitrogen species for July 2010. Same format as in Fig. 5.7.

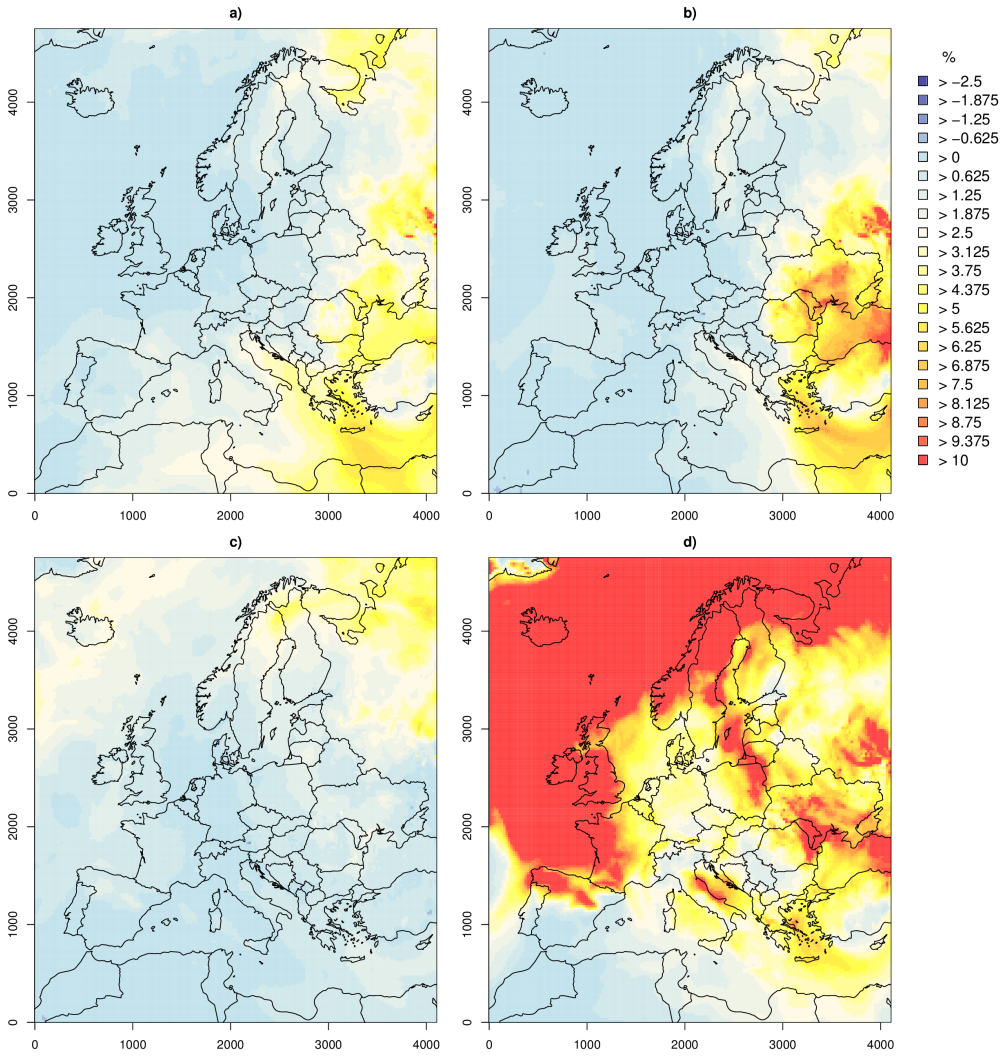

Figure 5.9: Near-ground concentration changes in ammonium nitrate for July 2010. Same format as in Fig. 5.7.

An evaluation of lightning emissions using the EMEP station network (see 5.1.8) showed that the impact on the air quality measurement was low but leads in some cases to significant differences (see Tab. 5.2 and 5.3). For example, the MNB had significantly higher values in the lightning case than in the base case. This could be interpreted as a model deterioration. The reason for this is that the base model run already overpredicted the nitrogen emissions as a result of the uncertainty in the anthropogenic emissions. Additional nitrogen emissions raise the concentration level and consequently the MNB. This indicated that the implementation of lightning emissions may improve the model in terms of processes considered without improving the performance of the model when evaluated against observations.

The dry deposition of oxidized nitrogen (Fig. 5.10) was spatially correlated with the increase in concentrations of oxidized nitrogen. The relative dry deposition change of NH_x (Fig. 5.11) was also positive and, to a smaller extent, spatially linked to the concentration increase in oxidized nitrogen. This was due to the additional formation of ammonium nitrate in the regions of higher emissions caused by lightning, where NH_4^+ deposition was then higher than before.

The pattern of wet deposition was closely linked to the rainfall pattern in the simulated month. The overall pattern resulting from the simulations was an combination of the dry deposition pattern already described and the rainfall pattern of the model. Where more rainfall occurs, deposition is higher; where less rainfall occurs, the deposition is lower than the dry deposition results or there is actually no deposition.

Table 5.2: EMEP evaluation values. First header row indicates the case, second the statistical parameter.

	BASE			TRMM		
	corr	RMSEP	MNB	corr	RMSEP	MNB
Vezin	0.74	1.17	0.03	0.74	1.17	0.03
Waldhof	0.51	1.43	-0.52	0.51	1.42	-0.52
Anholt	0.74	0.93	0.03	0.74	0.93	0.03
Lahemaa	0.48	1.14	-0.54	0.48	1.14	-0.53
Vilsandi	0.30	1.44	-0.59	0.30	1.44	-0.59
Aston Hill	0.69	0.69	-0.28	0.69	0.69	-0.28
St. Osyth	0.80	1.21	0.00	0.80	1.21	0.00
M. Harborough	0.39	0.75	0.02	0.39	0.75	0.03
Preila	0.38	0.44	-0.26	0.38	0.43	-0.26
Eibergen	0.64	2.12	-0.36	0.64	2.12	-0.36
Birkenes II	0.67	0.54	0.98	0.67	0.54	0.98
Hurdal	0.32	0.37	0.44	0.32	0.37	0.44
Leba	0.35	0.78	-0.51	0.35	0.78	-0.51
Råö	0.70	1.24	0.76	0.70	1.25	0.76

Table 5.3: EMEP evaluation values. Continued from 5.2. First header row indicates the case. second the statistical parameter.

	CTH			Old			New		
	corr	RMSEP	MNB	corr	RMSEP	MNB	corr	RMSEP	MNB
Vezin	0.74	1.17	0.03	0.74	1.17	0.04	0.74	1.17	0.03
Waldhof	0.51	1.43	-0.52	0.47	1.42	-0.51	0.51	1.43	-0.52
Anholt	0.74	0.92	0.03	0.74	0.92	0.03	0.74	0.93	0.03
Lahemaa	0.48	1.14	-0.53	0.48	1.13	-0.53	0.48	1.14	-0.53
Vilsandi	0.30	1.44	-0.59	0.28	1.43	-0.58	0.30	1.44	-0.59
Aston Hill	0.69	0.68	-0.27	0.69	0.67	-0.25	0.69	0.69	-0.28
St. Osyth	0.80	1.21	0.00	0.80	1.20	0.00	0.80	1.21	0.00
M. Harborough	0.39	0.75	0.03	0.39	0.74	0.04	0.39	0.75	0.03
Preila	0.38	0.43	-0.26	0.34	0.42	-0.20	0.39	0.43	-0.26
Eibergen	0.64	2.12	-0.36	0.63	2.11	-0.35	0.64	2.12	-0.36
Birkenes II	0.67	0.54	0.99	0.67	0.54	1.03	0.67	0.54	0.98
Hurdal	0.32	0.38	0.45	0.30	0.39	0.51	0.32	0.37	0.44
Leba	0.35	0.78	-0.51	0.28	0.78	-0.48	0.35	0.78	-0.51
Råö	0.70	1.24	0.76	0.70	1.25	0.78	0.70	1.24	0.76

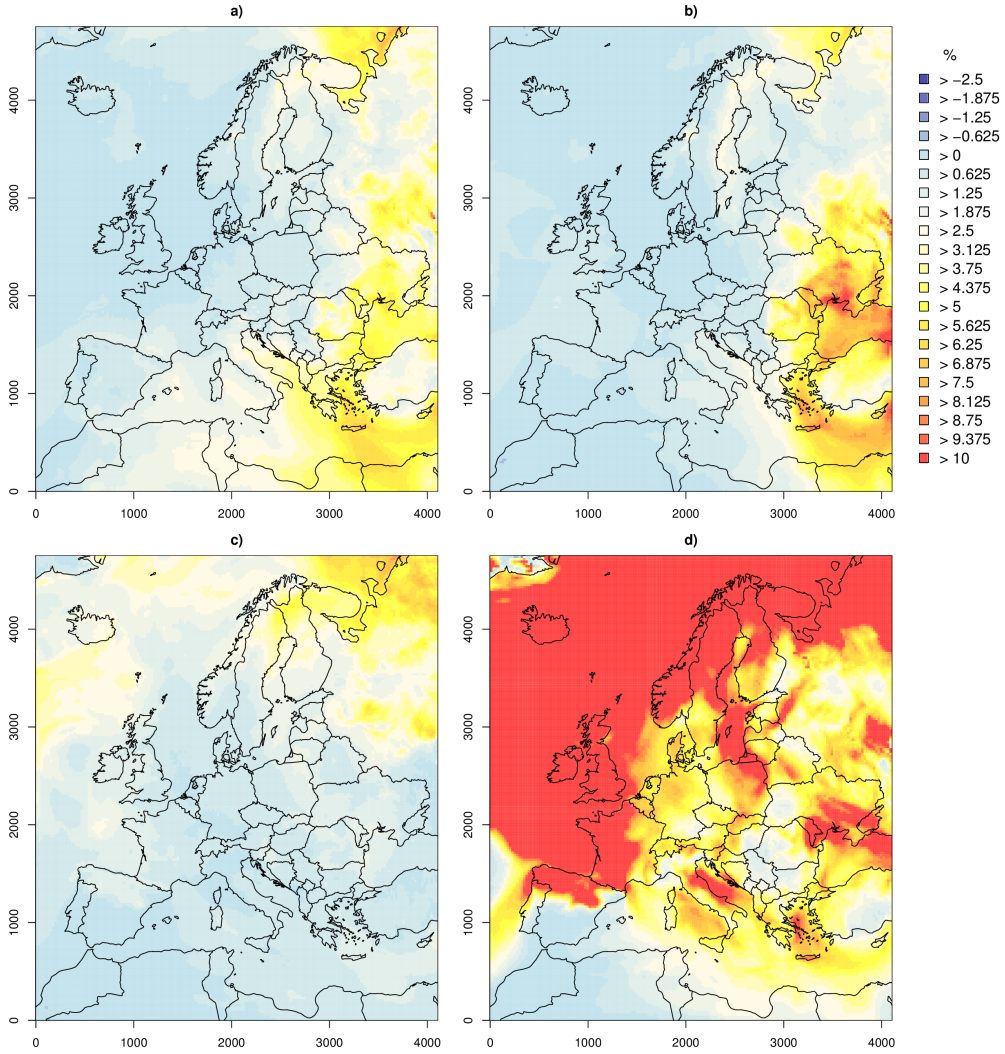

Figure 5.10: Dry deposition change in oxidized nitrogen for July 2010. a) is the TRMM data, b) is the parameterization as described in 5.2, c) is the CTH and d) is the old CMAQ parameterization. The change is mainly comparable to the change in figure 5.7 because dry deposition is proportional to the concentration.

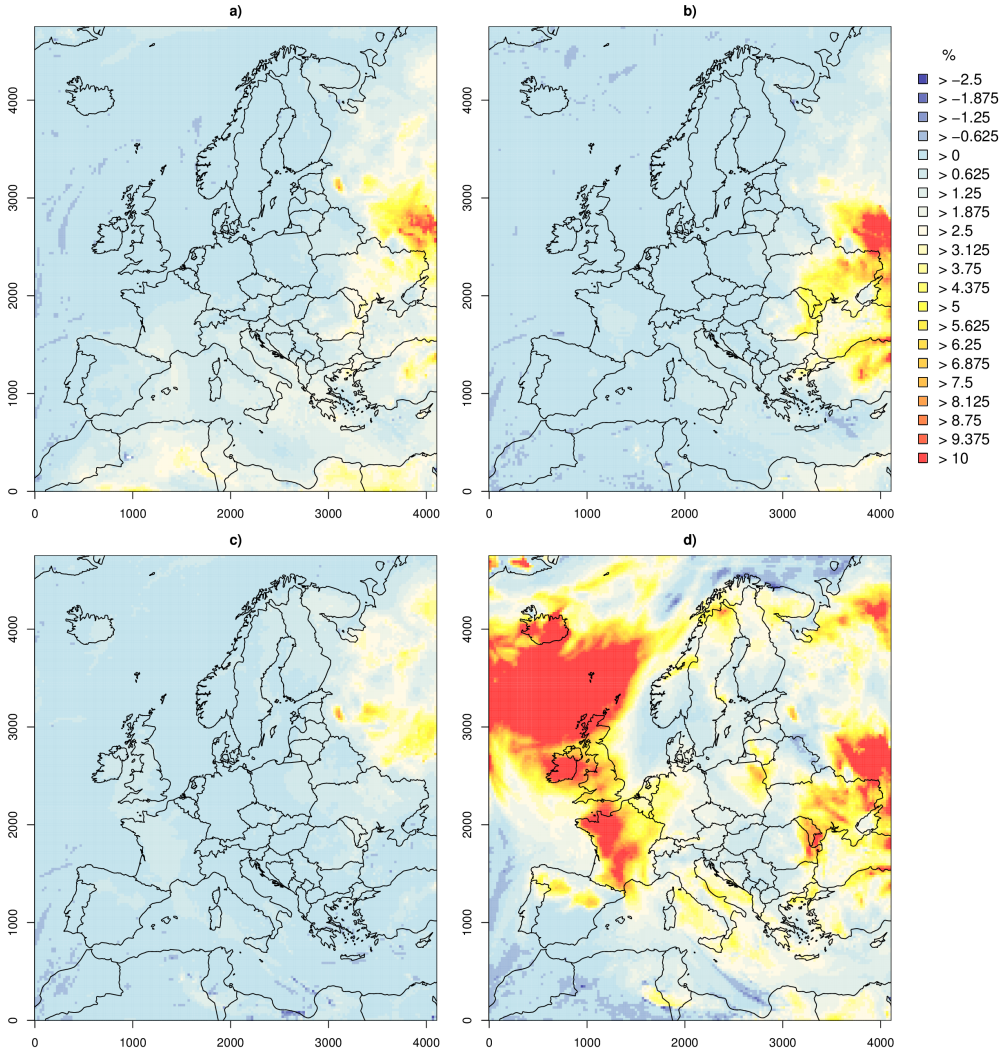

Figure 5.11: Dry deposition change of reduced nitrogen for July 2010. a) is the TRMM data, b) is the parameterization as described in 5.2, c) is the CTH and d) is the old CMAQ parameterization. The change is mainly comparable to the change in figure 5.8 because dry deposition is proportional to the concentration.

Upper Troposphere

The spatial N distribution in the upper atmosphere was different than that in the lower parts of the atmosphere. Anthropogenic emissions in the middle and high troposphere mainly stem from aircrafts. The emissions from aircraft are bound to the main flight paths over Europe, with large quantities over central Europe, the corridors to North America over the North Sea and Atlantic ocean and the corridors to Asia over the Baltic sea and southeastern Europe. For this study, the aircraft time and flight path profiles (and associated emissions) were assumed to be static. The emissions from aircraft were uniformly added to the emission dataset of the base and new lightning cases. The upper troposphere emissions from aircraft over the whole year 2012 were 128 Gg N and 10 Gg N for July (see table 5.4 for a source apportionment overview of the year 2010). This scaled to the lightning emissions that are mainly distributed in the upper troposphere (Fig. 5.12), as derived from the TRMM climatologies by about one third. A comparison of nitrogen oxide concentration caused by aircraft emissions and lightning emissions in the middle troposphere showed that lightning emissions had a considerably higher impact in the eastern part of the model domain than aircraft emissions (Fig. 5.13). There was a clear gradient from east to west in N contribution by lightning. In eastern Europe, N concentrations caused by lightning were over 6 times larger than those caused by aircraft. In western parts, in contrast, aircraft emissions were twice as large as lightning emissions.

Table 5.4: Total emissions per year for different regions of the model domain and for the different emission sources discussed in this study.

	Emission $\leq$ 10°E in Tg N	Emission $>$ 10°E in Tg N
Biogenic	0.15	0.22
Anthropogenic	1.88	2.33
Aircraft (above PBL)	0.07	0.06
Lightning	0.09	0.2

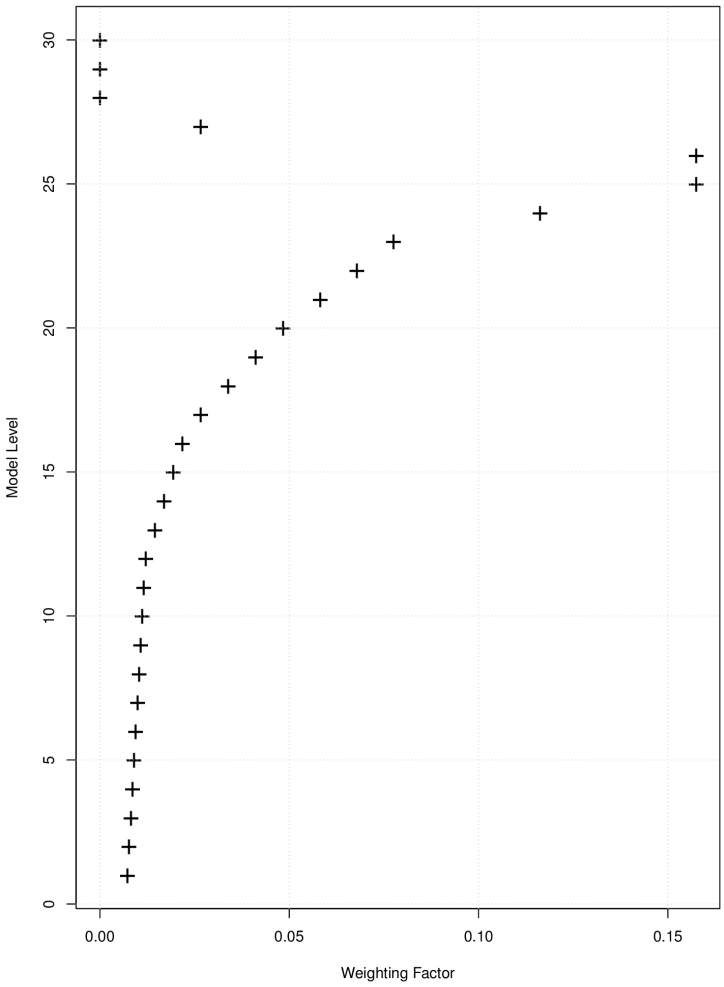

Figure 5.12: Vertical distribution of lightning emissions as mentioned in Koshak et al. (2014) and applied to the CMAQ model levels used in this study.

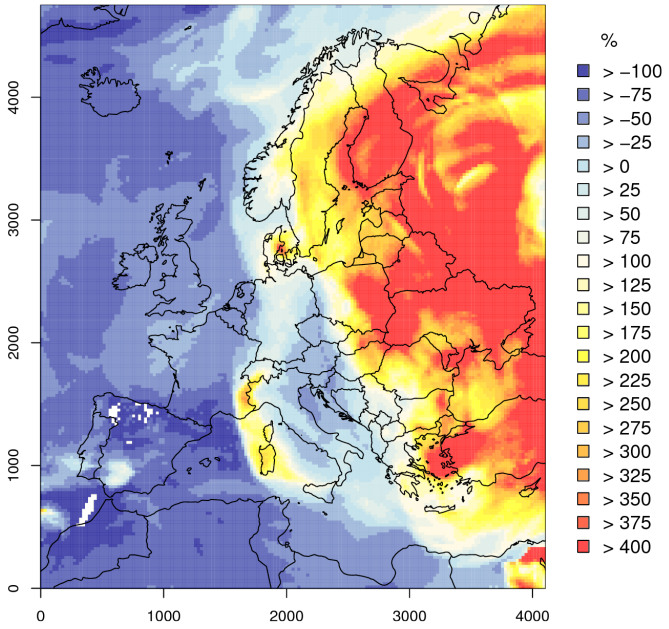

Figure 5.13: Share of contributions of lightning-caused oxidized nitrogen concentrations and aviation-caused oxidized nitrogen concentrations. Negative values indicate that the aviation contribution is higher, positive values indicate that the lightning contribution is higher.

Column values as derived by the OMI satellite instrument

The OMI data provides both column NO_2 data and the averaging kernel. The averaging kernel describes the height-dependent sensitivity of the satellite to the NO_2 concentration. With this information, the model data can be recalculated as the concentration that would have been seen by the satellite if the model atmosphere had been the real atmosphere. The averaging kernel was applied to the corresponding daylight overpasses of the satellite in July of 2010. The mean column NO_2 density for July was calculated for each case (Fig 5.14), and a field of uncertainties was also calculated (Fig. 5.15). The total amount of nitrogen dioxide in the columns deviate. The model columns show higher column densities than the observation column of the OMI.

The impact of the lightning emissions was high over the Black Sea, where the model cases with lightning emission agreed better with the observations than did the reference calculation without lightning. In this area, the relative differences are higher than the uncertainty of the observations. The differences between the different cases of parameterizations are small and all lie within the uncertainty of the observations. While the new parameterization matched the patterns over the Black Sea best, it overestimated the NO_2 column density over Eastern Europe. An interesting phenomenon might have been caused by the a priori information of the satellite data, which was provided by the GEOS-CHEM model. It used the CTH parameterization, which showed a comparably low column density in a very distinct way with a comparable pattern in the CTH case of this study over Romania and the OMI observation.

The satellite showed differences in the extent of the NO_2 fields between the model cases and the observations. The calculated column densities were broader and overestimated the NO_2 concentration in the areas outside the main pollution areas. The overestimation of column densities, as described in the previous paragraph, in conjunction with broader column densities of NO_2 around the high emission areas might indicate lowered depletion of NO_2 and an increased lifetime in the model. Another option is an overestimation of nitrogen emission in the SMOKE-EU emission model, which may lead to higher concentrations in the model area.

Compared to the satellite column densities, the emission dataset used in this study missed sources. There were hot spots of NO_2 concentrations along the northern coast of Africa that were observed by the satellite but not represented in the calculated concentration field or in the emissions used in this study. Furthermore, there are higher concentrations around Iceland and Greenland that were not present in the satellite measurements. The northern Baltic Sea showed smaller emissions from shipping than were observed in the satellite observations.

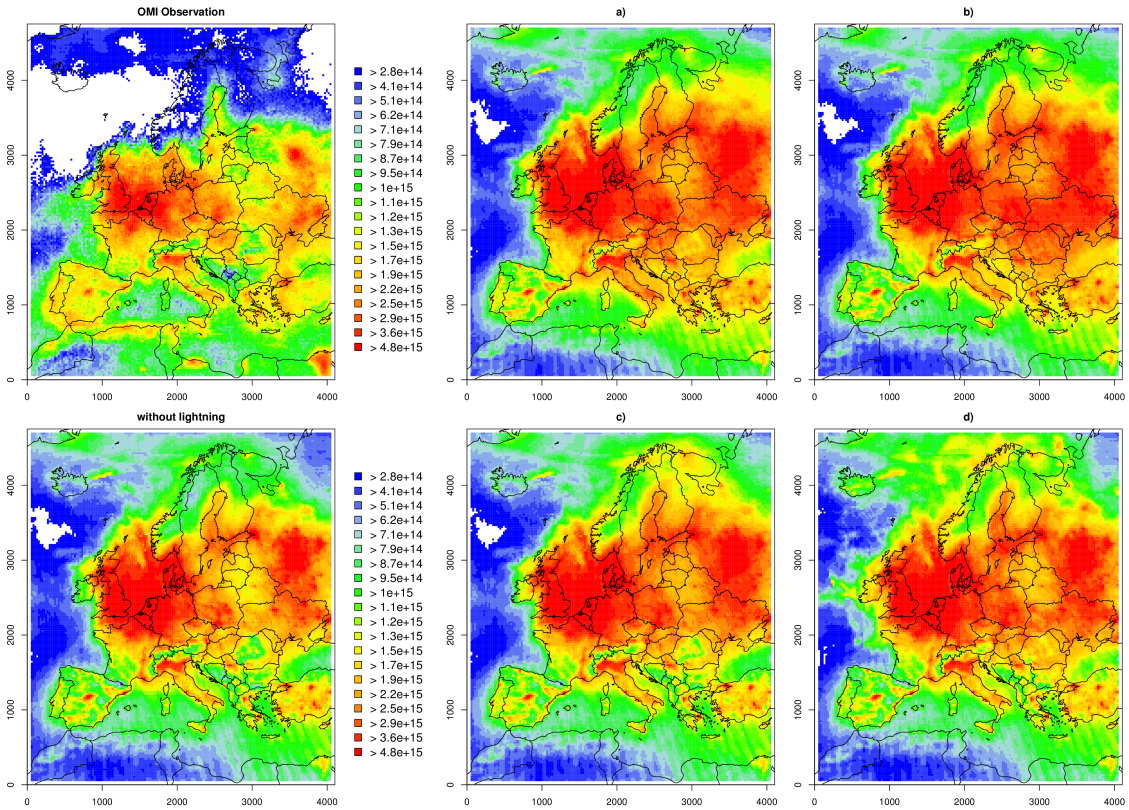

Figure 5.14: Vertical NO_2 column densities in molecules per square centimeter as seen from the OMI satellite. a) SAT, b) NEW, c) CTH and d) OLD parameterization. The model cases are calculated with the corresponding averaging kernels of the satellite overpasses per pixel in order to make them comparable. The OMI observation color scale is different from the model scales. All model cases use the color scale displayed with the „without lightning “ case. The OMI data has a priori information form GEOS-Chem, which incorporates a version of the CTH parameterization. Timespan of analysis is one month of July 2010.

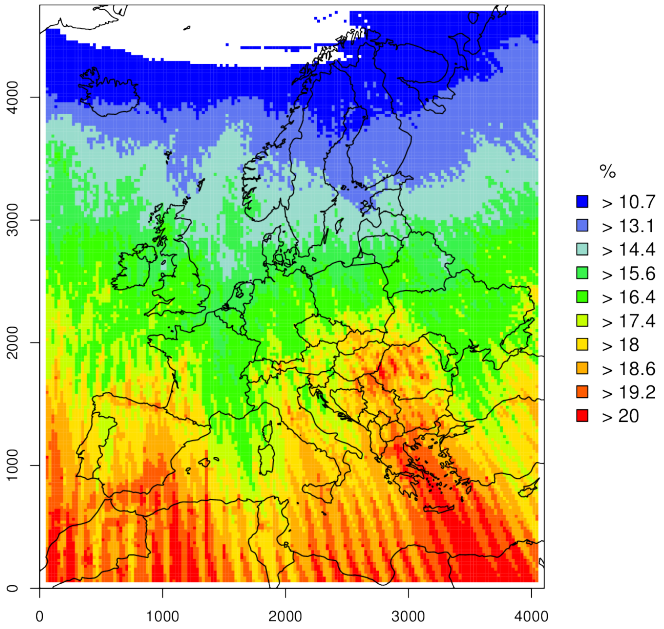

Figure 5.15: Uncertainty caused by random error in the OMI data in percent for every pixel for Figure 5.14.

5.5 Conclusion

This study investigates the impact of lightning nitrogen monoxide emissions on the European nitrogen budget. For reasons of better representativity, an adaptation of satellite climatologies of lightning to the particular model year is performed with a linear model of lightning dependent on convective rain. While the model itself is already implemented in the CMAQ model system, the ability to fit the linear model with globally and freely available satellite data instead of VHF network data is a sizable advantage for the modeling community. The described fit between lightning data from TRMM and rain data can be used as a globally applicable parameterization for lightning emissions in chemistry transport models. It is reliable enough to reproduce the TRMM satellite climatologies with special attention to the meteorological variation in the simulation year.

It was shown that lightning is an important natural source for reactive nitrogen in the European domain, especially in southern and eastern Europe. The estimated emissions from the TRMM lightning climatology were approximately 295 Gg N annually for Europe. For the model year, the emissions were 278 Gg N. This is approximately 6% of the total emissions of oxidized reactive nitrogen in Europe.

While these emissions had only a small impact on the near-ground concentrations in central and northern Europe, in southern Europe and in higher layers of the troposphere, the impact was considerably higher. Over broad areas of the eastern part of the model domain, the impact of lightning was more than 6 times higher than the impact of aircraft emissions on the nitrogen budget in the atmosphere.
The comparison with OMI satellite observations of NO_2 columns showed that the model overestimated NO_2 and that the emission dataset in this study included less emission sources than the satellite can show. Furthermore, it was shown that lightning has an observable impact on the column density over Europe.
A considerable uncertainty arises from the lack of knowledge of the best representing emission factor per flash. The value of 500 moles NO per flash that was assumed here is on the upper end of reliable estimates. An estimate with 320 moles NO per flash is in better agreement with the global estimate and leads to a 4% share of the total emissions in Europe.
In summary, the use of lightning data in chemistry transport simulations improves models of the rural areas of Europe, in southern Europe and in close proximity to and over larger water bodies, especially in southern Europe, because lightning influences the chemistry in these regions.

6 Natural nitrogen under largely reduced anthropogenic emissions

Natural oxidized reactive nitrogen air concentrations under largely reduced anthropogenic emissions in Europe

Jan A. Arndt, Armin Aulinger and Volker Matthias

Submitted as a conference presentation and abstract for the 37th International Technical Meeting on Air Pollution Modelling and its Application 2019 Conference in Hamburg, Germany. It is also planned to be published in a peer-reviewed journal in 2019.

Abstract

In populated areas, natural emissions sources of reactive oxidized nitrogen are of lower magnitude than anthropogenic emissions. Globally, the emissions from soil, fires and lightning have a share of 12-15% each. Anthropogenic emissions are supposed to decrease in the coming decades in Europe. Assuming that such emissions are decreased, the share of natural emissions will become more important in the coming decades. This study investigates the effect of decreasing anthropogenic emissions on the share and behavior of natural reactive oxidized nitrogen emissions and the resulting concentrations under these conditions.

Two years were considered, 2010 and 2040, featuring the anthropogenic emissions reduction of the IIASA ECLIPSE MTFR scenario. Natural emissions remain unchanged. In this case study, natural emissions will become as relevant as being responsible for up to 50% of the central and eastern European air concentrations of reactive nitrogen under the possible future of the MTFR scenario. These emissions alter the chemical composition of the atmosphere by an increasing share of organic nitrogen compounds and will contribute in a relatively larger share in the deposition processes affecting ecosystems in the future. Because it is the maximum technically feasible scenario, it shows the possible upper boundary of natural emissions contribution by today's technological achievements.

Acknowledgments
This work has been funded by the HGF through the PACES 2 project. The US EPA is gratefully acknowledged for the use of CMAQ, BEIS and SMOKE. We thank Dr. Beate Geyer for the meteorological data and Dr. Johannes Bieser for the generation of the anthropogenic emissions data. We thank the IIASA for providing the ECLIPSE scenario data for the emissions scenario.

This chapter consists of the manuscript that is planned to be submitted to a peer-reviewed scientific journal with a focus on atmospheric chemistry, as stated previously. It was written under my lead authorship for the purpose of this thesis. Major parts of the manuscript originate from me, with annotations and corrections made by Armin Aulinger and Volker Matthias. The analysis and discussion of the results were performed under the supervision of Armin Aulinger and Volker Matthias.
To avoid multiple introductions with very coherent content, the introduction of this manuscript was omitted.

6.1 Input data

6.1.1 Emissions, cases and scenarios

Anthropogenic emissions in hourly temporal resolution were produced with SMOKE-EU (Bieser et al., 2011a) for the year 2010. These emissions need to be taken into account to model and study the interactions of anthropogenic and natural nitrogen compounds correctly. Sea-, air- and land-based emissions sources in the model domain are used to create the emissions dataset. They are based on officially reported EMEP emissions, which are distributed in time and space using appropriate surrogates, such as population density, street maps or land use. Point sources were considered as long as information from the European Pollutant Release and Transfer Register (E-PRTR) register was available. The vertical distribution of the emissions was calculated online with the SMOKE model (Bieser et al., 2011b). Shipping emissions for the Baltic Sea and North Sea with high spatial and temporal resolutions for this study were obtained from the Ship Traffic Emission Assessment Model (STEAM) (Jalkanen et al., 2009, 2012; Johansson et al., 2013, 2017).

Natural emissions were created with methods specific for each type of emissions. Biogenic emissions were calculated with the meteorological data and the BEIS (Biogenic Emission Inventory System) model system. Biogenic emissions include nitrogen monoxide and VOCs such as isoprene and terpene. Canopy reduction of nitrogen monoxide was calculated with the approach of Wang et al. (1998) incorporated in BEIS as described in Arndt et al. (2018). The vegetation fire data were used from the FINN emission dataset for each day (Wiedinmyer et al., 2011). It was gridded and uniformly hourly distributed over the model day to the model grid. Vegetation fires emit nitrogen monoxide, nitrogen dioxide, ammonia and particles. The vertical distribution is uniform through the lower troposphere up to 200 m. Lightning emission data were added with the method described in Arndt et al. (2019) based on the LIS/OTD lightning climatologies.

For the purpose of this study, each emissions source was treated as a separate case. The cases are listed in table 6.1.

Table 6.1: Listing of emissions sources (rows) and denotation of cases (columns). Crosses indicate which emissions are considered in the respective cases.

	ant	biog	fire	lno
anthropogenic emissions	X	X	X	X
biogenic emissions		X	X	X
canopy reduction		X	X	X
wildfire emissions			X	X
lightning emissions				X

6.1.2 Base Emission 2010

The base case is an emissions dataset for the year 2010.The emissions model data for 2010 were used in the study of Solazzo et al. (2017), and the model performance with this dataset was tested, revealing that the model performed well. The emissions of 2010 were chosen because they have the most reliable background by highest primary inventory availability in this year.

Reactive oxidized nitrogen is emitted mainly by anthropogenic processes. Including all processes, the share of natural emissions on the total emissions of reactive oxidized nitrogen is approximately 10% for Europe. Total emissions are 7.2 Tg N, with 6.5 Tg N coming from anthropogenic sources (Fig. 6.1 a)). Emissions from soil have the greatest share to the total natural nitrogen oxide emissions, with 0.37 Tg N (5.3%), followed by lightning, with 0.3 Tg N (4.4%). Wildfires are of minor relevance, with 0.02 Tg (0.3%) for the total budget of reactive oxidized nitrogen, but they might be essential for limited time and region budget and air quality calculations. Canopy reduction reduces the amount of NO_y emitted by soil significantly from 0.43 Tg N to 0.37 Tg N (reduction of 14%). The natural emissions are shown in Figure 6.2.

Reduced nitrogen emissions are 5.8 Tg N in total (Fig. 6.1 b)). Livestock and manure are responsible for the majority of these emissions, while wildfires, industries and traffic are only responsible for a share of approximately 10%. Total emissions of reactive nitrogen are 13 Tg N.

6.1.3 2040 scenario data

For the effect of emissions reduction, a scenario was defined. The reduction fraction for 2040 is calculated based on countrywise emissions for 2010 and 2040 of the MTFR (maximum technically feasible reduction) for SO_X, NO_X, NH_3, VOC and

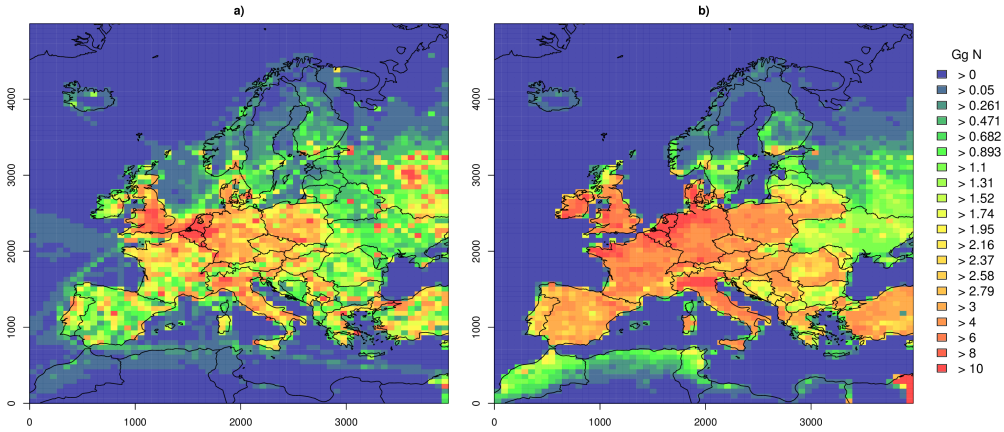

Figure 6.1: Total emissions of a) nitrogen oxides and b) ammonia for the model year used in this study. The unit is emission of NO_y in Gg N per grid cell and year.

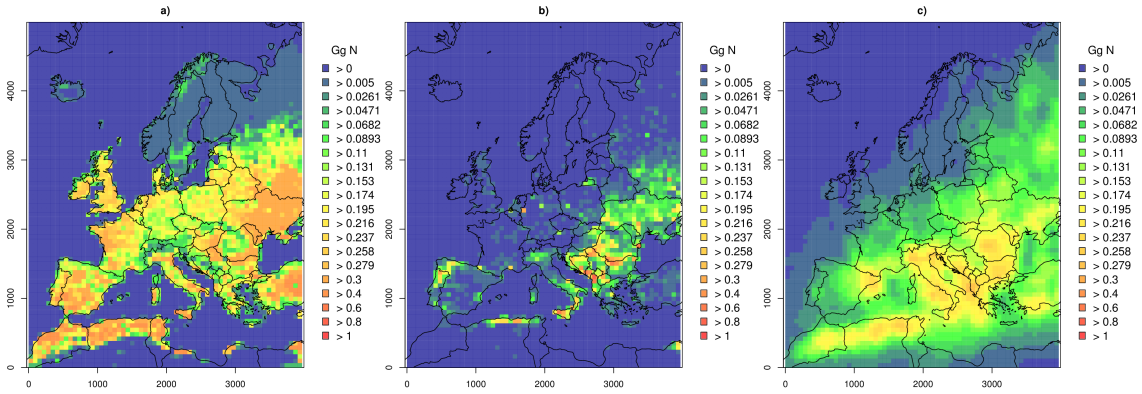

Figure 6.2: Total emissions of a) soil NO, b) wildfire NO_x and c) lightning NO emissions for the model year used in this study. The unit is emission of NO_y in Gg N per grid cell and year.

$PM_{2.5}$ from the IIASA ECLIPSE V5a Emission Inventory (see Table 6.2). Gridded 2010 emissions were scaled with the fractions to calculate 2040 gridded emissions (Fig. 6.3). Grid cells with contributions of two countries were treated with the average reduction of both countries.

Shipping emissions reduction is based on the scenarios „EEDI 2040“ described in Karl et al. (2018). For the purpose of this study, meteorology and natural emissions are considered to be unchanged.

Table 6.2: Emissions reduction of North Sea and Baltic Sea riparian states for 2040 emissions as fractions of 2010 emissions as taken from the IIASA ECLIPSE V5a MTFR scenario. Full table is provided in the appendix as table A.4.

Land	SO_X	NO_X	NH_3	VOC	$PM_{2.5}$
Belarus	0.93	0.95	0.20	0.46	0.74
Belgium	0.72	0.45	0.17	0.60	0.40
Denmark	0.49	0.35	0.17	0.32	0.19
Estonia	0.25	0.43	0.18	0.40	0.23
Finland	0.37	0.37	0.20	0.24	0.28
France	0.44	0.32	0.18	0.43	0.27
Germany	0.32	0.35	0.17	0.47	0.31
Latvia	0.89	0.46	0.25	0.31	0.29
Lithuania	0.50	0.34	0.15	0.38	0.27
Netherlands	0.60	0.38	0.16	0.49	0.52
Norway	1.29	0.77	0.32	0.45	0.48
Poland	0.29	0.33	0.18	0.42	0.55
Russian Federation	1.26	0.74	0.16	0.49	0.50
Sweden	0.71	0.32	0.19	0.54	0.55
Shipping Emissions	0.12	0.29	0.85	0.92	0.49
United Kingdom	0.19	0.29	0.20	0.51	0.39
Area-weighted average	0.42	0.42	0.52	0.68	0.47

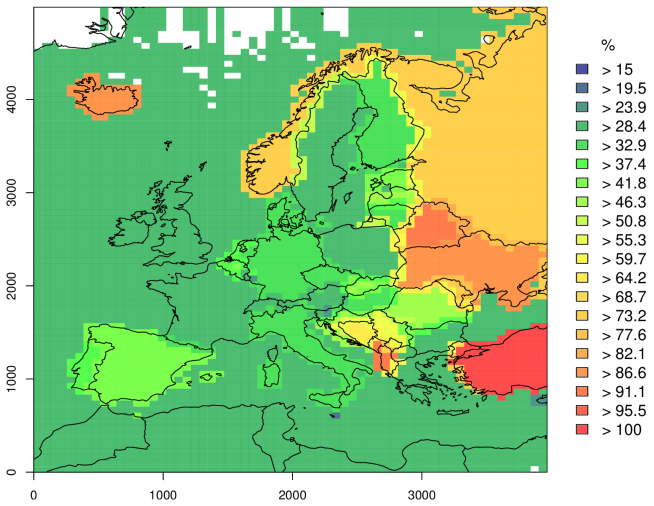

Figure 6.3: Emissions reduction ratio between 2010 and 2040 following the IIASA ECLIPSE V5a MTFR scenario. This figure only shows the fraction belonging to nitrogen oxides.

6.1.4 Meteorology Data from COSMO-CLM

The meteorological fields were simulated with the COSMO-CLM (Rockel et al., 2008) mesoscale meteorological model (version 5.0) for the year 2012 using ERA-Interim forcing data (Dee et al., 2011). COSMO-CLM is the climate version of the numerical weather prediction model COSMO (Schaettler et al., 2008), originally developed by Deutscher Wetterdienst (DWD) Steppeler et al. (2003); Schaettler et al. (2008). It was run on a 0.11° x 0.11° grid using 40 vertical layers up to 20 hPa for all of Europe. COSMO-CLM uses the TERRA-ML land surface model (Schrodin and Heise, 2001), a TKE turbulence closure scheme (Doms and Schättler, 2002; Doms et al., 2011), the Tiedtke scheme (Tiedtke, 1989) for cumulus clouds and a radiation transfer scheme following Ritter and Geleyn (1992). The meteorological fields were regridded to match the CMAQ grid with an adapted version of the Model-3 MCIP preprocessor. This study features the meteorology of 2012. The meteorological data are used and evaluated by the studies of Arndt et al. (2018) and Karl et al. (2019) and are based on Geyer (2014). These data were chosen rather than the emissions of the corresponding year 2010 because 2012 has a stronger winter and a hotter and dryer summer than 2010. This opens the span of the circulation and deposition in the context of climate change and made it a good reference year.

6.1.5 Chemistry transport modeling

The CMAQ model (Byun and Ching, 1999; Byun and Schere, 2006) version 5.0.1 was used (US EPA Office of Research and Development, 2012) with the CB05 photochemical mechanism (CB05tucl) (Kelly et al., 2010) and the AE6 aerosol mechanism. The model was run for the meteorology of 2012 with a spin-up time of 2 weeks in 2011 to avoid the influence of initial conditions on the modeled atmospheric concentrations. The model was setup on a grid with a grid cell size of 64 x 64 km^2 for all of Europe. Although the grid cell size is relatively coarse, it is sufficient for this study and computationally efficient. The emissions reduction scenario is an approximation of a future that might occur. Therefore, a spatially more detailed computation would suggest a higher detail of the model results than is consistent with the emissions scenario.
Chemical boundary conditions for the outer model domain were taken from the HTAP BASE dataset as described in Im et al. (2018). The vertical model extent

contains 30 layers up to 100 hPa. Twenty of these layers are below approximately 2000 m, with the lowest layer extending to approximately 36 m above ground.

6.2 Analysis metrics

Three different metrics describe the impact of natural emissions and the impact change with time under the MTFR emissions scenario. They first both analyze the year 2010

$$a = \frac{\overline{C_{case}} - \overline{C_{ant}}}{\overline{C_{case}}} \tag{6.1}$$

Eq. 6.1 defines the ratio where the natural emissions concentration increases the total concentration over the anthropogenic signal. The variables used are the spatially averaged variables over the entire model domain.

$$b = \frac{C_{lno} - C_{ant}}{C_{lno}} \times 100\% \tag{6.2}$$

Eq. 6.2 refers to the contribution of all natural emissions to the resulting concentrations of total emissions.

To represent the change in the natural emissions contribution share to the concentration in the future, the total difference of the share is calculated in Eq. 6.3. It shows the direct impact of the anthropogenic emissions reduction on the natural emissions contribution share.

$$c = \frac{C_{lno2040} - C_{ant2040}}{C_{lno2040}} \times 100\% - \frac{C_{lno2010} - C_{ant2010}}{C_{lno2010}} \times 100\% \tag{6.3}$$

The synopsis of both sources of information enables observing whether the amplitude of relative changes relate to small or large total changes.

6.3 Results and Discussion

6.3.1 Base case 2010 characteristics

Natural emissions are the highest in summer and lowest in winter, as shown in Fig. 6.4 a). This result was expected due to the lower temperatures in winter, which lead to reduced microbial activity and therefore lower nitrogen emissions from the

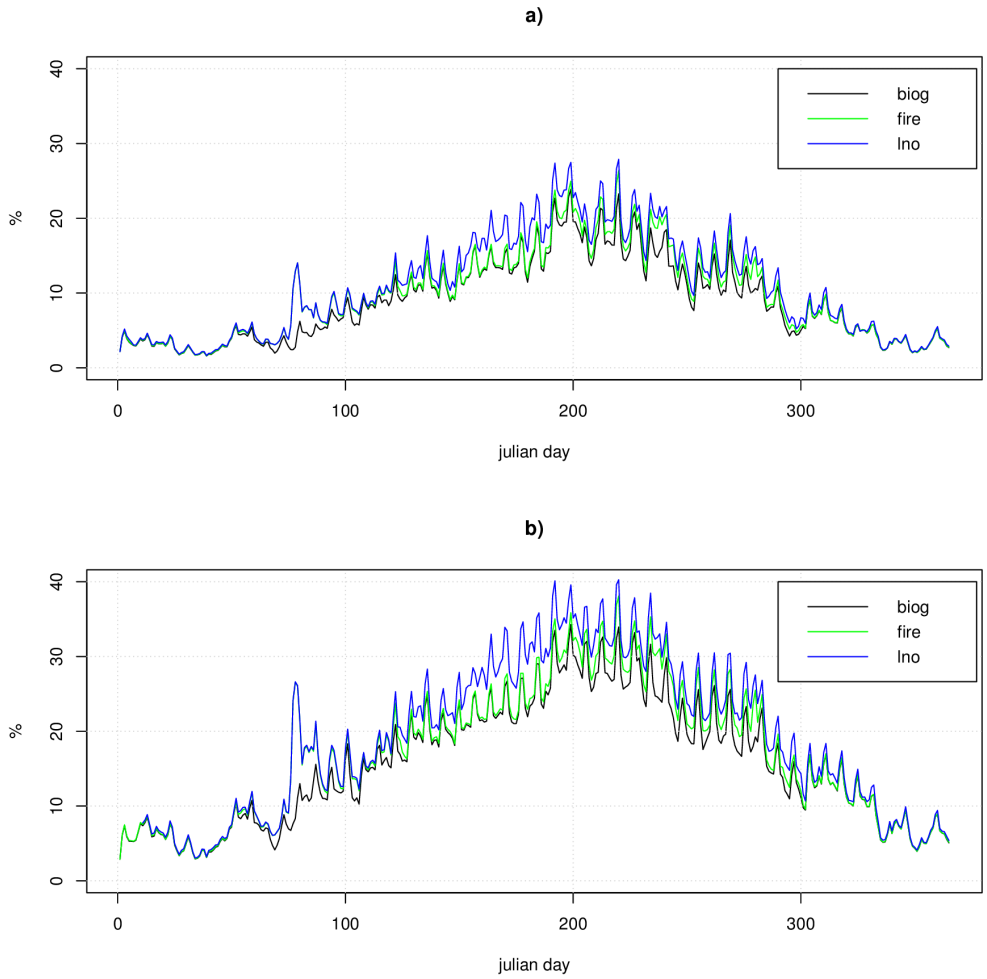

Figure 6.4: Share of natural-emissions-caused concentrations to the daily grid average concentration of oxidized nitrogen. a) For the base case, b) for the scenario case. Graphics are calculated with Eq. 6.1.

soil and lower convective activity of the atmosphere. Three cases are shown in Fig. 6.4 with respect to the model configurations described in Table 6.1. All of the cases are between 0 and 20% higher than the anthropogenic emissions alone. This result is consistent with the definition of the cases where every case contains a higher level of nitrogen emissions because the natural sources were added case by case.Although the case with the lowest share is that with biogenic emissions and canopy reduction, the one with the highest portion is that containing lightning emissions. It is approximately twice as high as the case without lightning. Vegetation fires contribute to a small percentage in the early summer but to a larger extent in the late summer.

Although vegetation fires do not occur noticeably in the winter months, there is a peak around Julian day 100. This is a fire event in southwest Europe leading to significant vegetation fire emissions. The higher percentage in the late summer is a result of the Russian 2010 forest fires. Wildfires in 2010 are lower in Europe than in the years before, but in conjunction with the wildfires in Russia in 2010 in total on the yearly average of the European domain. (San-Miguel-Ayanz et al., 2017). Stronger single fire events are also likely in the future (San-Miguel-Ayanz et al., 2017; Turco et al., 2018).

In winter (Fig. 6.5), the concentration share of natural emissions over northern and central Europe is low, and exceeding 5% share is limited to some areas in southern Europe. This result is expected because microbial activity is mainly driven by soil temperature and lightning activity by convective cloud formation. Those areas with a higher share are those with higher temperatures even during winter and are consistent with the expectations.
In summer (Fig. 6.6), the concentration share of natural nitrogen is high throughout the entire modeling domain, with minor shares over northwest central Europe and the waterbodies of the North and Baltic Seas. The portion is almost everywhere higher than 15%. This result is related to the higher temperatures in summer. For southern and eastern Europe, the formation of thunderstorms is associated with typical Mediterranean air masses with higher water vapor content leading to more and intense thunderstorms. This leads to a contribution higher than 20% in these areas.
Two unexpected effects could be observed, one of them in both winter and summer. The first effect is a higher concentration share around Iceland and the north Atlantic ocean off the coast of Norway. The higher emissions share here is a result of thunderstorms leading to lightning emissions and higher concentrations in otherwise clean maritime air. These thunderstorms are caused by relatively warm sea surface temperatures and forced convection by the orography of Iceland and western Norway. The other effect is a very high concentration share throughout the whole year in northern Africa. It is caused by strong emissions from soil and the absence of anthropogenic emissions.

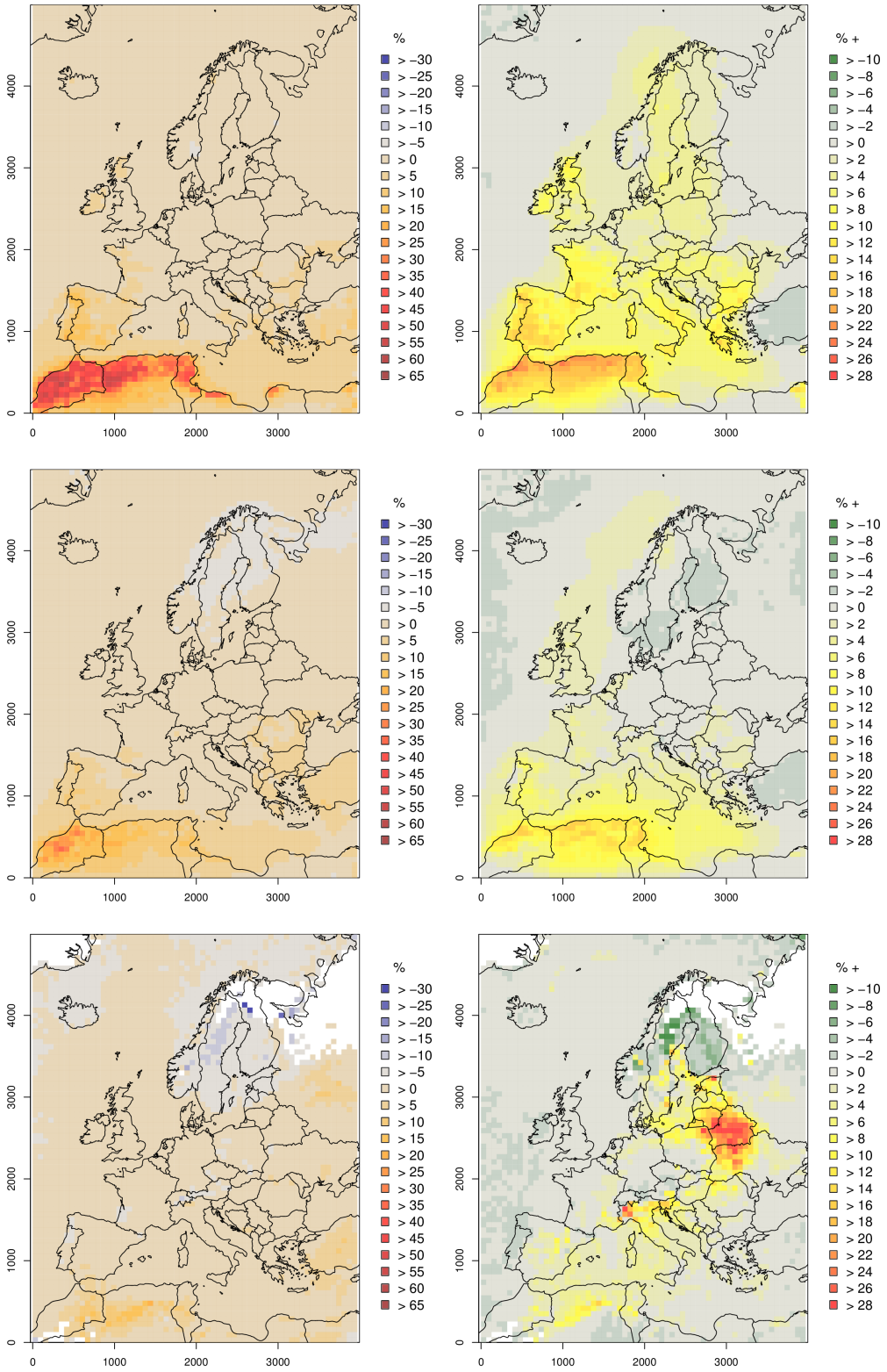

Figure 6.5: Spatial analysis of natural-emissions-caused concentrations to the seasonal average concentration for winter period. Top graphics refer to concentration, middle row refers to dry deposition, and the bottom row refers to wet deposition. Left graphics show the 2010 contribution after Eq. 6.2, and right shows the 2040 change following Eq. 6.3.

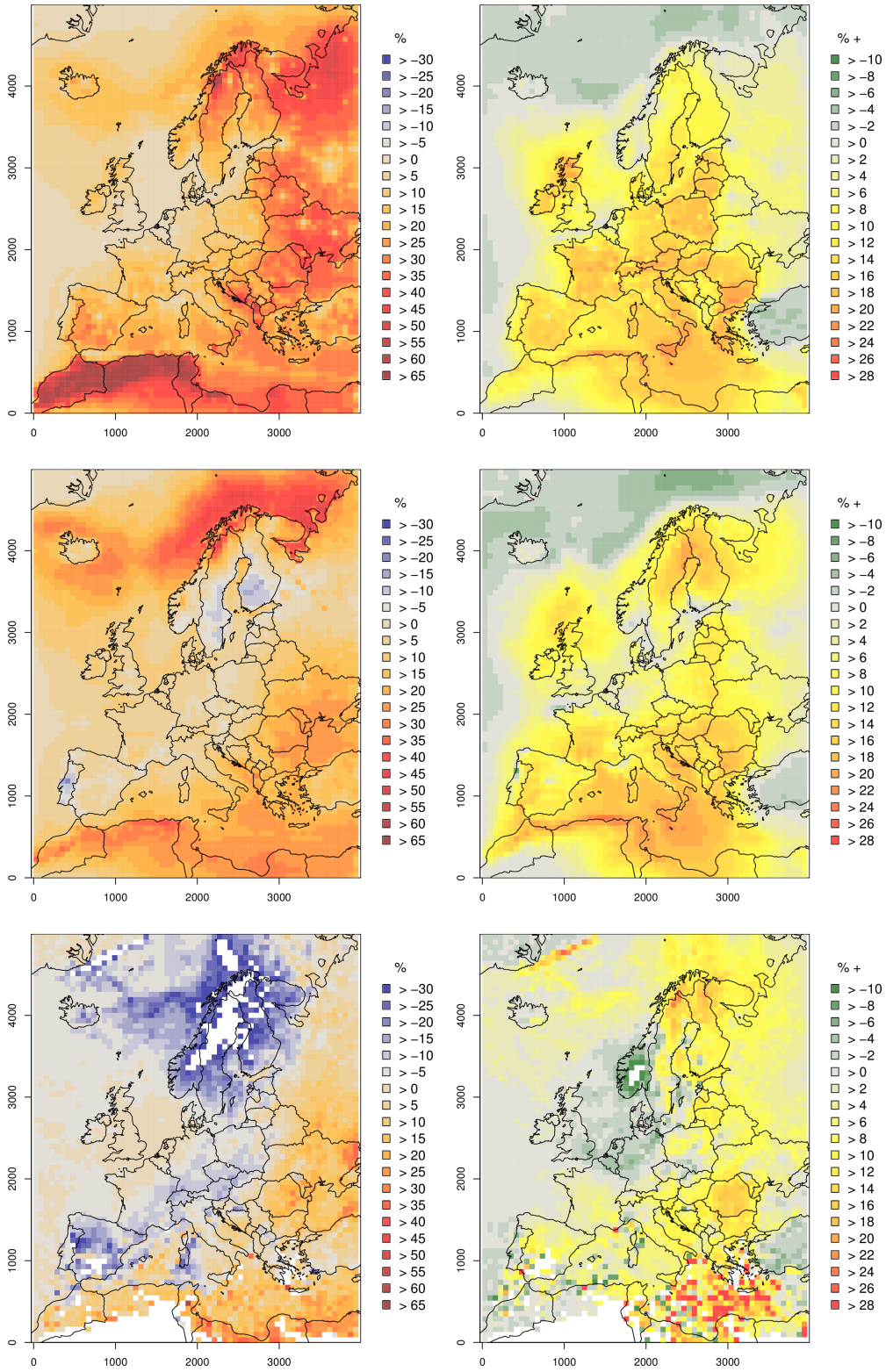

Figure 6.6: Spatial analysis of natural-emissions-caused concentrations to the seasonal average concentration for summer period. Top graphics refer to concentration, middle row refers to dry deposition, and the bottom row refers to wet deposition. Left graphics show the 2010 contribution after Eq. 6.2, and right shows the 2040 change following Eq. 6.3.

The aerosol concentration consisting of oxidized nitrate and reduced ammonia (Fig. 6.7) share shows that the concentration of particulate ammonium nitrate is reduced over most parts of central and northern Europe. The precisely located more positive share of nitrate aerosols in southeastern Europe and at the west coast of Europe is caused by the emission of NH_3 from vegetation fires. To understand why the particle concentration is reduced, it is important to mention the influence of biogenic VOCs. The **biog** case includes, in addition to nitrogen monoxide emissions, isoprene and terpene emissions. Those emissions change the impact of biogenic emissions significantly and form organic nitrates (denoted as PAN, PNAx, PNA and NTR) that are reservoir molecules for the oxidized nitrogen cycle. On average, the biogenic emission of VOCs lowers the concentration share of nitrogen monoxide and dioxide to the total oxidized nitrogen mass while increasing the share of organic nitrates (Fig. 6.8 a)). The shift into the reservoir species lowers the formation of particulate nitrate, which decreases the particulate ammonium nitrate concentration share. Nitrogen monoxide and VOCs react with ozone and reduce its concentration. This also leads to a smaller share of ozone caused by natural emissions (see Fig. 6.9).

Dry deposition is increased over the model domain belonging to higher concentrations of oxidized nitrogen. Its share is noticeably increased in areas with an increased concentration share to natural sources and in good agreement with the expectations. Deposition to the land surface by natural emissions is 134 Gg N, to the open sea surfaces is 34 Gg N, and to the direct coastal grid cells of the model domain is 39 Gg N. These are 8%, 5% and 5% of the total deposition to the respective areas. The negative deposition share is related to the concentration reduction of particulate nitrate.
The wet deposition share is negative over large parts of the northern model domain, while it is positive over the southern and eastern parts of the model domain. Deposition to the land surface by natural emissions is 15 Gg N and to the open sea surfaces is 5 Gg N. The coastal grid cells receive less deposition by natural emissions of approximately -0.6 Gg N. These are 3%, 1% and less than -0.2% of the total deposition to the respective areas. Because dry and wet deposition affect different categories of substances more efficiently, the wet deposition change indicates a lower concentration of particulate nitrogen in the air.This result is in good agreement with the findings for ammonium nitrate concentration.

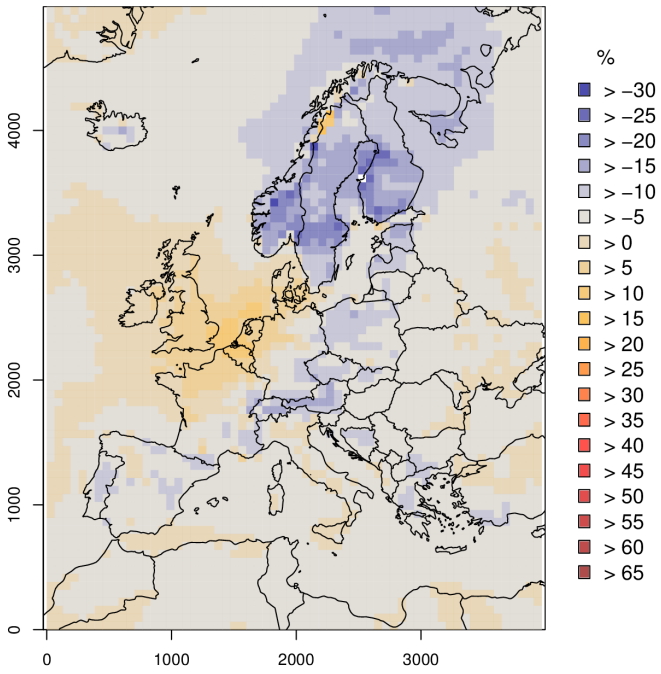

Figure 6.7: Spatial analysis of natural-emissions-caused concentrations of ammonium nitrate particles. Displayed is the share calculated with 6.2 for the summer period of the 2010 base case.

6.3.2 Scenario

Fig. 6.4 b) for the MTFR scenario basically shows an upscaling of the natural-emissions-induced concentration, as observed in 6.4 a), by a factor of 2. The observed relevance of processes for 2040 is comparable to 2010. This result is in general agreement with the design of the experiment of the scenario where the anthropogenic emissions are reduced and the natural emissions remain unchanged.
In summer (Fig. 6.6), the influence of natural emissions is enhanced over most parts of Europe by 10-20%. The central model domain is affected by an approximately 10-15% concentration change with the exception of the North Sea. Over eastern Europe, the concentration is enhanced by up to 20% by natural emissions. Relatively, the highest concentration change belongs to the North Sea. The relative impact change in conjunction with the low total change is a sign that very low concentrations caused by natural emissions are empowered in their relevance by greatly reducing the anthropogenic emissions here. The opposite effect indicated that these areas are already substantially influenced by natural emissions with a higher share

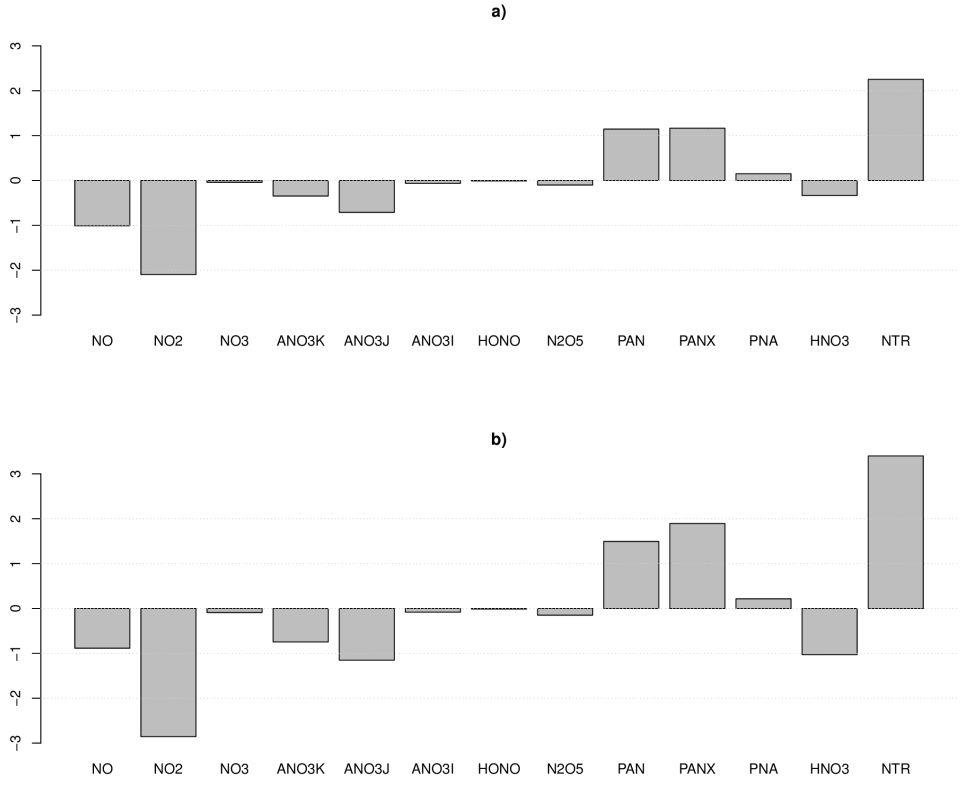

Figure 6.8: Concentration share changes of different nitrogen species between the ant and lno cases. A higher percentage shows increasing concentration share in the lno case. a) For 2010, b) for 2040. NO is nitrogen monoxide, NO2 is nitrogen dioxide, and NO3 is the nitrate radical. ANO3 I, J and K denote the three particle modes of particulate nitrate. HONO is nitrous acid, and N2O5 is dinitrogen pentoxide. PAN and PANX are peroxyacyl nitrates. HNO3 denotes nitric acid, and NTR denotes organic nitrates.

in the future due to the reduction of anthropogenic emissions.

In the Adriatic Sea, change is comparable to the remainder of the Mediterranean Sea area, but the total change in this area is higher. This results on the one hand from the anthropogenic reduction and on the other hand from the impact of vegetation fires and lightning in this area. This is clearly visible in winter (Fig. 6.5). When convective activity is low, the impact in central Europe is as high as in summer, but in the coastal areas of the Mediterranean and Adriatic Seas, which are more dependent on lightning emissions, the concentration impact change between

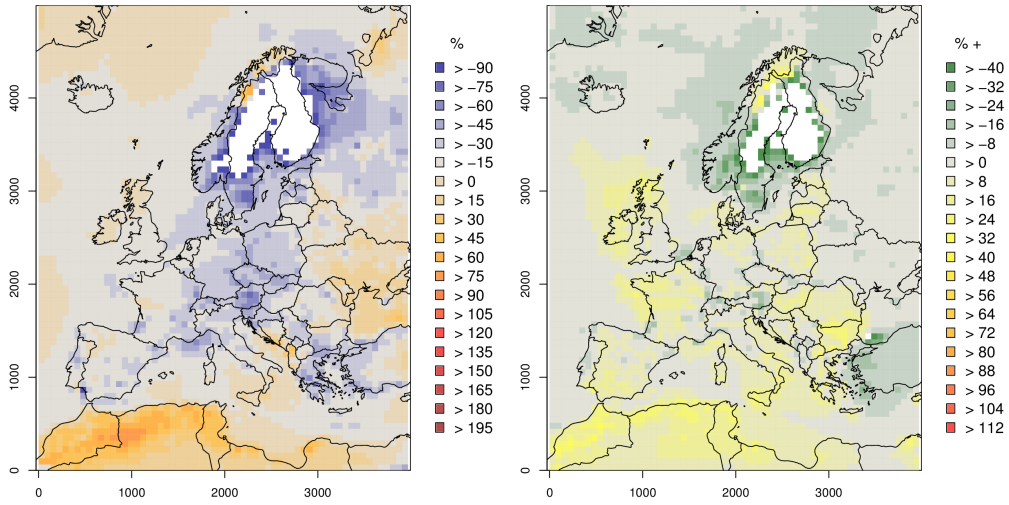

Figure 6.9: Ozone background concentration share by natural emissions in summer. Left graphics after Eq. 6.2, and right after Eq. 6.3.

the base case and the scenario case is less than in summer. Very little change can be observed in Turkey and around Moscow. Over Turkey, this is related to a very small emissions reduction. Over Moscow, anthropogenic emissions are so high and natural emissions are so low that a reduction of approximately 10% does not lead to a higher share of natural emissions. Emissions here are approximately 10 Gg N per grid cell. Comparable magnitudes of emissions in 2010, but approximately 10% more reduction to 2040, could be observed in the Netherlands. Because of the higher reduction factor, natural emissions gain importance in the Netherlands by approximately 2-5%, while natural emissions over Moscow gain only approximately 1%.

The species composition in Fig. 6.8 b) for 2040 resembles the composition in Fig. 6.8 a) for 2010. In detail, NO_2 and HNO_3 have a lower share, while the organic nitrogen species (PAN, PNA and NTR) have a higher share than 2010. This indicates a composition change toward more reservoir molecules and organic nitrogen compounds than inorganic, fast reactive oxidized nitrogen species.

The dry deposition reacts to the emissions change with intensification in most areas, relating to the pattern and strength of the concentration share change, both in summer and winter. The highest relative change is over the British Islands, and the highest absolute change is over southern Italy and the central Mediterranean Sea. The southern Baltic Sea and the corresponding riparian coastal areas are excluded

from this and remain with the same share as in 2010 by approximately +5% onshore to -5% offshore. This result indicates that there is no change of sign in the nitrate deposition behavior in 2040 evident in these areas. Dry deposition over land, sea and the coastal grid cells referring to natural emissions is very similar to the base case, with 136 Gg N, 33 Gg N and 41 Gg N, respectively. Relatively, the share is enhanced for land grid cells to 13%, sea cells to 9 % and coastal grid cells to 10% relative contribution of natural emissions to dry deposition.

Although an intensification in the wet deposition could also be observed, a negative contribution could be observed over central Europe. This is explainable with an increase in NH_x concentration in this area, which increases the particle-related wet deposition of NO_3. In those areas with negative change, less particles are available due to the additional emission of reactive oxidized nitrogen and VOCs from natural sources and even less in the future by less anthropogenic emissions. The winter dry deposition change related to the natural emissions under the scenario conditions is low, while the wet deposition change is approximately an additional 20%. This is especially observable in the region of the Baltic States. Wet deposition is less directly related to natural nitrogen oxide changes than dry deposition is. The total contribution of natural emissions in 2040 for the wet deposition for land grid cells is 20 Gg N, 9 Gg N for sea grid cells and 4 Gg N for coastal grid cells. The share of natural emissions contribution to wet deposition is significantly enhanced in contrast to 2010. The share is now 7% for land grid cells, 2% for sea cells and 2% for coastal grid cells.

The IIASA ECLIPSE MTFR scenario shows the maximum technically feasible emissions reduction future. Despite the large uncertainties, this simulation shows the upper boundary of natural emissions contribution by today's technological achievements for the years 2010 to 2040.

Whereas the method allows observing the emissions reduction effect very clearly, the effects of changing climate and changing meteorological conditions in 2040 are neglected. Although this is an uncertain approximation, it is necessary to measure only the anthropogenic emissions reduction impact and is sufficient for the purpose of this study. Thus, the natural emissions were considered as unchanged.
Furthermore, studies (Schefczyk and Heinemann, 2017; Lehmann et al., 2014; Riahi et al., 2007) indicate that thunderstorm activity for Europe is likely to decrease,

while warming will increase. On the one hand, these effects may be equal in magnitude regarding the natural emissions intensity and leave the natural emissions unchanged; on the other hand, changes are projected to be small for central Europe until 2100, so the effects until 2040 are supposed to be small enough to be neglected in this particular study.

As it was the aim of this study to obtain the first insights into the contribution change of natural emissions, it was decided to use only one year in the current emissions and one in the future emissions environment. This allows obtaining fast and computationally efficient results for the different cases but limits the representativity for other years. The results must be interpreted in this context as an insight, which provides the direction in which the contribution will move in the future.

6.4 Conclusion

The study investigates the future impact of natural emissions of reactive-nitrogen-related species by soil and vegetation, wildfires and lightning under changing anthropogenic emissions conditions. A base year of 2010 with an emissions dataset of 2010 with meteorology for 2012 was used as a reference. We created an anthropogenic emissions dataset for a future with the highest emissions reduction efforts based on the IIASA ECLIPSE V5a MTFR scenario. Because the scenario shows a large reduction in anthropogenic emissions, it shows the upper boundary of natural emissions contribution by today's technological achievements.

Natural emissions and their resulting air concentration and deposition contribution will be relatively more important in the future compared to now in the highly industrialized region of Europe. In general, it will be more important in those areas where anthropogenic emissions will be largely reduced. Even if the average concentration response is as expected, nonlinearities occur in certain regions that were not expected before and gain the understanding of natural emission interactions. This is particularly interesting in the chemical transformation context and the different deposition behaviors of particles and gases. Natural emissions of nitrogen and VOCs change the composition of species in the atmosphere toward more organic nitrogen compounds. In the future, this effect will be stronger. The formation and change of species lead to altered deposition characteristics. Regions will be less affected

by the deposition of oxidized nitrogen because more natural emissions occur than without them. Some regions will gain and some will lose nitrogen input in the future by natural emissions. Overall, the contribution and deposition of and by natural emissions in 2040 will be higher than in 2010.

An important finding for interpreting the chemistry transport model output under the scenario conditions was also determined by this study. In the interpretation of impact changes, relative and absolute changes are clearly observed in conjunction. Otherwise, the information of whether a large relative change is associated with a reasonable concentration or deposition change will be lost. The other finding regarding the technique is the use of longer time periods. Although an entire year was used, the emissions have some very year-specific patterns. To come closer to a generalized answer regarding contribution change, it would be necessary to repeat the performed calculations for several years.

Natural emissions will become as relevant as being responsible for up to 50% of the central and eastern European air concentrations of reactive nitrogen under the possible future of the MTFR scenario. They alter the chemical composition of the atmosphere by increasing the share of organic nitrogen compounds and will contribute in a relatively larger share to the deposition processes affecting ecosystems. Better representations of the spatial and temporal distributions and of the actual emission magnitude are important to meet the future needs of air pollution estimation and legislation. This enhances the need for more detailed and higher-dimensional observations even in rural areas and improved observation capabilities by satellites of fire and lightning to create a more reliable database for emission modeling by simultaneously improving model performance and detail.

7 Overarching Conclusions

7.1 Conclusion

This thesis asks how reactive oxidized nitrogen emissions from natural sources affect the air concentrations and deposition of nitrogen compounds in northern European coastal areas. Several studies regarding different sources, sinks and under the pressure of chemical composition change of the atmosphere were conducted. The research was focused on the nitrogen oxides NO and NO_2. Related oxidized species were covered by describing the interaction with nitrogen monoxide and dioxide. Ammonia was addressed regarding its role in the formation of the nitrogen aerosol ammonium nitrate.

It was determined that lightning emissions of nitrogen monoxide and soil emissions of nitrogen monoxide are the major emissions sources of oxidized nitrogen from natural processes. They are responsible for almost 10% of the total reactive oxidized nitrogen emissions in Europe. Wildfires have an impact on local air quality, but their contribution to the European budget is low, less than one percent. In addition to the loss of nitrogen through deposition, there is a loss of nitrogen to the vegetation during the primary emission from soil. Taking this into account, lightning and soil emissions are on the same order of magnitude as soil emissions, approximately 20% higher than lightning. Without the effect of canopy reduction, the emission from soil is higher (approximately 50%) than the emission from lightning.

Thus, how do natural emissions affect the air concentrations and deposition of nitrogen compounds in northern European coastal areas? Natural emissions modify the chemical composition, influence reaction pathways and change the deposition of reactive nitrogen compounds in the air. Oxidized nitrogen species are increased throughout the model domain. Those regions that are more naturally characterized by land use are clearly influenced to a greater extent than anthropogenically utilized

regions by natural emissions.

The emission of natural nitrogen oxides not only leads to higher concentrations of oxidized species on average but also to the formation of nitric acid, and in the presence of ammonia, particulate nitrate in form of the ammonium nitrate, aerosol is formed.
Particulate species differ in their physical behavior. These species are more efficiently washed out by rain. They settle less by gravity because their size makes them more vulnerable to friction forces than gas molecules. This influences the balance between the different nitrogen species and causes a reduction in reduced nitrogen air concentrations by deposition.

As it was shown, natural emissions are responsible for up to 20% of today's concentration of nitrogen oxides in the atmosphere over Europe on average. This depends on the period considered and is especially true in the summer months. Under the assumption of a maximum technically feasible reduction scenario, the contribution of natural emissions to the atmospheric concentration of nitrogen oxides will double in the period from 2010 to 2040. In this context, the influence of VOCs will lead to higher concentrations of organic nitrate reservoir molecules. This impacts aerosol formation and deposition behavior. Deposition is decreased in those regions where less aerosol is formed.

A topic not fully considered is cross-sensitivities to other species, such as ozone or sulfur, which are also important atmospheric pollutants. Ozone as a gaseous substance heavily influences the nitrogen oxide cycling in the atmosphere with different effects during day and night. The background concentration of ozone is generally decreased by the additional emission of reactive oxidized nitrogen. In regions where nitrogen air concentrations are low and VOC emissions are high, ozone is largely decreased.
Sulfur is a precursor for sulfate and therefore aerosol in the atmosphere. Ammonium bisulfate and ammonium sulfate are condensed by the gaseous precursors before ammonium nitrate will form. In the endeavor of reducing acidic rain and air pollution over the past decades, sulfur has been controlled very strictly, and its concentration has been decreased to a low level. Consequently, there is mostly an ammonia excess regime present, where enough ammonia is available for the formation of ammonium

nitrate, and cross-sensitivities to natural nitrogen emissions are of minor role.

With this in mind, the questions formulated in 1.7 can be answered as follows:

- Will vegetation act as a sink for natural reactive oxidized nitrogen emissions?

All type of leaves and needles of plants that have a curticula or stomata will act as a sink for the primary emission of natural reactive nitrogen. The freshly emitted nitrogen monoxide from soil is quickly converted into nitrogen dioxide and flows through the canopy of trees, plants and grasses. The stomata reduce the emission flux through the dissolution of NO_2. This reduces the natural emission flux by 20% on average, especially in heavily vegetated areas. In coniferous forests and big-leaf agriculturally utilized areas, the reduction is considerably more and could reach up to 50%.
As determined in this thesis, leaf area and meteorologically driven plant behavior lead for Europe to a reduction of approximately 5% of reactive oxidized nitrogen in the ambient air on average. In some areas that are strongly naturally utilized and are less anthropogenically influenced, the oxidized nitrogen concentration reduction is up to 30%.
The implementation analysis shows that emission models and chemistry transport models do need the canopy reduction parameterization to more correctly represent the air concentration of nitrogen, especially in less anthropogenically influenced regions.

- How important are natural sources of reactive nitrogen for the European atmospheric nitrogen budget?

All natural sources together account for approximately 10% of the atmospheric emissions of reactive oxidized nitrogen and cause an influence. During the summer season in particular, the concentration and deposition patterns are significantly influenced by natural reactive oxidized nitrogen emissions. Although the concentration and deposition patterns vary throughout the domain, the concentration is generally higher with natural emissions than without, and dry deposition is higher than without natural emissions but lower in those areas where wet deposition is also lower. Whereas

central Europe in summer is less influenced by 0% to 10%, eastern Europe is more influenced by 20% to 40%. Northern Africa and northern Norway and Sweden are highly influenced by natural oxidized nitrogen by up to 60%. In winter, this is considerably less, and only northern Africa is affected. Dry deposition is enhanced over broad areas of Europe relating to higher concentrations, with less deposition relating to those areas where particulate nitrogen is formed. This originates from less nitric acid formed by a greater formation of organic nitrates and is a side effect of biogenic emissions that do not only contain nitrogen but also VOCs. The largest natural oxidized nitrogen sources are nitrogen monoxide emissions with 0.37 Tg N (5.3%) from soil and with 0.3 Tg N (4.4%) from lightning. Although vegetation fires are responsible for a larger contribution of natural nitrogen emissions to the air concentrations on short time scales, they only contribute with 0.02 Tg (0.3%) to the total budget. The contribution is changing from year to year, but lightning and soil emissions calculations are based on the usual conditions around 2010. Wildfires are more unusual than the other emissions and may not be representative for 2010, but they provide a clue of the chemical contribution.
It is an important finding that depending on the source composition, reduced nitrogen acts in different manners. When only considering nitrogen from lightning, the air concentration through the whole model region is slightly reduced. Only in one case, when the nitrogen emissions by lighting exceed a certain level, is there also an increase in the reduced nitrogen. In the experiment where all biogenic emissions, including VOCs, were added, this has a significant regional impact on the behavior of the particulate species.

- What role will reactive nitrogen from natural sources play in Europe under largely reduced anthropogenic emissions?

Under the assumption that natural emissions remain unchanged while anthropogenic emissions are largely reduced, reactive oxidized nitrogen from natural sources will increase their share of the total reactive nitrogen in the atmosphere. Depending on the region and the reduction scenario, this might be as important as 20% more than actual. The total contribution change for the dry deposition is comparable to the concentration. The wet deposition portion is increased where it was positive before and decreased where it was reduced before. On average, this leads to

a contribution that doubles its share to the total reactive oxidized nitrogen share. Various cross-sensitivities to VOCs, ozone, reduced nitrogen and therefore particulate matter greatly increase the complexity of the system and make predictions and interpretations even more challenging. This underlines the need for complex nonlinear chemistry transport models for studies with this scope of investigation.
Emissions are supposed to decrease in the future, and this aim appears to be achieved. Nevertheless, the chosen scenario is the maximum technically feasible reduction scenario. The calculated gain in importance is therefore the most possible under the assumption that natural emissions do not change in total.

7.2 Outlook

Emissions modeling is continuously being improved. Natural emissions are uncertain in modeling because the database is often very thin. The modeling community needs better observations and new techniques for measuring emissions from soil, fire and lightning. This would improve emission factors and process understanding. A more reliable estimate for the nitrogen monoxide emissions of flashes and a better flux dataset under and above the canopy of different vegetation types would greatly improve the emissions and reduction calculations in this thesis.
Canopy reduction lacks the reduction of anthropogenic sources that might also be affected by absorption at the leaves. The implementation of this effect would again need a database of nitrogen oxide fluxes under and above the canopy layer. In a first step, this should be performed in areas with well-defined anthropogenic emissions. This could be a single road leading through a forest that would enable developing emission factor corrections for anthropogenic sources depending on the specific land use. A great challenge on the model side would be the differentiation of the dry deposition process from the atmosphere and the initial reduction by deposition of the primary emission. While it is pretty clear to differentiate when natural emissions are considered only affected by canopy reduction, the differentiation is far more complex if all emissions are influenced by the canopy.
The lightning emissions are calculated based on open-source climatology. Lightning data are often limited to restricted access. A comparison of the calculated flash density and flash density measurement would create a more robust statement for the reliability of the method.
This thesis gains knowledge regarding the importance of natural emissions for the

atmospheric nitrogen load in Europe. Note that the performed experiments are for selected test cases and time periods. Although it is possible to precisely answer the asked questions and comprehend the basic behavior of the species and the model, a generalization from the experiments to the general behavior of chemical substances in the atmosphere under the influence of natural nitrogen emissions is difficult. To gain more trust in the natural emissions contribution and to come closer to a generalized approach, it would be necessary to repeat the calculations made for several years.

The future emissions scenario is only one possible representation of the future. It should at be least improved by sector-specific emissions reduction. It is also recommended to vary the emissions reduction scenario and to create a variety of future realizations. The effect of climate change should be taken into account to substantially prove that climate change will not significantly change the emissions in Europe as assumed in the scenario calculation. Furthermore the effect of climate change on longer time scales and the natural emission contribution on the respective RCPs emission change should be evaluated.

Bibliography

[Ærtebjerg et al. 2001] Ærtebjerg, Gunni ; Carstensen, Jacob ; Dahl, Karsten ; Hansen, J; Nygaard, Kari ; Rygg, Brage ; Sörensen, Kai ; Severinsen, Gunnar: *Eutrophication in Europes Coastal Waters*. European Environment Agency (EEA), 2001

[Allen et al. 2012] Allen, D. J. ; Pickering, K. E. ; Pinder, R. W. ; Henderson, B. H. ; Appel, K. W. ; Prados, A.: Impact of lightning-NO on eastern United States photochemistry during the summer of 2006 as determined using the CMAQ model. In: *Atmospheric Chemistry and Physics* 12 (2012), Nr. 4, 1737–1758. http://dx.doi.org/10.5194/acp-12-1737-2012. – DOI 10.5194/acp–12–1737–2012

[Amann et al. 2012] Amann, M ; Borken-Kleefeld, J ; Cofala, J ; Heyes, C ; Klimont, Z ; Rafaj, P ; Purohit, P ; Schöpp, W ; Winiwarter, W: Future emissions of air pollutants in Europe: Current legislation baseline and the scope for further reductions. In: *TSAP Report No 1. Laxenburg, Austria: International Institute for Applied Systems Analysis* (2012)

[Amann et al. 2011] Amann, Markus ; Bertok, Imrich ; Borken-Kleefeld, Jens ; Cofala, Janusz ; Heyes, Chris ; Höglund-Isaksson, Lena ; Klimont, Zbigniew ; Nguyen, Binh ; Posch, Maximilian ; Rafaj, Peter ; Sandler, Robert ; Schöpp, Wolfgang ; Wagner, Fabian ; Winiwarter, Wilfried: Cost-effective control of air quality and greenhouse gases in Europe: Modeling and policy applications. In: *Environmental Modelling & Software* 26 (2011), Nr. 12, 1489 - 1501. http://dx.doi.org/https://doi.org/10.1016/j.envsoft.2011.07.012. – DOI https://doi.org/10.1016/j.envsoft.2011.07.012. – ISSN 1364–8152

[Amann et al. 2013] Amann, Markus ; Klimont, Zbigniew ; Wagner, Fabian: Regional and Global Emissions of Air Pollutants: Recent Trends and Future Scenarios. In: *Annual Review of Environment and Resources* 38 (2013), Nr. 1, 31-55. http://dx.doi.org/10.1146/annurev-environ-052912-173303. – DOI 10.1146/annurev–environ–052912–173303

[Anderson and Klugmann 2014] Anderson, G. ; Klugmann, D.: A European lightning density analysis using 5 years of ATDnet data. In: *Natural Hazards and Earth System Sciences* 14 (2014), Nr. 4, 815–829. http://dx.doi.org/10.5194/nhess-14-815-2014. – DOI 10.5194/nhess–14–815–2014

[Andreae and Merlet 2001] Andreae, M. O. ; Merlet, P.: Emission of trace gases and aerosols from biomass burning. In: *Global Biogeochemical Cycles* 15 (2001), Nr. 4, 955-966. http://dx.doi.org/10.1029/2000GB001382. – DOI 10.1029/2000GB001382

[Andreae and Crutzen 1997] Andreae, Meinrat O. ; Crutzen, Paul J.: Atmospheric Aerosols: Biogeochemical Sources and Role in Atmospheric Chemistry. In: *Science* 276 (1997), Nr. 5315, 1052–1058. http://dx.doi.org/10.1126/science.276.5315.1052. – DOI 10.1126/science.276.5315.1052. – ISSN 0036–8075

[Appel et al. 2017] Appel, K. W. ; Napelenok, S. L. ; Foley, K. M. ; Pye, H. O. T. ; Hogrefe, C. ; Luecken, D. J. ; Bash, J. O. ; Roselle, S. J. ; Pleim, J. E. ; Foroutan, H. ; Hutzell, W. T. ; Pouliot, G. A. ; Sarwar, G. ; Fahey, K. M. ; Gantt, B. ; Gilliam, R. C. ; Heath, N. K. ; Kang, D. ; Mathur, R. ; Schwede, D. B. ; Spero, T. L. ; Wong, D. C. ; Young, J. O.: Description and evaluation of the Community Multiscale Air Quality (CMAQ) modeling system version 5.1. In: *Geoscientific Model Development* 10 (2017), Nr. 4, 1703–1732. http://dx.doi.org/10.5194/gmd-10-1703-2017. – DOI 10.5194/gmd–10–1703–2017

[Arndt et al. 2018] Arndt, Jan A. ; Aulinger, Armin ; Matthias, Volker: Implementation of different big-leaf canopy reduction functions in the Biogenic Emission Inventory System (BEIS) and their impact on concentrations of oxidized nitrogen species in northern Europe.

In: *Atmospheric Environment* 191 (2018), 302 - 311. http://dx.doi.org/https://doi.org/10.1016/j.atmosenv.2018.07.035. – DOI https://doi.org/10.1016/j.atmosenv.2018.07.035. – ISSN 1352–2310

[Arndt et al. 2019] Arndt, Jan A. ; Aulinger, Armin ; Matthias, Volker: Quantification of lightning-induced nitrogen oxide emissions over Europe. In: *Atmospheric Environment* (2019). http://dx.doi.org/https://doi.org/10.1016/j.atmosenv.2018.12.059. – DOI https://doi.org/10.1016/j.atmosenv.2018.12.059. – ISSN 1352–2310

[Arneth et al. 2010] Arneth, A ; Harrison, Sandy ; Zaehle, Sönke ; Tsigaridis, Kostas ; Menon, Surabi ; Bartlein, Patrick ; Feichter, J ; Korhola, Atte ; Kulmala, Markku ; ODonnell, D ; Schurgers, G ; Sorvari, Sanna: Terrestrial biogeochemical feedbacks in the climate system: from past to future. (2010), 01

[Arnold et al. 2009] Arnold, S. R. ; Spracklen, D. V. ; Williams, J. ; Yassaa, N. ; Sciare, J. ; Bonsang, B. ; Gros, V. ; Peeken, I. ; Lewis, A. C. ; Alvain, S. ; Moulin, C.: Evaluation of the global oceanic isoprene source and its impacts on marine organic carbon aerosol. In: *Atmospheric Chemistry and Physics* 9 (2009), Nr. 4, 1253–1262. http://dx.doi.org/10.5194/acp-9-1253-2009. – DOI 10.5194/acp–9–1253–2009

[Atkinson and Arey 2003] Atkinson, Roger ; Arey, Janet: Atmospheric Degradation of Volatile Organic Compounds. In: *Chemical Reviews* 103 (2003), Nr. 12, 4605-4638. http://dx.doi.org/10.1021/cr0206420. – DOI 10.1021/cr0206420. – PMID: 14664626

[Aulinger et al. 2016] Aulinger, A. ; Matthias, V. ; Zeretzke, M. ; Bieser, J. ; Quante, M. ; Backes, A.: The impact of shipping emissions on air pollution in the greater North Sea region – Part 1: Current emissions and concentrations. In: *Atmospheric Chemistry and Physics* 16 (2016), Nr. 2, 739–758. http://dx.doi.org/10.5194/acp-16-739-2016. – DOI 10.5194/acp–16–739–2016

[Backes et al. 2016a] In: Backes, Anna ; Aulinger, A ; Bieser, Johannes ; Matthias, Volker ; Quante, M: *Infuence of Ammonia Emissions on Aerosol Formation in Northern and Central Europe*. Springer, 2016. – ISBN 978–3–319–24476–1, S. 29–36

[Backes et al. 2016b] Backes, Anna ; Aulinger, Armin ; Bieser, Johannes ; Matthias, Volker ; Quante, M: Ammonia emissions in Europe, Part II: How ammonia emission abatement strategies affect secondary aerosols. In: *Atmospheric Environment* 126 (2016), 01. http://dx.doi.org/10.1016/j.atmosenv.2015.11.039. – DOI 10.1016/j.atmosenv.2015.11.039

[Backes et al. 2016c] Backes, Anna ; Bieser, Johannes ; Aulinger, Armin ; Matthias, Volker ; Quante, M: Ammonia Emissions In Europe, Part I: Development Of A Dynamical Ammonia Emission Inventory. In: *Atmospheric Environment* 131 (2016), 01, S. 55–66. http://dx.doi.org/10.1016/j.atmosenv.2016.01.041. – DOI 10.1016/j.atmosenv.2016.01.041

[Bakwin et al. 1990] Bakwin, Peter ; Wofsy, Steven ; Fan, Song-Miao: Measurements of reactive nitrogen oxides (NOy) within and above a tropical forest canopy in the wet season. 95 (1990), 10

[Bartholomé and Belward 2005] Bartholomé, E. ; Belward, A. S.: GLC2000: a new approach to global land cover mapping from Earth observation data. In: *International Journal of Remote Sensing* 26 (2005), Nr. 9, 1959-1977. http://dx.doi.org/10.1080/01431160412331291297. – DOI 10.1080/01431160412331291297

[Bash et al. 2016] Bash, J. O. ; Baker, K. R. ; Beaver, M. R.: Evaluation of improved land use and canopy representation in BEIS v3.61 with biogenic VOC measurements in California. In: *Geoscientific Model Development* 9 (2016), Nr. 6, 2191–2207. http://dx.doi.org/10.5194/gmd-9-2191-2016. – DOI 10.5194/gmd–9–2191–2016

[Benton et al. 2000] Benton, J ; Fuhrer, Juerg ; Gimeno, Benjamín ; Skärby, Lena ; Palmer-Brown, Dominic ; Ball, Graham ; Roadknight, Chris ; Mills, G: An international cooperative program indicates the widespread occurrence of ozone injury on crops. In: *Agriculture, Ecosystems & Environment* 78 (2000), 03, S. 19–30. http://dx.doi.org/10.1016/S0167-8809(99)00107-3. – DOI 10.1016/S0167–8809(99)00107–3

[Bergström et al. 2012] Bergström, R. ; Gon, H. A. C. d. ; Prévôt, A. S. H. ; Yttri, K. E. ; Simpson, D.: Modelling of organic aerosols over Europe (2002 - 2007) using a volatility basis set (VBS) framework: application of different assumptions regarding the formation of secondary organic aerosol. In: *Atmospheric Chemistry and Physics* 12 (2012), Nr. 18, 8499–8527. http://dx.doi.org/10.5194/acp-12-8499-2012. – DOI 10.5194/acp–12–8499–2012

[Bieser et al. 2011a] Bieser, J. ; Aulinger, A. ; Matthias, V. ; Quante, M. ; Builtjes, P.: SMOKE for Europe - adaptation, modification and evaluation of a comprehensive emission model for Europe. In: *Geoscientific Model Development* 4 (2011), Nr. 1, S. 47–68. http://dx.doi.org/10.5194/gmd-4-47-2011. – DOI 10.5194/gmd–4–47–2011

[Bieser et al. 2011b] Bieser, J. ; Aulinger, A. ; Matthias, V. ; Quante, M. ; Gon, H. A. C. d.: Vertical emission profiles for Europe based on plume rise calculations. In: *Environmental Pollution* 159 (2011), Oktober, Nr. 10, S. 2935–2946. http://dx.doi.org/10.1016/j.envpol.2011.04.030. – DOI 10.1016/j.envpol.2011.04.030

[Birch 2016] In: Birch, Hayley: *Das Haber-Bosch-Verfahren*. Berlin, Heidelberg : Springer Berlin Heidelberg, 2016. – ISBN 978–3–662–48510–1, 68–71

[Blakeslee et al. 2014] Blakeslee, Richard J. ; Mach, Douglas M. ; Bateman, Monte G. ; Bailey, Jeffrey C.: Seasonal variations in the lightning diurnal cycle and implications for the global electric circuit. In: *Atmospheric Research* 135-136 (2014), 228 - 243. http://dx.doi.org/https://doi.org/10.1016/j.atmosres.2012.09.023. – DOI https://doi.org/10.1016/j.atmosres.2012.09.023. – ISSN 0169–8095

[Boersma et al. 2011] Boersma, K. F. ; Eskes, H. J. ; Dirksen, R. J. ; A, R. J. d. ; Veefkind, J. P. ; Stammes, P. ; Huijnen, V. ; Kleipool, Q. L. ; Sneep, M. ; Claas, J. ; Leitão, J. ; Richter, A. ; Zhou, Y. ; Brunner, D.: An improved tropospheric NO_2 column retrieval algorithm for the Ozone Monitoring Instrument. In: *Atmospheric Measurement Techniques* 4 (2011), Nr. 9, 1905–1928. http://dx.doi.org/10.5194/amt-4-1905-2011. – DOI 10.5194/amt–4–1905–2011

[Boersma et al. 2005] Boersma, K. F. ; Eskes, H. J. ; Meijer, E. W. ; Kelder, H. M.: Estimates of lightning NO_x production from GOME satellite observations. In: *Atmospheric Chemistry and Physics* 5 (2005), Nr. 9, 2311–2331. http://dx.doi.org/10.5194/acp-5-2311-2005. – DOI 10.5194/acp–5–2311–2005

[Bossioli et al. 2008] Bossioli, Elizabeth ; Builtjes, P.J.H. ; Denby, B ; Deserti, M ; Douros, Ioannis ; Fay, Barbara ; Geersema, G ; Kaasik, Marko ; Labancz, Krisztina ; Matthias, Volker ; Miranda, A.I. ; Moussiopoulos, Nicolas ; , Viel ; Pernigotti, Denise ; Persson, Christer ; García, Roberto ; Schlünzen, Heinke ; Sokhi, Ranjeet ; Struzewska, Joanna ; Yu, Ye: *Overview of tools and methods for meteorological and air pollution mesoscale model evaluation and user training*. GAW Report No. 181. WMO/TD-No. 1457, 2008. – ISBN 978–1–905313–59–4

[Butterbach-Bahl et al. 2011] Butterbach-Bahl, Klaus ; Gundersen, Per ; Ambus, Per ; Augustin, Jürgen ; Beier, Claus ; Boeckx, Pascal ; Dannenmann, Michael ; Gimeno, Benjamin S. ; Ibrom, Andreas ; Kiese, Ralf ; Sutton, Mark A. (Hrsg.) ; Howard, Clare M. (Hrsg.) ; Erisman, Jan W. (Hrsg.) ; Billen, Gilles (Hrsg.) ; Bleeker, Albert (Hrsg.) ; Grennfelt, Peringe (Hrsg.) ; Grinsven, Hans van (Hrsg.) ; Grizzetti, Bruna (Hrsg.): *Nitrogen processes in terrestrial ecosystems*. Cambridge University Press, 2011. – 99–125 S. http://dx.doi.org/10.1017/CBO9780511976988.009. http://dx.doi.org/10.1017/CBO9780511976988.009

[Buttner et al. 2004] Buttner, George ; Feranec, Jan ; Jaffrain, G ; Mari, Laszlo ; Maucha, Gergely ; Soukup, Tomas: The CORINE land cover 2000 project. 3 (2004), 01, S. 331–346

[Byun and Schere 2006] Byun, D. ; Schere, K.L.: Review of the Governing Equations, Computational Algorithms, and Other Components of the Models-3 Community Multiscale Air Quality (CMAQ) Modeling System. In: *Applied Mechanics Reviews* 59 (2006), S. 51–77

[Byun and Ching 1999] Byun, D.W. ; Ching, J.K.S.: Science Algorithms of the EPA Models-3 Community Multiscale Air Quality Modeling System / US Environmental Protection Agency, Office of Research and Development. Washington DC, 1999. – EPA/600/R-99/030

[Cavalli et al. 2006] Cavalli, F. ; Facchini, M. C. ; Decesari, S. ; Emblico, L. ; Mircea, M. ; Jensen, N. R. ; Fuzzi, S.: Size-segregated aerosol chemical composition at a boreal site in southern Finland, during the QUEST project. In: *Atmospheric Chemistry and Physics* 6 (2006), Nr. 4, 993–1002. http://dx.doi.org/10.5194/acp-6-993-2006. – DOI 10.5194/acp–6–993–2006

[Cecil et al. 2014] Cecil, Daniel J. ; Buechler, Dennis E. ; Blakeslee, Richard J.: Gridded lightning climatology from TRMM-LIS and OTD: Dataset description. In: *Atmospheric Research* 135-136 (2014), 404 - 414. http://dx.doi.org/https://doi.org/10.1016/j.atmosres.2012.06.028. – DOI https://doi.org/10.1016/j.atmosres.2012.06.028. – ISSN 0169–8095

[Churkina et al. 2017] Churkina, Galina ; Kuik, Friderike ; Bonn, Boris ; Lauer, Axel ; Grote, Rüdiger ; Tomiak, Karolina ; Butler, Tim M.: Effect of VOC Emissions from Vegetation on Air Quality in Berlin during a Heatwave. In: *Environmental Science & Technology* 51 (2017), Nr. 11, 6120-6130. http://dx.doi.org/10.1021/acs.est.6b06514. – DOI 10.1021/acs.est.6b06514. – PMID: 28513175

[Crutzen 1979] Crutzen, P J.: The Role of NO and NO2 in the Chemistry of the Troposphere and Stratosphere. In: *Annual Review of Earth and Planetary Sciences* (1979), S. 443–472

[Curci et al. 2009] Curci, G. ; Beekmann, M. ; Vautard, R. ; Smiatek, G. ; Steinbrecher, R. ; Theloke, J. ; Friedrich, R.: Modelling study of the impact of isoprene and terpene biogenic emissions on European ozone levels. In: *Atmospheric Environment* 43 (2009), Nr. 7, 1444 - 1455. http://dx.doi.org/https://doi.org/10.1016/j.atmosenv.2008.02.070. – DOI https://doi.org/10.1016/j.atmosenv.2008.02.070. – ISSN 1352–2310. – Natural and Biogenic Emissions of Environmentally Relevant Atmospheric Trace Constituents in Europe

[Davidson and Kingerlee 1997] Davidson, E.A. ; Kingerlee, W.: A global inventory of nitric oxide emissions from soils. In: *Nutrient Cycling in Agroecosystems* 48 (1997). http://dx.doi.org/10.1023/A:1009738715891. – DOI 10.1023/A:1009738715891

[Dee et al. 2011] Dee, D. P. ; Uppala, A. J. S. M.and Simmons S. S. M.and Simmons ; Berrisford, P. ; Poli, P. ; Kobayashi, S. ; Andrae, U. ; Balmaseda, M. A. ; Balsamo, G. ; Bauer, P. ; Bechtold, P. ; Beljaars, A. C. M. ; Berg, L. van d. ; Bidlot, J. ; Bormann, N. ; Delsol, C. ; Dragani, R. ; Fuentes, M. ; Geer, A. J. ; Haimberger, L. ; Healy, S. B. ; Hersbach, E. V. H.and Hólm H. H.and Hólm ; Isaksen, L. ; Kallberg, P. ; Köhler, M. ; Matricardi, M. ; McNally, A. P. ; Monge-Sanz, B. M. ; Morcrette, J.-J. ; Park, B.-K. ; Peubey, C. ; Rosnay, P. de ; Tavolato, C. ; Thépaut, J.-N. ; Vitart, F.: The ERA-Interim reanalysis: configuration and performance of the data assimilation system. In: *Q.J.R. Meteorol* 137 (2011), S. 553–597. http://dx.doi.org/10.1002/qj.828. – DOI 10.1002/qj.828

[Di Giuseppe et al. 2017] Di Giuseppe, Francesca ; Remy, Samuel ; Pappenberger, Florian ; Wetterhall, Fredrik: Improving Forecasts of Biomass Burning Emissions with the Fire Weather Index. In: *Journal of Applied Meteorology and Climatology* 56 (2017), Nr. 10, 2789-2799. http://dx.doi.org/10.1175/JAMC-D-16-0405.1. – DOI 10.1175/JAMC–D–16–0405.1

[Doms et al. 2011] Doms, G. ; J., Foerstner ; Heise, E. ; Herzog, H.-J. ; Mrionow, D. ; Raschendorfer, M. ; Reinhart, T. ; Ritter, B. ; Schrodin, R. ; Schulz, J.-P. ; Vogel, G.: A Description of the Nonhydrostatic Regional COSMO Model. Part II: Physical Parameterization / Deutscher Wetterdienst. Version: 2011. http://www.cosmo-model.org/content/model/documentation/core/cosmoPhysParamtr.pdf. 2011. – Forschungsbericht. – Accessed: 2014-04-09

[Doms and Schättler 2002] Doms, G. ; Schättler, U.: A Description of the Nonhydrostatic Regional Model LM. Part I: Dynamics and Numerics. / Deutscher Wetterdienst. Version: 2002. http://www.cosmo-model.org/content/model/documentation/core/cosmoDyncsNumcs.pdf. 2002. – Forschungsbericht

[Doney et al. 2007] Doney, Scott C. ; Mahowald, Natalie ; Lima, Ivan ; Feely, Richard A. ; Mackenzie, Fred T. ; Lamarque, Jean-Francois ; Rasch, Phil J.: Impact of anthropogenic atmospheric nitrogen and sulfur deposition on ocean acidification and the inorganic carbon system. In: *Proceedings of the National Academy of Sciences* 104 (2007), Nr. 37, 14580–14585.

http://dx.doi.org/10.1073/pnas.0702218104. – DOI 10.1073/pnas.0702218104. – ISSN 0027–8424

[Drewniak et al. 2014] Drewniak, Beth A. ; Snyder, Peter K. ; Steiner, Allison L. ; Twine, Tracy E. ; Wuebbles, Donald J.: Simulated changes in biogenic VOC emissions and ozone formation from habitat expansion of Acer Rubrum(red maple). In: *Environmental Research Letters* 9 (2014), jan, Nr. 1, 014006. http://dx.doi.org/10.1088/1748-9326/9/1/014006. – DOI 10.1088/1748–9326/9/1/014006

[Durand et al. 2011] *Kapitel* Nitrogen processes in aquatic ecosystems. In: Durand, Patrick ; Breuer, Lutz ; Johnes, Penny ; Billen, Gilles ; De Klein, Jeroen: *Nitrogen processes in aquatic ecosystems*. Cambridge University Press, 2011

[Eskes and Boersma 2003] Eskes, H. J. ; Boersma, K. F.: Averaging kernels for DOAS total-column satellite retrievals. In: *Atmospheric Chemistry and Physics* 3 (2003), Nr. 5, 1285–1291. http://dx.doi.org/10.5194/acp-3-1285-2003. – DOI 10.5194/acp–3–1285–2003

[Etling 1996] Etling, Dieter: Theoretische Meteorologie. In: *Vieweg, Braunschweig, Wiesbaden* (1996). http://link.springer.com/content/pdf/10.1007/978-3-540-75979-9.pdf. ISBN 9783540759782

[Fehr et al. 2004] Fehr, Thorsten ; Hüller, Hartmut ; Huntrieser, Heidi: Model study on production and transport of lightning-produced NOx in a EULINOX supercell storm. In: *Journal of Geophysical Research: Atmospheres* 109 (2004), Nr. D9. http://dx.doi.org/10.1029/2003JD003935. – DOI 10.1029/2003JD003935

[Finlayson-Pitts and Pitts 2000] Finlayson-Pitts, Barbara J. ; Pitts, James N.: CHAPTER 2 - The Atmospheric System. Version: 2000. http://dx.doi.org/https://doi.org/10.1016/B978-012257060-5/50004-6. In: Finlayson-Pitts, Barbara J. (Hrsg.) ; Pitts, James N. (Hrsg.): *Chemistry of the Upper and Lower Atmosphere*. San Diego : Academic Press, 2000. – DOI https://doi.org/10.1016/B978–012257060–5/50004–6. – ISBN 978–0–12–257060–5, 15 - 42

[Finney et al. 2014] Finney, D. L. ; Doherty, R. M. ; Wild, O. ; Huntrieser, H. ; Pumphrey, H. C. ; Blyth, A. M.: Using cloud ice flux to parametrise large-scale lightning. In: *Atmospheric Chemistry and Physics* 14 (2014), Nr. 23, 12665–12682. http://dx.doi.org/10.5194/acp-14-12665-2014. – DOI 10.5194/acp–14–12665–2014

[FORESTS 2017] FORESTS, ICP: http://icp-forests.net (accessed November 2017). (2017)

[Fountoukis et al. 2014] Fountoukis, C. ; Megaritis, A. G. ; Skyllakou, K. ; Charalampidis, P. E. ; Pilinis, C. ; Gon, H. A. C. d. ; Crippa, M. ; Canonaco, F. ; Mohr, C. ; Prévôt, A. S. H. ; Allan, J. D. ; Poulain, L. ; Petäjä, T. ; Tiitta, P. ; Carbone, S. ; Kiendler-Scharr, A. ; Nemitz, E. ; O'Dowd, C. ; Swietlicki, E. ; Pandis, S. N.: Organic aerosol concentration and composition over Europe: insights from comparison of regional model predictions with aerosol mass spectrometer factor analysis. In: *Atmospheric Chemistry and Physics* 14 (2014), Nr. 17, 9061–9076. http://dx.doi.org/10.5194/acp-14-9061-2014. – DOI 10.5194/acp–14–9061–2014

[Fountoukis and Nenes 2007] Fountoukis, C ; Nenes, Athanasios: ISORROPIA II: a computationally efficient thermodynamic equilibrium model for K+–Ca 2+–Mg 2+–NH 4+–Na+–SO 4 2—NO 3—Cl—H 2 O aerosols. In: *Atmospheric Chemistry and Physics* 7 (2007), Nr. 17, S. 4639–4659

[Fowler et al. 2013] Fowler, David ; Coyle, Mhairi ; Skiba, U ; A Sutton, Mark ; Neil Cape, J ; Reis, Stefan ; Sheppard, Lucy ; Jenkins, Alan ; Grizzetti, Bruna ; Galloway, James ; Vitousek, Peter ; Leach, Allison ; Bouwman, Alexander ; Butterbach-Bahl, Klaus ; Dentener, Frank ; Stevenson, David ; Amann, Markus ; Voss, Maren: The Global Nitrogen Cycle in the Twenty-First Century. In: *Philosophical transactions of the Royal Society of London. Series B, Biological sciences* 368 (2013), 07, S. 20130164. http://dx.doi.org/10.1098/rstb.2013.0164. – DOI 10.1098/rstb.2013.0164

[Freitas et al. 2011] Freitas, S. R. ; Longo, K. M. ; Alonso, M. F. ; Pirre, M. ; Marecal, V. ; Grell, G. ; Stockler, R. ; Mello, R. F. ; Sánchez Gácita, M.: PREP-CHEM-SRC – 1.0: a preprocessor of trace gas and aerosol emission fields for regional and global

atmospheric chemistry models. In: *Geoscientific Model Development* 4 (2011), Nr. 2, 419–433. http://dx.doi.org/10.5194/gmd-4-419-2011. – DOI 10.5194/gmd–4–419–2011

[Freitas et al. 2006] Freitas, S. R. ; Longo, K. M. ; Andreae, M. O.: Impact of including the plume rise of vegetation fires in numerical simulations of associated atmospheric pollutants. In: *Geophysical Research Letters* 33 (2006), Nr. 17. http://dx.doi.org/10.1029/2006GL026608. – DOI 10.1029/2006GL026608

[Frost et al. 2013] Frost, Gregory J. ; Middleton, Paulette ; Tarrason, Leonor ; Granier, Claire ; Guenther, Alex ; Cardenas, Beatriz ; Gon, Hugo D. d. ; Janssens-Maenhout, Greet ; Kaiser, Johannes W. ; Keating, Terry ; Klimont, Zbigniew ; Lamarque, Jean-Francois ; Liousse, Catherine ; Nickovic, Slobodan ; Ohara, Toshimasa ; Schultz, Martin G. ; Skiba, Ute ; Aardenne, John van ; Wang, Yuxuan: New Directions: GEIA's 2020 vision for better air emissions information. In: *Atmospheric Environment* 81 (2013), 710 - 712. http://dx.doi.org/https://doi.org/10.1016/j.atmosenv.2013.08.063. – DOI https://doi.org/10.1016/j.atmosenv.2013.08.063. – ISSN 1352–2310

[Fuest 2000] Fuest, Stefan: Regionale Grundwassergefährdung durch Nitrat. In: *Vergleich von räumlich differenzierten Überwachungsdaten und Modellrechnungen* (2000)

[Fuzzi et al. 2015] Fuzzi, S. ; Baltensperger, U. ; Carslaw, K. ; Decesari, S. ; Gon, H. Denier van d. ; Facchini, M. C. ; Fowler, D. ; Koren, I. ; Langford, B. ; Lohmann, U. ; Nemitz, E. ; Pandis, S. ; Riipinen, I. ; Rudich, Y. ; Schaap, M. ; Slowik, J. G. ; Spracklen, D. V. ; Vignati, E. ; Wild, M. ; Williams, M. ; Gilardoni, S.: Particulate matter, air quality and climate: lessons learned and future needs. In: *Atmospheric Chemistry and Physics* 15 (2015), Nr. 14, 8217–8299. http://dx.doi.org/10.5194/acp-15-8217-2015. – DOI 10.5194/acp–15–8217–2015

[Galle et al. 2010] Galle, Bo ; Johansson, Mattias ; Rivera, Claudia ; Zhang, Yan ; Kihlman, Manne ; Kern, Christoph ; Lehmann, Thomas ; Platt, Ulrich ; Arellano, Santiago ; Hidalgo, Silvana: Network for Observation of Volcanic and Atmospheric Change (NOVAC): A global network for volcanic gas monitoring: Network layout and instrument description. In: *Journal of Geophysical Research: Atmospheres* 115 (2010), Nr. D5. http://dx.doi.org/10.1029/2009JD011823. – DOI 10.1029/2009JD011823

[Galloway et al. 2004] Galloway, James N. ; Dentener, Frank J. ; Capone, Douglas G. ; Boyer, Elisabeth W. ; Howarth, Robert W. ; Seitzinger, Sybil P. ; Asner, Gregory P. ; Cleveland, Cory C. ; Green, PA ; Holland, Elizabeth A. et al.: Nitrogen cycles: past, present, and future. In: *Biogeochemistry* 70 (2004), Nr. 2, S. 153–226

[Ganzeveld et al. 2002] Ganzeveld, L. N. ; Lelieveld, J. ; Dentener, F. J. ; Krol, M. C. ; Bouwman, A. J. ; Roelofs, G.-J.: Global soil-biogenic NOx emissions and the role of canopy processes. In: *J. Geophys. Res., 107(D16)* (2002). http://dx.doi.org/10.1029/2001JD001289. – DOI 10.1029/2001JD001289

[Geyer 2014] Geyer, B.: High-resolution atmospheric reconstruction for Europe 1948-2012: coastDat2. In: *Earth System Science Data* 6 (2014), Nr. 1, 147–164. http://dx.doi.org/10.5194/essd-6-147-2014. – DOI 10.5194/essd–6–147–2014

[GFED 2017] GFED: Emissions Database (GFED). 2017. Global Fire Emissions Database, version 4.1 (GFEDv4), summary. In: *https://daac.ornl.gov/VEGETATION/guides/fire_emissions_v4_R1.html(accessed November* 2017), 2017

[Giglio et al. 2003] Giglio, Louis ; Descloitres, Jacques ; Justice, Christopher O. ; Kaufman, Yoram J.: An Enhanced Contextual Fire Detection Algorithm for MODIS. In: *Remote Sensing of Environment* 87 (2003), Nr. 2, 273 - 282. http://dx.doi.org/https://doi.org/10.1016/S0034-4257(03)00184-6. – DOI https://doi.org/10.1016/S0034–4257(03)00184–6. – ISSN 0034–4257

[Denier van der Gon et al. 2015] Gon, H. A. C. d. ; Bergström, R. ; Fountoukis, C. ; Johansson, C. ; Pandis, S. N. ; Simpson, D. ; Visschedijk, A. J. H.: Particulate emissions from residential wood combustion in Europe: revised estimates and an evaluation. In: *Atmospheric Chemistry and Physics* 15 (2015), Nr. 11, 6503–6519. http://dx.doi.org/10.5194/

acp-15-6503-2015. – DOI 10.5194/acp–15–6503–2015

[Guenther et al. 2006] Guenther, A. ; Karl, T. ; Harley, P. ; Wiedinmyer, C. ; Palmer, P. I. ; Geron, C.: Estimates of global terrestrial isoprene emissions using MEGAN (Model of Emissions of Gases and Aerosols from Nature). In: *Atmospheric Chemistry and Physics* 6 (2006), Nr. 11, 3181–3210. http://dx.doi.org/10.5194/acp-6-3181-2006. – DOI 10.5194/acp–6–3181–2006

[Guenther et al. 2012] Guenther, A. B. ; Jiang, X. ; Heald, C. L. ; Sakulyanontvittaya, T. ; Duhl, T. ; Emmons, L. K. ; Wang, X.: The Model of Emissions of Gases and Aerosols from Nature version 2.1 (MEGAN2.1): an extended and updated framework for modeling biogenic emissions. In: *Geoscientific Model Development* 5 (2012), Nr. 6, 1471–1492. http://dx.doi.org/10.5194/gmd-5-1471-2012. – DOI 10.5194/gmd–5–1471–2012

[Guenther 2013] Guenther, Alex: Biological and Chemical Diversity of Biogenic Volatile Organic Emissions into the Atmosphere. In: *SRN Atmospheric Sciences, vol 2013, Article ID 786290* 27 (2013), S. pages,

[Guenther et al. 1995] Guenther, Alex ; Hewitt, C. N. ; Erickson, David ; Fall, Ray ; Geron, Chris ; Graedel, Tom ; Harley, Peter ; Klinger, Lee ; Lerdau, Manuel ; Mckay, W. A. ; Pierce, Tom ; Scholes, Bob ; Steinbrecher, Rainer ; Tallamraju, Raja ; Taylor, John ; Zimmerman, Pat: A global model of natural volatile organic compound emissions. In: *Journal of Geophysical Research: Atmospheres* 100 (1995), Nr. D5, 8873-8892. http://dx.doi.org/10.1029/94JD02950. – DOI 10.1029/94JD02950

[Hallquist et al. 2009] Hallquist, M. ; Wenger, J. C. ; Baltensperger, U. ; Rudich, Y. ; Simpson, D. ; Claeys, M. ; Dommen, J. ; Donahue, N. M. ; George, C. ; Goldstein, A. H. ; Hamilton, J. F. ; Herrmann, H. ; Hoffmann, T. ; Iinuma, Y. ; Jang, M. ; Jenkin, M. E. ; Jimenez, J. L. ; Kiendler-Scharr, A. ; Maenhaut, W. ; McFiggans, G. ; Mentel, Th. F. ; Monod, A. ; Prévôt, A. S. H. ; Seinfeld, J. H. ; Surratt, J. D. ; Szmigielski, R. ; Wildt, J.: The formation, properties and impact of secondary organic aerosol: current and emerging issues. In: *Atmospheric Chemistry and Physics* 9 (2009), Nr. 14, 5155–5236. http://dx.doi.org/10.5194/acp-9-5155-2009. – DOI 10.5194/acp–9–5155–2009

[Hamra et al. 2015] Hamra, Ghassan B. ; Laden, Francine ; Cohen, Aaron J. ; Raaschou-Nielsen, Ole ; Brauer, Michael ; Loomis, Dana: Lung Cancer and Exposure to Nitrogen Dioxide and Traffic: A Systematic Review and Meta-Analysis. In: *Environmental Health Perspectives* 123 (2015), Nr. 11, 1107-1112. http://dx.doi.org/10.1289/ehp.1408882. – DOI 10.1289/ehp.1408882

[Heffer and Prudhomme 2010] Heffer, Patrick ; Prudhomme, Michel: Fertilizer outlook 2010–2014. 2010. – Forschungsbericht

[Heffer and Prudhomme 2016] Heffer, Patrick ; Prudhomme, Michel: Fertilizer Outlook 2016–2020, 2016

[Hemond and Fechner 2015] Hemond, Harold F. ; Fechner, Elizabeth J.: Chapter 4 - The Atmosphere. Version: Third Edition, 2015. http://dx.doi.org/https://doi.org/10.1016/B978-0-12-398256-8.00004-9. In: Hemond, Harold F. (Hrsg.) ; Fechner, Elizabeth J. (Hrsg.): *Chemical Fate and Transport in the Environment (Third Edition)*. Third Edition. Boston : Academic Press, 2015. – DOI https://doi.org/10.1016/B978–0–12–398256–8.00004–9. – ISBN 978–0–12–398256–8, 311 - 454

[Hertel et al. 2011] Hertel, Ole ; Reis, Stefan ; Skjøth, Carsten A. ; Bleeker, Albert ; Harrison, Roy ; Cape, John N. ; Fowler, David ; Skiba, Ute ; Simpson, David ; Jickells, Tim ; Sutton, Mark A. (Hrsg.) ; Howard, Clare M. (Hrsg.) ; Erisman, Jan W. (Hrsg.) ; Billen, Gilles (Hrsg.) ; Bleeker, Albert (Hrsg.) ; Grennfelt, Peringe (Hrsg.) ; Grinsven, Hans van (Hrsg.) ; Grizzetti, BrunaEditors (Hrsg.): *Nitrogen processes in the atmosphere*. Cambridge University Press, 2011. – 177–208 S. http://dx.doi.org/10.1017/CBO9780511976988.012. http://dx.doi.org/10.1017/CBO9780511976988.012

[Hoelzemann et al. 2004] Hoelzemann, Judith J. ; Schultz, Martin G. ; Brasseur, Guy P. ; Granier, Claire ; Simon, Muriel: Global Wildland Fire Emission Model (GWEM): Evaluating

the use of global area burnt satellite data. In: *Journal of Geophysical Research: Atmospheres* 109 (2004), Nr. D14. http://dx.doi.org/10.1029/2003JD003666. – DOI 10.1029/2003JD003666

[Holtappels et al. 2009] Holtappels, Moritz ; Lam, Phyllis ; M.M. Kuypers, Marcel: Der Stickstoffkreislauf im ozean. In: *BIOspektrum* (2009), 01

[Huntrieser et al. 2000] Huntrieser, Heidi ; Feigl, Ch ; Schlager, H ; Schr, F ; Gerbig, C ; Velthoven, Peter ; Flatoy, F ; Théry, C ; Höller, H ; Schumann, Ulrich: Contribution of Lightning-produced NOx to the European and Global NOx Budget: Results and Estimates from Airborne EULINOX Measurements. (2000), 01, S. 43–76

[Ichoku and Kaufman 2005] Ichoku, C. ; Kaufman, Y. J.: A method to derive smoke emission rates from MODIS fire radiative energy measurements. In: *IEEE Transactions on Geoscience and Remote Sensing* 43 (2005), Nov, Nr. 11, S. 2636–2649. http://dx.doi.org/10.1109/TGRS.2005.857328. – DOI 10.1109/TGRS.2005.857328. – ISSN 0196–2892

[Im et al. 2018] Im, U. ; Christensen, J. H. ; Geels, C. ; Hansen, K. M. ; Brandt, J. ; Solazzo, E. ; Alyuz, U. ; Balzarini, A. ; Baro, R. ; Bellasio, R. ; Bianconi, R. ; Bieser, J. ; Colette, A. ; Curci, G. ; Farrow, A. ; Flemming, J. ; Fraser, A. ; Jimenez-Guerrero, P. ; Kitwiroon, N. ; Liu, P. ; Nopmongcol, U. ; Palacios-Peña, L. ; Pirovano, G. ; Pozzoli, L. ; Prank, M. ; Rose, R. ; Sokhi, R. ; Tuccella, P. ; Unal, A. ; Vivanco, M. G. ; Yarwood, G. ; Hogrefe, C. ; Galmarini, S.: Influence of anthropogenic emissions and boundary conditions on multi-model simulations of major air pollutants over Europe and North America in the framework of AQMEII3. In: *Atmospheric Chemistry and Physics* 18 (2018), Nr. 12, 8929–8952. http://dx.doi.org/10.5194/acp-18-8929-2018. – DOI 10.5194/acp–18–8929–2018

[Intergovernmental Panel on Climate Change 2001] Intergovernmental Panel on Climate Change: Climate change 2001, the scientific basic. 2001. – Forschungsbericht

[Jacob and Bakwin 1991] Jacob, Daniel J. ; Bakwin, Peter S.: Cycling of NOx in tropical forest canopies. In: *American Society for Microbiology, Microbial Production and Consumption of Greenhouse Gases: Methane, Nitrogen Oxides and Halomethanes* (1991), S. 237–253

[Jacobson 1999] Jacobson, Mark Z.: *Fundamentals of Atmospheric Modeling*. 2. Cambridge University Press, 1999. – 828 S. http://www.cambridge.org/us/academic/subjects/earth-and-environmental-science/atmospheric-science-and-meteorology/fundamentals-atmospheric-modeling-2nd-edition. – ISBN 9780521548656

[Jalkanen et al. 2009] Jalkanen, J.-P. ; Brink, A. ; Kalli, J. ; Pettersson, H. ; Kukkonen, J. ; Stipa, T.: A modelling system for the exhaust emissions of marine traffic and its application in the Baltic Sea area. In: *Atmospheric Chemistry and Physics* 9 (2009), Nr. 23, 9209–9223. http://dx.doi.org/10.5194/acp-9-9209-2009. – DOI 10.5194/acp–9–9209–2009

[Jalkanen et al. 2012] Jalkanen, J.-P. ; Johansson, L. ; Kukkonen, J. ; Brink, A. ; Kalli, J. ; Stipa, T.: Extension of an assessment model of ship traffic exhaust emissions for particulate matter and carbon monoxide. In: *Atmospheric Chemistry and Physics* 12 (2012), Nr. 5, 2641–2659. http://dx.doi.org/10.5194/acp-12-2641-2012. – DOI 10.5194/acp–12–2641–2012

[Johansson et al. 2013] Johansson, L. ; Jalkanen, J.-P. ; Kalli, J. ; Kukkonen, J.: The evolution of shipping emissions and the costs of regulation changes in the northern EU area. In: *Atmospheric Chemistry and Physics* 13 (2013), Nr. 22, 11375–11389. http://dx.doi.org/10.5194/acp-13-11375-2013. – DOI 10.5194/acp–13–11375–2013

[Johansson et al. 2017] Johansson, Lasse ; Jalkanen, Jukka-Pekka ; Kukkonen, Jaakko: Global assessment of shipping emissions in 2015 on a high spatial and temporal resolution. In: *Atmospheric Environment* 167 (2017), 403 - 415. http://dx.doi.org/https://doi.org/10.1016/j.atmosenv.2017.08.042. – DOI https://doi.org/10.1016/j.atmosenv.2017.08.042. – ISSN 1352–2310

[Kaiser et al. 2012] Kaiser, J. W. ; Heil, A. ; Andreae, M. O. ; Benedetti, A. ; Chubarova, N. ; Jones, L. ; Morcrette, J.-J. ; Razinger, M. ; Schultz, M. G. ; Suttie, M. ; Werf, G. R. d.: Biomass burning emissions estimated with a global fire assimilation system based on observed fire radiative power. In: *Biogeosciences* 9 (2012), Nr. 1, 527–554. http://dx.doi.

org/10.5194/bg-9-527-2012. – DOI 10.5194/bg–9–527–2012

[Kanakidou et al. 2005] Kanakidou, M. ; Seinfeld, J. H. ; Pandis, S. N. ; Barnes, I. ; Dentener, F. J. ; Facchini, M. C. ; Van Dingenen, R. ; Ervens, B. ; Nenes, A. ; Nielsen, C. J. ; Swietlicki, E. ; Putaud, J. P. ; Balkanski, Y. ; Fuzzi, S. ; Horth, J. ; Moortgat, G. K. ; Winterhalter, R. ; Myhre, C. E. L. ; Tsigaridis, K. ; Vignati, E. ; Stephanou, E. G. ; Wilson, J.: Organic aerosol and global climate modelling: a review. In: *Atmospheric Chemistry and Physics* 5 (2005), Nr. 4, 1053–1123. http://dx.doi.org/10.5194/acp-5-1053-2005. – DOI 10.5194/acp–5–1053–2005

[Kang et al. 2018] Kang, Daiwen ; Heath, Nicholas ; Foley, Kristen ; Bash, Jesse ; Roselle, Shawn ; Mathur, Rohit: On the Relationship Between Observed NLDN Lightning Strikes and Modeled Convective Precipitation Rates: Parameterization of Lightning NOx Production in CMAQ. In: Mensink, Clemens (Hrsg.) ; Kallos, George (Hrsg.): *Air Pollution Modeling and its Application XXV*. Cham : Springer International Publishing, 2018. – ISBN 978–3–319–57645–9, S. 413–419

[Karl et al. 2018] Karl, M. ; Bieser, J. ; Geyer, B. ; Matthias, V. ; Jalkanen, J.-P. ; Johansson, L. ; Fridell, E.: Impact of a nitrogen emission control area (NECA) on the future air quality and nitrogen deposition to seawater in the Baltic Sea region. In: *Atmospheric Chemistry and Physics Discussions* 2018 (2018), 1–58. http://dx.doi.org/10.5194/acp-2018-1107. – DOI 10.5194/acp–2018–1107

[Karl et al. 2009] Karl, M. ; Guenther, A. ; Köble, R. ; Leip, A. ; Seufert, G.: A new European plant-specific emission inventory of biogenic volatile organic compounds for use in atmospheric transport models. In: *Biogeosciences* 6 (2009), Nr. 6, 1059–1087. http://dx.doi.org/10.5194/bg-6-1059-2009. – DOI 10.5194/bg–6–1059–2009

[Karl et al. 2019] Karl, Matthias ; Jonson, Jan ; Uppstu, Andreas ; Aulinger, A ; Prank, Marja ; Jalkanen, Jukka-Pekka ; Johansson, Lasse ; Quante, M ; Matthias, Volker: Effects of ship emissions on air quality in the Baltic Sea region simulated with three different chemistry transport models. In: *Atmospheric Chemistry and Physics Discussions* (2019), 01, S. 1–48. http://dx.doi.org/10.5194/acp-2018-1317. – DOI 10.5194/acp–2018–1317

[Kelly et al. 2010] Kelly, J. T. ; Bhave, P. V. ; Nolte, C. G. ; Shankar, U. ; Foley, K. M.: Simulating emission and chemical evolution of coarse sea-salt particles in the Community Multiscale Air Quality (CMAQ) model. In: *Geoscientific Model Development* 3 (2010), April, Nr. 1, 257–273. http://dx.doi.org/10.5194/gmd-3-257-2010. – DOI 10.5194/gmd–3–257–2010. – ISSN 1991–9603

[Kesselmeier and Staudt 1999] Kesselmeier, J ; Staudt, Michael: Biogenic Volatile Organic Compounds (VOC): An Overview on Emission, Physiology and Ecology. In: *Journal of Atmospheric Chemistry, v.33, 23-88 (1999)* 33 (1999), 05. http://dx.doi.org/10.1023/A:1006127516791. – DOI 10.1023/A:1006127516791

[Khaniabadi et al. 2018] Khaniabadi, Yusef O. ; Daryanoosh, Mohammad ; Sicard, Pierre ; Takdastan, Afshin ; Hopke, Philip K. ; Esmaeili, Shirin ; De Marco, Alessandra ; Rashidi, Rajab: Chronic obstructive pulmonary diseases related to outdoor PM10, O3, SO2, and NO2 in a heavily polluted megacity of Iran. In: *Environmental Science and Pollution Research* 25 (2018), Jun, Nr. 18, 17726–17734. http://dx.doi.org/10.1007/s11356-018-1902-9. – DOI 10.1007/s11356–018–1902–9. – ISSN 1614–7499

[Kim et al. 2007] Kim, Brian Y. ; Fleming, Gregg G. ; Lee, Joosung J. ; Waitz, Ian A. ; Clarke, John-Paul ; Balasubramanian, Sathya ; Malwitz, Andrew ; Klima, Kelly ; Locke, Maryalice ; Holsclaw, Curtis A. ; Maurice, Lourdes Q. ; Gupta, Mohan L.: System for assessing Aviation's Global Emissions (SAGE), Part 1: Model description and inventory results. In: *Transportation Research Part D: Transport and Environment* 12 (2007), Nr. 5, 325 - 346. http://dx.doi.org/https://doi.org/10.1016/j.trd.2007.03.007. – DOI https://doi.org/10.1016/j.trd.2007.03.007. – ISSN 1361–9209

[Klimont et al. 2017] Klimont, Z. ; Kupiainen, K. ; Heyes, C. ; Purohit, P. ; Cofala, J. ; Rafaj, P. ; Borken-Kleefeld, J. ; Schöpp, W.: Global anthropogenic emissions of

particulate matter including black carbon. In: *Atmospheric Chemistry and Physics* 17 (2017), Nr. 14, 8681–8723. http://dx.doi.org/10.5194/acp-17-8681-2017. – DOI 10.5194/acp–17–8681–2017

[Köble and Seufert 2001] Köble, R ; Seufert, G: Novel maps for forest tree species in Europe. Proceedings of the 8th European symposium on the physico-chemical behaviour of air pollutants. In: *A changing atmosphere, ed. Turino, Italy, September 17-20 2001*, 2001

[Koshak et al. 2014] Koshak, William ; Peterson, Harold ; Biazar, Arastoo ; Khan, Maudood ; Wang, Lihua: The NASA Lightning Nitrogen Oxides Model (LNOM): Application to air quality modeling. In: *Atmospheric Research* 135-136 (2014), 363 - 369. http://dx.doi.org/https://doi.org/10.1016/j.atmosres.2012.12.015. – DOI https://doi.org/10.1016/j.atmosres.2012.12.015. – ISSN 0169–8095

[Kühlwein et al. 2002] Kühlwein, J. ; Friedrich, R. ; Kalthoff, N. ; Corsmeier, U. ; Slemr, F. ; Habram, M. ; Möllmann-Coers, M.: Comparison of modelled and measured total CO and NOx emission rates. In: *Atmospheric Environment* 36 (2002), 53 - 60. http://dx.doi.org/https://doi.org/10.1016/S1352-2310(02)00207-8. – DOI https://doi.org/10.1016/S1352–2310(02)00207–8. – ISSN 1352–2310. – Evaluation of Modeled Emission Inventories of Ozone Precursors. A Case Study for an Urban Area (Augsburg, Germany)

[Kulshrestha 2017] Kulshrestha, U.: 26 - Assessment of Atmospheric Emissions and Depositions of Major Nr Species in Indian Region. Version: 2017. http://dx.doi.org/https://doi.org/10.1016/B978-0-12-811836-8.00026-4. In: Abrol, Yash P. (Hrsg.) ; Adhya, Tapan K. (Hrsg.) ; Aneja, Viney P. (Hrsg.) ; Raghuram, Nandula (Hrsg.) ; Pathak, Himanshu (Hrsg.) ; Kulshrestha, Umesh (Hrsg.) ; Sharma, Chhemendra (Hrsg.) ; Singh, Bijay (Hrsg.): *The Indian Nitrogen Assessment*. Elsevier, 2017. – DOI https://doi.org/10.1016/B978–0–12–811836–8.00026–4. – ISBN 978–0–12–811836–8, 427 - 444

[Langmann et al. 2012] Langmann, Baerbel ; Folch, Arnau ; Hensch, Martin ; Matthias, Volker: Volcanic ash over Europe during the eruption of Eyjafjallajökull on Iceland, April-May 2010. In: *Atmospheric Environment* 48 (2012), 1 - 8. http://dx.doi.org/https://doi.org/10.1016/j.atmosenv.2011.03.054. – DOI https://doi.org/10.1016/j.atmosenv.2011.03.054. – ISSN 1352–2310. – Volcanic ash over Europe during the eruption of Eyjafjallajöekull on Iceland, April-May 2010

[Langmann et al. 2009] Langmann, Bärbel ; Duncan, Bryan ; Textor, Christiane ; Trentmann, Jörg ; Werf, Guido R. d.: Vegetation fire emissions and their impact on air pollution and climate. In: *Atmospheric Environment* 43 (2009), Nr. 1, 107 - 116. http://dx.doi.org/https://doi.org/10.1016/j.atmosenv.2008.09.047. – DOI https://doi.org/10.1016/j.atmosenv.2008.09.047. – ISSN 1352–2310. – Atmospheric Environment - Fifty Years of Endeavour

[Lee et al. 2009] Lee, David S. ; Fahey, David W. ; Forster, Piers M. ; Newton, Peter J. ; Wit, Ron C. ; Lim, Ling L. ; Owen, Bethan ; Sausen, Robert: Aviation and global climate change in the 21st century. In: *Atmospheric Environment* 43 (2009), Nr. 22, 3520 - 3537. http://dx.doi.org/https://doi.org/10.1016/j.atmosenv.2009.04.024. – DOI https://doi.org/10.1016/j.atmosenv.2009.04.024. – ISSN 1352–2310

[Lee et al. 1997] Lee, D.S. ; Köhler, I. ; Grobler, E. ; Rohrer, F. ; Sausen, R. ; Gallardo-Klenner, L. ; Olivier, J.G.J. ; Dentener, F.J. ; Bouwman, A.F.: Estimations of global no, emissions and their uncertainties. In: *Atmospheric Environment* 31 (1997), Nr. 12, 1735 - 1749. http://dx.doi.org/https://doi.org/10.1016/S1352-2310(96)00327-5. – DOI https://doi.org/10.1016/S1352–2310(96)00327–5. – ISSN 1352–2310

[Lehmann et al. 2014] Lehmann, Jascha ; Coumou, Dim ; Frieler, Katja ; Eliseev, Alexey V. ; Levermann, Anders: Future changes in extratropical storm tracks and baroclinicity under climate change. In: *Environmental Research Letters* 9 (2014), aug, Nr. 8, 084002. http://dx.doi.org/10.1088/1748-9326/9/8/084002. – DOI 10.1088/1748–9326/9/8/084002

[Lelieveld et al. 2015] Lelieveld, J ; Evans, J S. ; Fnais, M ; Giannadaki, D ; Pozzer, A: The contribution of outdoor air pollution sources to premature mortality on a global scale. In:

Nature 525, 2015, S. 367–371

[Li et al. 1992] Li, Changsheng ; Frolking, Steve ; Frolking, Tod A.: A model of nitrous oxide evolution from soil driven by rainfall events: 1. Model structure and sensitivity. In: *Journal of Geophysical Research: Atmospheres* 97 (1992), Nr. D9, 9759-9776. http://dx.doi.org/10.1029/92JD00509. – DOI 10.1029/92JD00509

[Liousse et al. 2004] Liousse, C ; Andreae, M O. ; Artaxo, P ; Barbosa, P ; Cachier, H ; Gregoire, J M. ; Hobbs, P ; Lavoué, D ; Mouillot, F ; Penner, J: Deriving global quantitative estimates for spatial and temporal distributions of biomass burning emissions. In Emissions of atmospheric trace compounds – Advances in global change research, Kluwer Academic Publishers, 2004

[Martin et al. 2003] Martin, Randall V. ; Jacob, Daniel J. ; Chance, Kelly ; Kurosu, Thomas P. ; Palmer, Paul I. ; Evans, Mathew J.: Global inventory of nitrogen oxide emissions constrained by space-based observations of NO2 columns. In: *Journal of Geophysical Research: Atmospheres* 108 (2003), Nr. D17. http://dx.doi.org/10.1029/2003JD003453. – DOI 10.1029/2003JD003453

[Mastin et al. 2009] Mastin, L.G. ; Guffanti, M. ; Servranckx, R. ; Webley, P. ; Barsotti, S. ; Dean, K. ; Durant, A. ; Ewert, J.W. ; Neri, A. ; Rose, W.I. ; Schneider, D. ; Siebert, L. ; Stunder, B. ; Swanson, G. ; Tupper, A. ; Volentik, A. ; Waythomas, C.F.: A multidisciplinary effort to assign realistic source parameters to models of volcanic ash-cloud transport and dispersion during eruptions. In: *Journal of Volcanology and Geothermal Research* 186 (2009), Nr. 1, 10 - 21. http://dx.doi.org/https://doi.org/10.1016/j.jvolgeores.2009.01.008. – DOI https://doi.org/10.1016/j.jvolgeores.2009.01.008. – ISSN 0377–0273. – Improved Prediction and Tracking of Volcanic Ash Clouds

[Matthias et al. 2009] Matthias, V. ; Quante, M. ; Aulinger, A.: Determination of the optimum MM5 configuration for long term CMAQ simulations of aerosol bound pollutants in Europe. In: *Environmental Fluid Mechanics* 9 (2009), S. 91–108. http://dx.doi.org/10.1007/s10652-008-9103-6. – DOI 10.1007/s10652–008–9103–6

[Matthias et al. 2012] Matthias, Volker ; Aulinger, Armin ; Bieser, Johannes ; Cuesta, Juan ; Geyer, Beate ; Langmann, Bärbel ; Serikov, Ilya ; Mattis, Ina ; Minikin, Andreas ; Mona, Lucia ; Quante, Markus ; Schumann, Ulrich ; Weinzierl, Bernadett: The ash dispersion over Europe during the Eyjafjallajökull eruption: Comparison of CMAQ simulations to remote sensing and air-borne in-situ observations. In: *Atmospheric Environment* 48 (2012), 184 - 194. http://dx.doi.org/https://doi.org/10.1016/j.atmosenv.2011.06.077. – DOI https://doi.org/10.1016/j.atmosenv.2011.06.077. – ISSN 1352–2310. – Volcanic ash over Europe during the eruption of Eyjafjallajöekull on Iceland, April-May 2010

[Meijer et al. 2001] Meijer, E.W. ; Velthoven, P.F.J. van ; Brunner, D.W. ; Huntrieser, H. ; Kelder, H.: Improvement and evaluation of the parameterisation of nitrogen oxide production by lightning. In: *Physics and Chemistry of the Earth, Part C: Solar, Terrestrial & Planetary Science* 26 (2001), Nr. 8, 577 - 583. http://dx.doi.org/https://doi.org/10.1016/S1464-1917(01)00050-2. – DOI https://doi.org/10.1016/S1464–1917(01)00050–2. – ISSN 1464–1917

[Michel et al. 2005] Michel, C. ; Liousse, C. ; Grégoire, J.-M. ; Tansey, K. ; Carmichael, G. R. ; Woo, J.-H.: Biomass burning emission inventory from burnt area data given by the SPOT-VEGETATION system in the frame of TRACE-P and ACE-Asia campaigns. In: *Journal of Geophysical Research: Atmospheres* 110 (2005), Nr. D9. http://dx.doi.org/10.1029/2004JD005461. – DOI 10.1029/2004JD005461

[Mieville et al. 2010] Mieville, A. ; Granier, C. ; Liousse, C. ; Guillaume, B. ; Mouillot, F. ; Lamarque, J.-F. ; Gregoire, J.-M. ; Petron, G.: Emissions of gases and particles from biomass burning during the 20th century using satellite data and an historical reconstruction. In: *Atmospheric Environment* 44 (2010), Nr. 11, 1469 - 1477. http://dx.doi.org/https://doi.org/10.1016/j.atmosenv.2010.01.011. – DOI https://doi.org/10.1016/j.atmosenv.2010.01.011. – ISSN 1352–2310

[Moritz et al. 2014] Moritz, M A. ; Batllori, E ; Bradstock, R A. ; Gill, A M. ; Handmer, J ; Hessburg, P F. ; Leonard, J ; McCaffrey, S ; Odion, D C. ; Schoennagel, T: Learning to coexist with wildfire. In: *Nature 515*, 2014, S. 58–66

[Mu et al. 2011] Mu, M. ; Randerson, J. T. ; Werf, G. R. d. ; Giglio, L. ; Kasibhatla, P. ; Morton, D. ; Collatz, G. J. ; DeFries, R. S. ; Hyer, E. J. ; Prins, E. M. ; Griffith, D. W. T. ; Wunch, D. ; Toon, G. C. ; Sherlock, V. ; Wennberg, P. O.: Daily and 3-hourly variability in global fire emissions and consequences for atmospheric model predictions of carbon monoxide. In: *Journal of Geophysical Research: Atmospheres* 116 (2011), Nr. D24. http://dx.doi.org/10.1029/2011JD016245. – DOI 10.1029/2011JD016245

[Müller et al. 2008] Müller, J.-F. ; Stavrakou, T. ; Wallens, S. ; De Smedt, I. ; Van Roozendael, M. ; Potosnak, M. J. ; Rinne, J. ; Munger, B. ; Goldstein, A. ; Guenther, A. B.: Global isoprene emissions estimated using MEGAN, ECMWF analyses and a detailed canopy environment model. In: *Atmospheric Chemistry and Physics* 8 (2008), Nr. 5, 1329–1341. http://dx.doi.org/10.5194/acp-8-1329-2008. – DOI 10.5194/acp–8–1329–2008

[Murray et al. 2012] Murray, Lee T. ; Jacob, Daniel J. ; Logan, Jennifer A. ; Hudman, Rynda C. ; Koshak, William J.: Optimized regional and interannual variability of lightning in a global chemical transport model constrained by LIS/OTD satellite data. In: *Journal of Geophysical Research: Atmospheres* 117 (2012), Nr. D20. http://dx.doi.org/10.1029/2012JD017934. – DOI 10.1029/2012JD017934

[Neely and Schmidt 2016] Neely, R R. ; Schmidt, A: VolcanEESM: Global volcanic sulphur dioxide (SO2) emissions database from 1850 to present - Version 1.0. In: *Centre for Environmental Data Analysis* 04 (2016). – http://dx.doi.org/10.5285/76ebdc0b-0eed-4f70-b89e-55e606bcd568

[Nesbit et al. 2016] Nesbit, Martin ; Fergusson, Malcolm ; Colsa, Alejandro ; Ohlendorf, Jana ; Hayes, Christina ; Paquel, Kamila ; Schweitzer, Jean-Pierre: The Differences between the EU and US Legislation on Emissions in the Automotive Sector. In: *Policy Department A: Economic and Scientific Policy, European Parliament* (2016)

[Ng et al. 2017] Ng, N L. ; Brown, S S. ; Archibald, A T. ; Atlas, E ; Cohen, R C. ; Crowley, J N. ; Day, D A. ; Donahue, N M. ; Fry, J L. ; Fuchs, H ; Griffin, R J. ; Guzman, M I. ; Herrmann, H ; Hodzic, A ; Iinuma, Y ; Jimenez, J L. ; Kiendler-Scharr, A ; Lee, B H. ; Luecken, D J. ; Mao, J ; McLaren, R ; Mutzel, A ; Osthoff, H D. ; Ouyang, B ; Picquet-Varrault, B ; Platt, U ; Pye, H ; Rudich, Y ; Schwantes, R H. ; Shiraiwa, M ; Stutz, J ; Thornton, J A. ; Tilgner, A ; Williams, B J.: Nitrate radicals and biogenic volatile organic compounds: oxidation, mechanisms, and organic aerosol. Atmospheric chemistry and physics. In: *Atmos Chem Phys.* 17 (2017), Nr. 3, S. 2103–2162

[von Nieding and Wagner 1979] Nieding, G von ; Wagner, H M.: Effects of NO2 on chronic bronchitics. In: *Environmental Health Perspectives* 29 (1979), 137-142. http://dx.doi.org/10.1289/ehp.7929137. – DOI 10.1289/ehp.7929137

[Oderbolz et al. 2013] Oderbolz, D. C. ; Aksoyoglu, S. ; Keller, J. ; Barmpadimos, I. ; Steinbrecher, R. ; Skjøth, C. A. ; Plass-Dülmer, C. ; Prévôt, A. S. H.: A comprehensive emission inventory of biogenic volatile organic compounds in Europe: improved seasonality and land-cover. In: *Atmospheric Chemistry and Physics* 13 (2013), Nr. 4, 1689–1712. http://dx.doi.org/10.5194/acp-13-1689-2013. – DOI 10.5194/acp–13–1689–2013

[Oenema et al. 2011] Oenema, Oene ; Bleeker, Albert ; Braathen, Nils ; Budňáková, Michaela ; Bull, Keith ; Čermák, Pavel ; Geupel, Markus ; Hicks, Kevin ; Hoft, Robert ; Kozlova, Natalia ; Leip, Adrian ; Spranger, T ; Valli, Laura ; Velthof, Gerard ; Winiwarter, Wilfried: Nitrogen in current European policies. In: *The European Nitrogen Assessment* (2011), 01, S. 62–81. http://dx.doi.org/10.1017/CBO9780511976988.007. – DOI 10.1017/CBO9780511976988.007

[Ortiz-Suslow et al. 2016] Ortiz-Suslow, D. G. ; Haus, B. K. ; Williams, N. J. ; Graber, H. C.: Field Observations of Coastal Air-Sea Interaction. In: *AGU Fall Meeting Abstracts* (2016), Dezember

[Ott et al. 2010] Ott, Lesley E. ; Pickering, Kenneth E. ; Stenchikov, Georgiy L. ; Allen, Dale J. ; DeCaria, Alex J. ; Ridley, Brian ; Lin, Ruei-Fong ; Lang, Stephen ; Tao, Wei-Kuo: Production of lightning NOx and its vertical distribution calculated from three-dimensional cloud-scale chemical transport model simulations. In: *Journal of Geophysical Research: Atmospheres* 115 (2010), Nr. D4. http://dx.doi.org/10.1029/2009JD011880. – DOI 10.1029/2009JD011880

[Peterson and Beasley 2011] Peterson, H. S. ; Beasley, W. H.: Possible catalytic effects of ice particles on the production of NO_x by lightning discharges. In: *Atmospheric Chemistry and Physics* 11 (2011), Nr. 19, 10259–10268. http://dx.doi.org/10.5194/acp-11-10259-2011. – DOI 10.5194/acp–11–10259–2011

[Pierce et al. 2002] Pierce, T ; Geron, C ; Pouliot, G ; Kinnee, E ; Vukovich, J: Integration of the Biogenic Emission Inventory System (BEIS3) into the Community Multiscale Air Quality modeling system. In: *Preprints, 12th Joint Conf. on the Application of Air Pollution Meteorology with the Air and Waste Management Association, Amer. Meteor. Soc., Norfolk, VA, J85?J86.*, 2002

[Pierce and Waldruff 1991] Pierce, Thomas E. ; Waldruff, Paul S.: PC-BEIS: A Personal Computer Version of the Biogenic Emissions Inventory System. In: *Journal of the Air & Waste Management Association* 41 (1991), Nr. 7, 937-941. http://dx.doi.org/10.1080/10473289.1991.10466890. – DOI 10.1080/10473289.1991.10466890

[Pope III et al. 2002] Pope III, C ; Burnett, RT ; Thun, MJ: Lung cancer, cardiopulmonary mortality, and long-term exposure to fine particulate air pollution. In: *JAMA* 287 (2002), Nr. 9, 1132-1141. http://dx.doi.org/10.1001/jama.287.9.1132. – DOI 10.1001/jama.287.9.1132

[Pouliot and Pierce 2009] Pouliot ; Pierce: Integration of the Model of Emissions of Gases and Aerosols from Nature (MEGAN) into the CMAS Modeling System. In: *Presented at 18th Annual International Emission Inventory Conference, Baltimore, MD , April 14-17, accessed: 2017-06-19.* (2009)

[Price and Rind 1992] Price, Colin ; Rind, David: A simple lightning parameterization for calculating global lightning distributions. In: *Journal of Geophysical Research: Atmospheres* 97 (1992), Nr. D9, S. 9919–9933. http://dx.doi.org/10.1029/92JD00719. – DOI 10.1029/92JD00719

[Price and Rind 1993] Price, Colin ; Rind, David: What determines the cloud-to-ground lightning fraction in thunderstorms? In: *Geophysical Research Letters* 20 (1993), Nr. 6, S. 463–466. http://dx.doi.org/10.1029/93GL00226. – DOI 10.1029/93GL00226

[Randerson et al. 2015] Randerson, J T. ; Werf, G R. d. ; Giglio, L ; Collatz, G J. ; Kasibhatla, P S.: Global Fire Emissions Database, version 4 (GFEDv4). In: *Oak Ridge, TN: Oak Ridge National Laboratory Distributed Active Archive Center. doi:10.3334/ORNLDAAC/1293* (2015)

[Rasool et al. 2016] Rasool, Q. Z. ; Zhang, R. ; Lash, B. ; Cohan, D. S. ; Cooter, E. J. ; Bash, J. O. ; Lamsal, L. N.: Enhanced representation of soil NO emissions in the Community Multiscale Air Quality (CMAQ) model version 5.0.2. In: *Geoscientific Model Development* 9 (2016), Nr. 9, 3177–3197. http://dx.doi.org/10.5194/gmd-9-3177-2016. – DOI 10.5194/gmd–9–3177–2016

[Remke et al. 2009] Remke, Eva ; Brouwer, Emiel ; Kooijman, Annemieke ; Blindow, Irmgard ; Esselink, Hans ; Roelofs, Jan G.: Even low to medium nitrogen deposition impacts vegetation of dry, coastal dunes around the Baltic Sea. In: *Environmental Pollution* 157 (2009), Nr. 3, 792 - 800. http://dx.doi.org/https://doi.org/10.1016/j.envpol.2008.11.020. – DOI https://doi.org/10.1016/j.envpol.2008.11.020. – ISSN 0269–7491

[Riahi et al. 2007] Riahi, Keywan ; Grübler, Arnulf ; Nakicenovic, Nebojsa: Scenarios of long-term socio-economic and environmental development under climate stabilization. In: *Technological Forecasting and Social Change* 74 (2007), Nr. 7, 887 - 935. http://dx.doi.org/https://doi.org/10.1016/j.techfore.2006.05.026. – DOI https://doi.org/10.1016/j.techfore.2006.05.026. – ISSN 0040–1625. – Greenhouse Gases - In-

tegrated Assessment

[Ritter and Geleyn 1992] Ritter, B. ; Geleyn, J. F.: A Comprehensive Radiation Scheme For Numerical Weather Prediction Models With Potential Applications In Climate Simulations. In: *Monthly Weather Review* 120 (1992), Februar, Nr. 2, S. 303–325. http://dx.doi.org/10.1175/1520-0493(1992)120<0303:ACRSFN>2.0.CO;2. – DOI 10.1175/1520–0493(1992)120<0303:ACRSFN>2.0.CO;2

[Rockel et al. 2008] Rockel, B. ; Will, A. ; Hense, A.: The Regional Climate Model COSMO-CLM(CCLM). In: *Meteorologische Zeitschrift* 17 (2008), Nr. 4, S. 347–348

[Rogers et al. 1979] Rogers, H. ; Campbell, J. ; Volk, R.: Nitrogen-15 Dioxide Uptake and Incorporation by Phaseolus vulgaris (L.). In: *Science* 206(4416) (1979)

[Rostami et al. 2015] Rostami, Majid ; Monaco, Stefano ; Sacco, Dario ; Grignani, Carlo ; Dinuccio, Elio: Comparison of ammonia emissions from animal wastes and chemical fertilizers after application in the soil. In: *International Journal of Recycling of Organic Waste in Agriculture* 4 (2015), Jun, Nr. 2, 127–134. http://dx.doi.org/10.1007/s40093-015-0092-4. – DOI 10.1007/s40093–015–0092–4. – ISSN 2251–7715

[Sakulyanontvittaya et al. 2010] Sakulyanontvittaya, T ; Piyachaturawat, P ; Yarwood, G ; Guenther, A: Enhancement of GLOBEIS. Final report. In: *Austin, TX:Texas Commission on Environmental Quality* (2010)

[Sakulyanontvittaya et al. 2012] Sakulyanontvittaya, T ; Yarwood, G ; Guenther, A: Improved biogenic emission inventories across the west. Final report. Vintage 19, ENVIRON International Corporation, 2012

[Sala et al. 2000] Sala, O.E. ; F.S., Chapin I. ; Armesto, J.J. ; Berlow, Eric ; Bloomfield, J ; Dirzo, R: Biodiversity: global biodiversity scenarios for the year 2100. In: *Science* 287 (2000), 01, S. 1170–1174

[San-Miguel-Ayanz et al. 2017] San-Miguel-Ayanz, Jesús ; Houston Durrant, Tracy ; Boca, Roberto ; Libertà, Giorgio ; Boccacci, Francesco ; Di Leo, Margherita ; López Pérez, Jorge ; Schulte, Ernst ; Benchikha, Abdelhafid ; Abbas, Mohamed ; Humer, Franz ; Konstantinov, Vladimir ; Pešut, Ivana ; Szabo, Neven ; Papageorgiou, Kostas ; Toumasis, Ioannis ; Kütt, Veljo ; Kõiv, Kadi ; Ruuska, Rami ; Anastasov, Tatjana ; Timovska, Maja ; Michaut, Philippe ; Joannelle, Philippe ; Lachmann, Michaela ; Alexiou, Eirini ; Debreceni, Peter ; Nagy, Dániel ; Nugent, Ciaran ; Piccoli, Daniela ; Micillo, Filippo ; Colletti, Lorenza ; Di Fonzo, Marco ; Di Liberto, Fabrizio ; Leisavnieks, Edijs ; Mitri, George ; Glazko, Zbignev ; Assali, Fouad ; Alaoui M'harzi, Hicham ; Botnen, Dag ; Piwnicki, Joseph ; Szczygieł, Ryszard ; Janeira, Marta ; Borges, Alexandre ; Mara, Septimius ; Sbirnea, Radu ; Eritsov, Andrey ; Longauerová, Valéria ; Jakša, Jošt ; Enriquez, Elsa ; Sandahl, Leif ; Reinhard, Michael ; Conedera, Marco ; Pezzatti, Boris: *Forest fires in Europe, Middle East and North Africa 2016*. 2017. http://dx.doi.org/10.2760/17690. http://dx.doi.org/10.2760/17690. – ISBN 978–92–79–71292–0

[Sausen and Schumann 2000] Sausen, Robert ; Schumann, Ulrich: Estimates of the Climate Response to Aircraft CO2 and NOxEmissions Scenarios. In: *Climatic Change* 44 (2000), Jan, Nr. 1, 27–58. http://dx.doi.org/10.1023/A:1005579306109. – DOI 10.1023/A:1005579306109. – ISSN 1573–1480

[Sauvage et al. 2007] Sauvage, B. ; Martin, R. V. ; Donkelaar, A. van ; Liu, X. ; Chance, K. ; Jaeglé, L. ; Palmer, P. I. ; Wu, S. ; Fu, T.-M.: Remote sensed and in situ constraints on processes affecting tropical tropospheric ozone. In: *Atmospheric Chemistry and Physics* 7 (2007), Nr. 3, 815–838. http://dx.doi.org/10.5194/acp-7-815-2007. – DOI 10.5194/acp–7–815–2007

[Saylor 2013] Saylor, R. D.: The Atmospheric Chemistry and Canopy Exchange Simulation System (ACCESS): model description and application to a temperate deciduous forest canopy. In: *Atmospheric Chemistry and Physics* 13 (2013), Nr. 2, 693–715. http://dx.doi.org/10.5194/acp-13-693-2013. – DOI 10.5194/acp–13–693–2013

[Schaettler et al. 2008] Schaettler, U. ; Doms, G. ; Schraff, C.: A Description of the Nonhydrostatic Regional COSMO-Model Part VII: User's Guide / Deutscher Wetterdienst. 2008. – Forschungsbericht

[Schefczyk and Heinemann 2017] Schefczyk, Lukas ; Heinemann, Günther: Climate change impact on thunderstorms: Analysis of thunderstorm indices using high-resolution regional climate simulations. In: *Meteorologische Zeitschrift* 26 (2017), 10, Nr. 4, 409-419. http://dx.doi.org/10.1127/metz/2017/0749. – DOI 10.1127/metz/2017/0749

[Schimel and Bennett 2004] Schimel, Joshua P. ; Bennett, Jennifer: NITROGEN MINERALIZATION: CHALLENGES OF A CHANGING PARADIGM. In: *Ecology* 85 (2004), Nr. 3, 591-602. http://dx.doi.org/10.1890/03-8002. – DOI 10.1890/03–8002

[Schlünzen et al. 2012] Schlünzen, K H. ; Bungert, Ursula ; Flagg, David D. ; Fock, Björn H ; Gierisch, Andrea ; Grawe, David ; Kirschner, Peter ; Lüpkes, Christof ; Reinhardt, Volker ; Ries, Hinnerk et al.: Technical Documentation of the Multiscale Model System M-SYS. 2012. – Forschungsbericht

[Schlünzen and Sokhi 2008] Schlünzen, K. H. ; Sokhi, Ranjeet S.: Joint Report of COST Action 728 and GURME - Overview of Tools and Methods for Meteorological and Air Pollution Mesoscale Model Evaluation and User Training / WMO. 2008. – Forschungsbericht

[Schrodin and Heise 2001] Schrodin, R. ; Heise, E.: The multi-layer-version of the DWD soil model TERRA/LM. In: *Consortium for Small-Scale Modelling (COSMO) Tech. Rep* 2 (2001), S. 16

[Schumann and Huntrieser 2007] Schumann, U. ; Huntrieser, H.: The global lightning-induced nitrogen oxides source. In: *Atmospheric Chemistry and Physics* 7 (2007), Nr. 14, 3823–3907. http://dx.doi.org/10.5194/acp-7-3823-2007. – DOI 10.5194/acp–7–3823–2007

[Schwede et al. 2005] Schwede, D. ; Pouliot, G. ; Pierce, T.: Changes to the Biogenic Emissions Inventory System Version 3 (BEIS3). In: *Proceedings of the 4th CMAS Models-3 Users Conference 26-28 September 2005. Chapel Hill, NC.*, 2005

[Seinfeld and Pandis 1998] Seinfeld, J ; Pandis, S: *Atmospheric Chemistry and Physics: From Air Pollution to Climate Change.* John Wiley & Sons, 1998. – 1326 S.

[Shepson 2007] *Kapitel* 7. In: Shepson, Paul B.: *Organic Nitrates.* John Wiley & Sons, Ltd, 2007. – ISBN 9780470988657, 269-291

[Simpson et al. 2012] Simpson, D. ; Benedictow, A. ; Berge, H. ; Bergström, R. ; Emberson, L. D. ; Fagerli, H. ; Flechard, C. R. ; Hayman, G. D. ; Gauss, M. ; Jonson, J. E. ; Jenkin, M. E. ; Nyíri, A. ; Richter, C. ; Semeena, V. S. ; Tsyro, S. ; Tuovinen, J.-P. ; Valdebenito, Á. ; Wind, P.: The EMEP MSC-W chemical transport model - technical description. In: *Atmospheric Chemistry and Physics* 12 (2012), Nr. 16, 7825–7865. http://dx.doi.org/10.5194/acp-12-7825-2012. – DOI 10.5194/acp–12–7825–2012

[Simpson et al. 1999] Simpson, David ; Winiwarter, Wilfried ; Börjesson, Gunnar ; Cinderby, Steve ; Ferreiro, Antonio ; Guenther, Alex ; Hewitt, C. N. ; Janson, Robert ; Khalil, M ; Owen, Susan ; E. Pierce, Tom ; Puxbaum, Hans ; Shearer, Martha ; Skiba, U ; Steinbrecher, Rainer ; Tarrasan, Leonor ; G. Oquist, M: Inventorying emissions from nature in Europe. In: *Journal of Geophysical Research-Atmospheres* 104 (1999), 04, S. 8113–8152. http://dx.doi.org/10.1029/98JD02747. – DOI 10.1029/98JD02747

[Sindelarova et al. 2014] Sindelarova, K. ; Granier, C. ; Bouarar, I. ; Guenther, A. ; Tilmes, S. ; Stavrakou, T. ; Müller, J.-F. ; Kuhn, U. ; Stefani, P. ; Knorr, W.: Global data set of biogenic VOC emissions calculated by the MEGAN model over the last 30 years. In: *Atmospheric Chemistry and Physics* 14 (2014), Nr. 17, 9317–9341. http://dx.doi.org/10.5194/acp-14-9317-2014. – DOI 10.5194/acp–14–9317–2014

[Soares and Sofiev 2014] Soares, J ; Sofiev, M: A global wildfire emission and atmospheric composition: Refinement of the integrated system for wild-land fires IS4FIRES. In: *Air Pollut. Model. Appl.* (2014). – xxiii:253-258

[Sofiev et al. 2009] Sofiev, M. ; Vankevich, R. ; Lotjonen, M. ; Prank, M. ; Petukhov, V. ; Ermakova, T. ; Koskinen, J. ; Kukkonen, J.: An operational system for the assimilation of

the satellite information on wild-land fires for the needs of air quality modelling and forecasting. In: *Atmospheric Chemistry and Physics* 9 (2009), Nr. 18, 6833–6847. http://dx.doi.org/10.5194/acp-9-6833-2009. – DOI 10.5194/acp–9–6833–2009

[Sokhi et al. 2018] Sokhi, R. ; Baklanov, A. ; Schlünzen, K.: *Mesoscale Modelling for Meteorological and Air Pollution Applications*. Anthem Press, 2018 http://www.jstor.org/stable/j.ctv80cdh5. – ISBN 9781783088263

[Solazzo et al. 2017] Solazzo, E. ; Bianconi, R. ; Hogrefe, C. ; Curci, G. ; Tuccella, P. ; Alyuz, U. ; Balzarini, A. ; Baró, R. ; Bellasio, R. ; Bieser, J. ; Brandt, J. ; Christensen, J. H. ; Colette, A. ; Francis, X. ; Fraser, A. ; Vivanco, M. G. ; Jiménez-Guerrero, P. ; Im, U. ; Manders, A. ; Nopmongcol, U. ; Kitwiroon, N. ; Pirovano, G. ; Pozzoli, L. ; Prank, M. ; Sokhi, R. S. ; Unal, A. ; Yarwood, G. ; Galmarini, S.: Evaluation and error apportionment of an ensemble of atmospheric chemistry transport modeling systems: multivariable temporal and spatial breakdown. In: *Atmospheric Chemistry and Physics* 17 (2017), Nr. 4, 3001–3054. http://dx.doi.org/10.5194/acp-17-3001-2017. – DOI 10.5194/acp–17–3001–2017

[Sorgoná et al. 2011] Sorgoná, Agostino ; Lupini, Antonio ; Mercati, Francesco ; Di Dio, Luigi ; Sunseri, Francesco ; Abenavoli, Maria: Nitrate uptake along the maize primary root: An integrated physiological and molecular approach. In: *Plant, cell & environment* 34 (2011), 03, S. 1127–40. http://dx.doi.org/10.1111/j.1365-3040.2011.02311.x. – DOI 10.1111/j.1365–3040.2011.02311.x

[Sparks et al. 1997] Sparks, R S J. ; Bursik, M I. ; Carey, S N. ; Gilbert, J ; Glaze, L S. ; Sigurdsson, H ; Woods, A W.: *Volcanic plumes*. Wiley. ISBN: 0471939013, 1997

[Stavrakou et al. 2009] Stavrakou, T. ; Müller, J.-F. ; De Smedt, I. ; Van Roozendael, M. ; Werf, G. R. d. ; Giglio, L. ; Guenther, A.: Global emissions of non-methane hydrocarbons deduced from SCIAMACHY formaldehyde columns through 2003-2006. In: *Atmospheric Chemistry and Physics* 9 (2009), Nr. 11, 3663–3679. http://dx.doi.org/10.5194/acp-9-3663-2009. – DOI 10.5194/acp–9–3663–2009

[Steppeler et al. 2003] Steppeler, J. ; Doms, G. ; Schattler, U. ; Bitzer, H. W. ; Gassmann, A. ; Damrath, U. ; Gregoric, G.: Meso-gamma scale forecasts using the nonhydrostatic model LM. In: *Meteorology and Atmospheric Physics* 82 (2003), Nr. 1-4, S. 75–96. http://dx.doi.org/10.1007/s00703-001-0592-9. – DOI 10.1007/s00703–001–0592–9

[Stockwell et al. 2015] Stockwell, C. E. ; Veres, P. R. ; Williams, J. ; Yokelson, R. J.: Characterization of biomass burning emissions from cooking fires, peat, crop residue, and other fuels with high-resolution proton-transfer-reaction time-of-flight mass spectrometry. In: *Atmospheric Chemistry and Physics* 15 (2015), Nr. 2, 845–865. http://dx.doi.org/10.5194/acp-15-845-2015. – DOI 10.5194/acp–15–845–2015

[Stockwell et al. 2014] Stockwell, C. E. ; Yokelson, R. J. ; Kreidenweis, S. M. ; Robinson, A. L. ; DeMott, P. J. ; Sullivan, R. C. ; Reardon, J. ; Ryan, K. C. ; Griffith, D. W. T. ; Stevens, L.: Trace gas emissions from combustion of peat, crop residue, domestic biofuels, grasses, and other fuels: configuration and Fourier transform infrared (FTIR) component of the fourth Fire Lab at Missoula Experiment (FLAME-4). In: *Atmospheric Chemistry and Physics* 14 (2014), Nr. 18, 9727–9754. http://dx.doi.org/10.5194/acp-14-9727-2014. – DOI 10.5194/acp–14–9727–2014

[Stohl et al. 2015] Stohl, A. ; Aamaas, B. ; Amann, M. ; Baker, L. H. ; Bellouin, N. ; Berntsen, T. K. ; Boucher, O. ; Cherian, R. ; Collins, W. ; Daskalakis, N. ; Dusinska, M. ; Eckhardt, S. ; Fuglestvedt, J. S. ; Harju, M. ; Heyes, C. ; Hodnebrog, Ø. ; Hao, J. ; Im, U. ; Kanakidou, M. ; Klimont, Z. ; Kupiainen, K. ; Law, K. S. ; Lund, M. T. ; Maas, R. ; MacIntosh, C. R. ; Myhre, G. ; Myriokefalitakis, S. ; Olivié, D. ; Quaas, J. ; Quennehen, B. ; Raut, J.-C. ; Rumbold, S. T. ; Samset, B. H. ; Schulz, M. ; Seland, Ø. ; Shine, K. P. ; Skeie, R. B. ; Wang, S. ; Yttri, K. E. ; Zhu, T.: Evaluating the climate and air quality impacts of short-lived pollutants. In: *Atmospheric Chemistry and Physics* 15 (2015), Nr. 18, 10529–10566. http://dx.doi.org/10.5194/acp-15-10529-2015. –

DOI 10.5194/acp–15–10529–2015

[Stohl et al. 2011] Stohl, A. ; Prata, A. J. ; Eckhardt, S. ; Clarisse, L. ; Durant, A. ; Henne, S. ; Kristiansen, N. I. ; Minikin, A. ; Schumann, U. ; Seibert, P. ; Stebel, K. ; Thomas, H. E. ; Thorsteinsson, T. ; Tørseth, K. ; Weinzierl, B.: Determination of time- and height-resolved volcanic ash emissions and their use for quantitative ash dispersion modeling: the 2010 Eyjafjallajökull eruption. In: *Atmospheric Chemistry and Physics* 11 (2011), Nr. 9, 4333–4351. http://dx.doi.org/10.5194/acp-11-4333-2011. – DOI 10.5194/acp–11–4333–2011

[Strand et al. 1998] Strand, V ; Svartengren, M ; Rak, S ; Barck, C ; Bylin, G: Repeated exposure to an ambient level of NO2 enhances asthmatic response to a nonsymptomatic allergen dose. In: *European Respiratory Journal* 12 (1998), Nr. 1, 6–12. https://erj.ersjournals.com/content/12/1/6. – ISSN 0903–1936

[Sutton et al. 2011a] In: Sutton, M. A. ; Howard, C. M. ; Erisman, J. W. ; Billen, G. ; Bleeker, A. ; Grennfelt, P. ; Grinsven, H. van ; Grizzetti, B.: *Managing nitrogen in relation to key societal threats.* Cambridge University Press, 2011, S. 377–378

[Sutton et al. 2011b] In: Sutton, M. A. ; Howard, C. M. ; Erisman, J. W. ; Billen, G. ; Bleeker, A. ; Grennfelt, P. ; Grinsven, H. van ; Grizzetti, B.: *Nitrogen processing in the biosphere.* Cambridge University Press, 2011, S. 97–98

[Syakila and Kroeze 2011] Syakila, Alfi ; Kroeze, Carolien: The global nitrous oxide budget revisited. In: *Greenhouse Gas Measurement and Management* 1 (2011), Nr. 1, 17-26. http://dx.doi.org/10.3763/ghgmm.2010.0007. – DOI 10.3763/ghgmm.2010.0007

[Tiedtke 1989] Tiedtke, M.: A Comprehensive Mass Flux Scheme For Cumulus Parameterization In Large-scale Models. In: *Monthly Weather Review* 117 (1989), August, Nr. 8, S. 1779–1800. http://dx.doi.org/10.1175/1520-0493(1989)117<1779:ACMFSF>2.0.CO;2. – DOI 10.1175/1520–0493(1989)117<1779:ACMFSF>2.0.CO;2

[Tischner 2000] Tischner, R.: Nitrate uptake and reduction in higher and lower plants. In: *Plant, Cell & Environment* 23 (2000), Nr. 10, 1005-1024. http://dx.doi.org/10.1046/j.1365-3040.2000.00595.x. – DOI 10.1046/j.1365–3040.2000.00595.x

[Tørseth et al. 2012] Tørseth, K. ; Aas, W. ; Breivik, K. ; Fjæraa, A. M. ; Fiebig, M. ; Hjellbrekke, A. G. ; Lund Myhre, C. ; Solberg, S. ; Yttri, K. E.: Introduction to the European Monitoring and Evaluation Programme (EMEP) and observed atmospheric composition change during 1972-2009. In: *Atmos. Chem. Phys.* 12 (2012). http://dx.doi.org/10.5194/acp-12-5447-2012. – DOI 10.5194/acp–12–5447–2012

[Townsend et al. 2003] Townsend, Alan ; Howarth, R ; A. Bazzaz, Fakhri ; Booth, Mary ; Cleveland, Cory ; Collinge, Sharon ; Dobson, Andy ; R. Epstein, Paul ; Holland, Elisabeth ; R. Keeney, Dennis ; A. Mallin, Michael ; Rogers, Christine ; Wayne, Peter ; H. Wolfe, Amir: Human Health Effects of a Changing Global Nitrogen Cycle. In: *Christine A Rogers* 1 (2003), 06. http://dx.doi.org/10.2307/3868011. – DOI 10.2307/3868011

[Turco et al. 2018] Turco, Marco ; Rosa-Cánovas, Juan ; Bedia, Joaquín ; Jerez, Sonia ; Montávez, J ; Carmen Llasat, Maria ; Provenzale, Antonello: Exacerbated fires in Mediterranean Europe due to anthropogenic warming projected with non-stationary climate-fire models. In: *Nature Communications* 9 (2018), 12. http://dx.doi.org/10.1038/s41467-018-06358-z. – DOI 10.1038/s41467–018–06358–z

[US EPA Office of Research and Development 2012] US EPA Office of Research and Development: CMAQv5.0. (2012), Februar. http://dx.doi.org/10.5281/zenodo.1079888. – DOI 10.5281/zenodo.1079888. – For up-to-date documentation, source code, and sample run scripts, please clone or download the CMAQ git repository available through GitHub: https://github.com/USEPA/CMAQ/tree/5.0

[Vedrenne et al. 2016] Vedrenne, Michel ; Borge, Rafael ; Lumbreras, Julio ; Rodriguez, Encarnacion ; Paz, David ; Perez, Javier ; Andres Almeida, Juan M. ; Quaassdorff, Christina: A comprehensive approach for the evaluation and comparison of emission inventories in Madrid. In: *Atmospheric Environment* 145 (2016), 29

- 44. http://dx.doi.org/https://doi.org/10.1016/j.atmosenv.2016.09.020. – DOI https://doi.org/10.1016/j.atmosenv.2016.09.020. – ISSN 1352–2310

[Vinken et al. 2014] Vinken, G. C. M. ; Boersma, K. F. ; Donkelaar, A. van ; Zhang, L.: Constraints on ship NO_x emissions in Europe using GEOS-Chem and OMI satellite NO_2 observations. In: *Atmospheric Chemistry and Physics* 14 (2014), Nr. 3, 1353–1369. http://dx.doi.org/10.5194/acp-14-1353-2014. – DOI 10.5194/acp–14–1353–2014

[Voss et al. 2011] Voss, Maren ; Baker, A ; Bange, Hermann ; Conley, Daniel ; Cornell, Sarah ; Deutsch, Barbara ; Engel, Anja ; Ganeshram, Raja ; Garnier, Josette ; Heiskanen, Anna-Stiina ; Jickells, T ; Lancelot, C ; McQuatters-Gollop, Abigail ; Middelburg, Jack ; Schiedek, D ; Slomp, C.P. ; Conley, D.P.: Chapter 8: Nitrogen processes in coastal and marine ecosystems. In: *Continental Shelf Research* 21 (2011), 01, S. 2073–2094

[Vukovich and Pierce 2002] Vukovich, J ; Pierce, T.: The Implementation of BEIS3 within the SMOKE Modeling Framework. In: *Proceedings of the 11th International Emissions Inventory Conference. Atlanta, Georgia. April 15-18* (2002)

[Wang et al. 2013] Wang, Lihua ; Newchurch, M.J. ; Pour-Biazar, Arastoo ; Kuang, Shi ; Khan, Maudood ; Liu, Xiong ; Koshak, William ; Chance, Kelly: Estimating the influence of lightning on upper tropospheric ozone using NLDN lightning data and CMAQ model. In: *Atmospheric Environment* 67 (2013), 219 - 228. http://dx.doi.org/https://doi.org/10.1016/j.atmosenv.2012.11.001. – DOI https://doi.org/10.1016/j.atmosenv.2012.11.001. – ISSN 1352–2310

[Wang et al. 1998] Wang, Y. ; Jacob, D.J. ; Logan, J.A.: Global Simulation of tropospheric O3-NOx-hydrocarbon chemistry: 1. Model formulation. In: *J. Geophys. Res.* 103(D9) (1998), S. 10713–10725. http://dx.doi.org/10.1029/98JD00158. – DOI 10.1029/98JD00158

[Ward et al. 2005] Ward, Mary ; M deKok, Theo ; Levallois, Patrick ; Brender, Jean ; Gulis, Gabriel ; T Nolan, Bernard ; Vanderslice, James: Drinking Water Nitrate and Health - Recent Findings and Research Needs. In: *Environmental health perspectives* 113 (2005), 12, S. 1607–14. http://dx.doi.org/10.1289/ehp.8043. – DOI 10.1289/ehp.8043

[Wasiuk et al. 2016] Wasiuk, Donata ; Khan, Md ; Shallcross, Dudley ; Lowenberg, Mark: A Commercial Aircraft Fuel Burn and Emissions Inventory for 2005-2011. In: *Atmosphere* 7 (2016), Jun, Nr. 6, 78. http://dx.doi.org/10.3390/atmos7060078. – DOI 10.3390/atmos7060078. – ISSN 2073–4433

[van der Werf et al. 2006] Werf, G. R. d. ; Randerson, J. T. ; Giglio, L. ; Collatz, G. J. ; Kasibhatla, P. S. ; Arellano Jr., A. F.: Interannual variability in global biomass burning emissions from 1997 to 2004. In: *Atmospheric Chemistry and Physics* 6 (2006), Nr. 11, 3423–3441. http://dx.doi.org/10.5194/acp-6-3423-2006. – DOI 10.5194/acp–6–3423–2006

[van der Werf et al. 2010] Werf, G. R. d. ; Randerson, J. T. ; Giglio, L. ; Collatz, G. J. ; Mu, M. ; Kasibhatla, P. S. ; Morton, D. C. ; DeFries, R. S. ; Jin, Y. ; Leeuwen, T. T.: Global fire emissions and the contribution of deforestation, savanna, forest, agricultural, and peat fires (1997–2009). In: *Atmospheric Chemistry and Physics* 10 (2010), Nr. 23, 11707–11735. http://dx.doi.org/10.5194/acp-10-11707-2010. – DOI 10.5194/acp–10–11707–2010

[van der Werf et al. 2017] Werf, G. R. d. ; Randerson, J. T. ; Giglio, L. ; Leeuwen, T. T. ; Chen, Y. ; Rogers, B. M. ; Mu, M. ; Marle, M. J. E. ; Morton, D. C. ; Collatz, G. J. ; Yokelson, R. J. ; Kasibhatla, P. S.: Global fire emissions estimates during 1997–2016. In: *Earth System Science Data* 9 (2017), Nr. 2, 697–720. http://dx.doi.org/10.5194/essd-9-697-2017. – DOI 10.5194/essd–9–697–2017

[Wesely 1989] Wesely, M.L.: Parameterization of surface resistances to gaseous dry deposition in regional-scale numerical models. In: *Atmospheric Environment (1967)* 23 (1989), Nr. 6, 1293 - 1304. http://dx.doi.org/https://doi.org/10.1016/0004-6981(89)90153-4. – DOI https://doi.org/10.1016/0004–6981(89)90153–4. – ISSN 0004–6981

[Weyer 2018] Weyer, Jost: *Geschichte der Chemie Band 1 Altertum, Mittelalter, 16. bis 18. Jahrhundert*. 1. Springer Spektrum, 2018. http://dx.doi.org/10.1007/978-3-662-55798-3. http://dx.doi.org/10.1007/978-3-662-55798-3

[Wiedinmyer et al. 2011] Wiedinmyer, C. ; Akagi, S. K. ; Yokelson, R. J. ; Emmons, L. K. ; Al-Saadi, J. A. ; Orlando, J. J. ; Soja, A. J.: The Fire INventory from NCAR (FINN): a high resolution global model to estimate the emissions from open burning. In: *Geoscientific Model Development* 4 (2011), Nr. 3, 625–641. http://dx.doi.org/10.5194/gmd-4-625-2011. – DOI 10.5194/gmd–4–625–2011

[Wiedinmyer et al. 2006] Wiedinmyer, Christine ; Quayle, Brad ; Geron, Chris ; Belote, Angie ; McKenzie, Don ; Zhang, Xiaoyang ; Neill, Susan O. ; Wynne, Kristina K.: Estimating emissions from fires in North America for air quality modeling. In: *Atmospheric Environment* 40 (2006), Nr. 19, 3419 - 3432. http://dx.doi.org/https://doi.org/10.1016/j.atmosenv.2006.02.010. – DOI https://doi.org/10.1016/j.atmosenv.2006.02.010. – ISSN 1352–2310

[Wilkerson et al. 2010] Wilkerson, J. T. ; Jacobson, M. Z. ; Malwitz, A. ; Balasubramanian, S. ; Wayson, R. ; Fleming, G. ; Naiman, A. D. ; Lele, S. K.: Analysis of emission data from global commercial aviation: 2004 and 2006. In: *Atmospheric Chemistry and Physics* 10 (2010), Nr. 13, 6391–6408. http://dx.doi.org/10.5194/acp-10-6391-2010. – DOI 10.5194/acp–10–6391–2010

[Williams and Fehsenfeld 1991] Williams, E.J. ; Fehsenfeld, F.C.: MEASUREMENT OF SOIL NITROGEN OXIDE EMISSIONS AT THREE NORTH AMERICAN ECOSYSTEMS. In: *JOURNAL OF GEOPHYSICAL RESEARCH* 96 (1991)

[Yarwood et al. 2010] Yarwood, G ; Jung, J ; Whitten, G Z. ; Heo, G ; Mellberg, J ; Estes, M: Updates to the Carbon Bond mechanism for version 6 (CB6. In: *2010 CMAS Conference, Chapel Hill*, 2010. – pdf (accessed

[Yarwood et al. 1999] Yarwood, G ; Wilson, G ; Emery, C ; Guenther, A: Development of GLOBEIS-A State of the science biogenic emissions modeling system. Final report to the Texas. In: *Austin, TX: Natural Resource Conservation Commission* (1999)

[Yienger and Levy 1995] Yienger, J. J. ; Levy, H.: Empirical model of global soil-biogenic NOx emissions. In: *Journal of Geophysical Research: Atmospheres* 100 (1995), Nr. D6, 11447–11464. http://dx.doi.org/10.1029/95JD00370. – DOI 10.1029/95JD00370. – ISSN 2156–2202

[Yokelson et al. 2013] Yokelson, R. J. ; Burling, I. R. ; Gilman, J. B. ; Warneke, C. ; Stockwell, C. E. ; Gouw, J. de ; Akagi, S. K. ; Urbanski, S. P. ; Veres, P. ; Roberts, J. M. ; Kuster, W. C. ; Reardon, J. ; Griffith, D. W. T. ; Johnson, T. J. ; Hosseini, S. ; Miller, J. W. ; Cocker III, D. R. ; Jung, H. ; Weise, D. R.: Coupling field and laboratory measurements to estimate the emission factors of identified and unidentified trace gases for prescribed fires. In: *Atmospheric Chemistry and Physics* 13 (2013), Nr. 1, 89–116. http://dx.doi.org/10.5194/acp-13-89-2013. – DOI 10.5194/acp–13–89–2013

[Zhang et al. 2003] Zhang, Xingjun ; Helsdon, John H. ; Farley, Richard D.: Numerical modeling of lightning-produced NOx using an explicit lightning scheme: 2. Three-dimensional simulation and expanded chemistry. In: *Journal of Geophysical Research: Atmospheres* 108 (2003), Nr. D18

[Zhao et al. 2016] Zhao, C. ; Huang, M. ; Fast, J. D. ; Berg, L. K. ; Qian, Y. ; Guenther, A. ; Gu, D. ; Shrivastava, M. ; Liu, Y. ; Walters, S. ; Pfister, G. ; Jin, J. ; Shilling, J. E. ; Warneke, C.: Sensitivity of biogenic volatile organic compounds to land surface parameterizations and vegetation distributions in California. In: *Geoscientific Model Development* 9 (2016), Nr. 5, 1959–1976. http://dx.doi.org/10.5194/gmd-9-1959-2016. – DOI 10.5194/gmd–9–1959–2016

List of Figures

List of Tables

A Appendix

A.1 Supplement to manuscript 2

Implementation of different big-leaf canopy reduction functions in the Biogenic Emission Inventory System (BEIS) and their impact on concentrations of oxidized nitrogen species in northern Europe

Supplementary material of the original publication

In this appendix chapter the supplement with the publication of manuscript 2 is presented. The supplement includes the full evaluation result table of the EMEP measurement stations from chapter 4 and table 4.3 in the table A.1 and A.2. Furthermore the flowcharts describing the technical model process are presented in figures A.1 to A.4.

Table A.1: EMEP evaluation table (part 1) from the supplement of the manuscript for the three canopy reduction parameterizations. For evaluation description, see the full manuscript.

	Cor				FB				IOA			
Station	Ref	VP02	WA98	YL95	Ref	VP02	WA98	YL95	Ref	VP02	WA98	YL95
Offagne	0,565	0,569	0,561	0,570	0,089	0,102	0,087	0,103	0,591	0,563	0,589	0,562
Eupen	0,290	0,288	0,290	0,289	0,145	0,151	0,147	0,152	0,457	0,445	0,455	0,445
Vezin	0,747	0,738	0,749	0,738	0,103	0,111	0,105	0,110	0,797	0,775	0,798	0,775
Westerland	0,668	0,668	0,668	0,668	-0,136	-0,135	-0,136	-0,135	0,743	0,749	0,745	0,750
Waldhof	0,552	0,543	0,560	0,544	-0,039	-0,025	-0,037	-0,025	0,704	0,717	0,711	0,718
Schauinsland	0,353	0,360	0,355	0,360	0,271	0,276	0,271	0,276	0,258	0,252	0,260	0,251
Neuglobsow	0,666	0,671	0,664	0,672	-0,078	-0,054	-0,077	-0,054	0,681	0,730	0,676	0,731
Schmücke	0,458	0,448	0,469	0,449	0,010	0,018	0,009	0,019	0,609	0,588	0,618	0,588
Zingst	0,729	0,726	0,728	0,726	-0,013	-0,003	-0,014	-0,003	0,752	0,743	0,753	0,743
Keldsnor	0,699	0,701	0,699	0,701	0,037	0,040	0,038	0,040	0,822	0,822	0,821	0,822
Anholt	0,686	0,686	0,686	0,687	-0,035	-0,031	-0,034	-0,031	0,665	0,663	0,665	0,663
Risoe	0,814	0,814	0,813	0,814	0,034	0,044	0,035	0,044	0,877	0,868	0,876	0,868
Lahemaa	0,557	0,558	0,557	0,558	0,130	0,155	0,139	0,155	0,372	0,367	0,369	0,367
Vilsandi	0,276	0,277	0,275	0,277	0,001	0,011	0,005	0,011	0,310	0,311	0,309	0,311
Utö	0,505	0,505	0,505	0,505	0,006	0,023	0,019	0,023	0,538	0,538	0,538	0,538
Virolahti II	0,710	0,710	0,710	0,710	-0,052	-0,041	-0,048	-0,041	0,730	0,727	0,728	0,727
Oulanka	0,320	0,325	0,316	0,325	-0,266	-0,241	-0,255	-0,241	0,470	0,483	0,473	0,483
Ähtäri II	0,453	0,447	0,458	0,447	-0,034	-0,025	-0,032	-0,025	0,677	0,677	0,680	0,677
Hyytiälä	0,539	0,534	0,539	0,534	0,047	0,058	0,048	0,058	0,678	0,667	0,675	0,667
Preila	0,469	0,483	0,471	0,483	-0,093	-0,080	-0,089	-0,080	0,619	0,642	0,624	0,642
Rucava	0,184	0,174	0,202	0,174	0,052	0,093	0,060	0,093	0,383	0,342	0,401	0,342
Eibergen	0,696	0,698	0,698	0,698	0,005	0,016	0,009	0,016	0,826	0,821	0,827	0,821
Kollumerwaard	0,735	0,736	0,740	0,736	0,318	0,324	0,319	0,324	0,239	0,231	0,238	0,231
Vredepeel	0,791	0,794	0,793	0,794	-0,010	-0,002	-0,008	-0,002	0,879	0,886	0,881	0,886
De Zilk	0,751	0,752	0,752	0,752	0,300	0,301	0,300	0,301	0,267	0,264	0,267	0,264
Birkenes II	0,545	0,539	0,545	0,539	0,121	0,130	0,121	0,130	0,471	0,460	0,470	0,460
Tustervatn	0,164	0,171	0,169	0,171	-0,086	-0,066	-0,076	-0,066	0,499	0,503	0,502	0,503
Kårvatn	-0,048	-0,065	-0,056	-0,065	-0,029	-0,006	-0,008	-0,006	0,317	0,294	0,302	0,294
Hurdal	0,426	0,424	0,427	0,424	0,110	0,114	0,110	0,114	0,430	0,424	0,431	0,424
Jarczew	0,373	0,366	0,370	0,365	-0,175	-0,154	-0,164	-0,154	0,484	0,512	0,488	0,512
Sniezka	-0,022	-0,018	-0,021	-0,018	-0,005	0,011	-0,008	0,011	0,346	0,356	0,345	0,356
Leba	0,572	0,573	0,576	0,573	-0,051	-0,046	-0,049	-0,046	0,733	0,738	0,736	0,738
Diabla Gora	0,182	0,158	0,181	0,159	0,048	0,087	0,047	0,087	0,458	0,435	0,451	0,436
Vavihill	0,568	0,563	0,571	0,563	0,063	0,084	0,063	0,084	0,657	0,622	0,660	0,622
Aspvreten	0,457	0,455	0,457	0,455	0,110	0,112	0,110	0,112	0,425	0,419	0,423	0,419
Råö	0,289	0,292	0,290	0,292	0,038	0,040	0,039	0,040	0,395	0,393	0,395	0,393
Mean	0,522	0,522	5,525	0,523	0,0387	0,0386	0,0291	0,026	0,556	0,556	0,561	0,560

Table A.2: EMEP evaluation table (part 2) from the supplement of the manuscript for the three canopy reduction parameterizations. For evaluation description, see the full manuscript.

	RMSEP				MNB			
Station	Ref	VP02	WA98	YL95	Ref	VP02	WA98	YL95
Offagne	1,026	1,125	1,028	1,127	0,422	0,489	0,423	0,491
Eupen	2,149	2,244	2,156	2,245	0,890	0,947	0,899	0,948
Vezin	1,234	1,336	1,228	1,337	0,390	0,446	0,395	0,447
Westerland	0,760	0,754	0,758	0,754	-0,348	-0,337	-0,345	-0,336
Waldhof	0,621	0,611	0,613	0,610	-0,129	-0,059	-0,124	-0,057
Schauinsland	1,009	1,049	1,000	1,049	2,386	2,481	2,365	2,484
Neuglobsow	0,466	0,420	0,470	0,419	-0,257	-0,195	-0,261	-0,194
Schmücke	0,417	0,447	0,412	0,447	0,090	0,133	0,092	0,135
Zingst	0,875	0,902	0,872	0,902	0,083	0,119	0,086	0,119
Keldsnor	1,191	1,199	1,193	1,199	0,078	0,091	0,083	0,092
Anholt	1,183	1,194	1,184	1,194	0,078	0,089	0,082	0,089
Risoe	0,677	0,710	0,676	0,711	0,132	0,164	0,134	0,165
Lahemaa	1,140	1,163	1,152	1,163	1,196	1,321	1,244	1,321
Vilsandi	0,953	0,950	0,955	0,950	0,750	0,782	0,762	0,782
Utö	1,110	1,111	1,110	1,111	0,321	0,330	0,325	0,330
Virolahti II	0,551	0,556	0,555	0,556	-0,004	0,023	0,005	0,023
Oulanka	0,144	0,137	0,142	0,137	-0,644	-0,590	-0,627	-0,590
Ähtäri II	0,097	0,097	0,096	0,097	-0,006	0,033	-0,002	0,033
Hyytiälä	0,122	0,127	0,123	0,127	0,439	0,484	0,450	0,484
Preila	0,398	0,392	0,395	0,392	-0,256	-0,210	-0,243	-0,210
Rucava	0,355	0,443	0,342	0,443	0,485	0,739	0,480	0,740
Eibergen	0,957	0,990	0,952	0,991	0,075	0,112	0,081	0,114
Kollumerwaard	2,075	2,162	2,084	2,163	3,787	3,937	3,807	3,940
Vredepeel	1,036	1,020	1,029	1,020	-0,026	0,005	-0,022	0,005
De Zilk	3,810	3,863	3,817	3,865	3,627	3,665	3,634	3,666
Birkenes II	0,401	0,413	0,402	0,413	1,212	1,284	1,220	1,285
Tustervatn	0,098	0,096	0,097	0,096	0,104	0,181	0,153	0,181
Kårvatn	0,107	0,110	0,109	0,110	0,411	0,518	0,490	0,518
Hurdal	0,528	0,540	0,528	0,540	1,066	1,106	1,068	1,106
Jarczew	1,105	1,009	1,080	1,008	-0,410	-0,343	-0,396	-0,342
Sniezka	0,491	0,495	0,491	0,495	0,203	0,280	0,202	0,282
Leba	0,442	0,440	0,439	0,440	-0,146	-0,111	-0,143	-0,110
Diabla Gora	0,352	0,414	0,355	0,414	0,381	0,615	0,390	0,615
Vavihill	0,598	0,666	0,590	0,667	0,369	0,470	0,367	0,471
Aspvreten	0,362	0,367	0,363	0,367	0,634	0,656	0,639	0,656
Råö	1,045	1,057	1,044	1,057	0,452	0,477	0,458	0,478
Mean	0,851	0,850	0,829	0,830	0,560	0,559	0,505	0,495

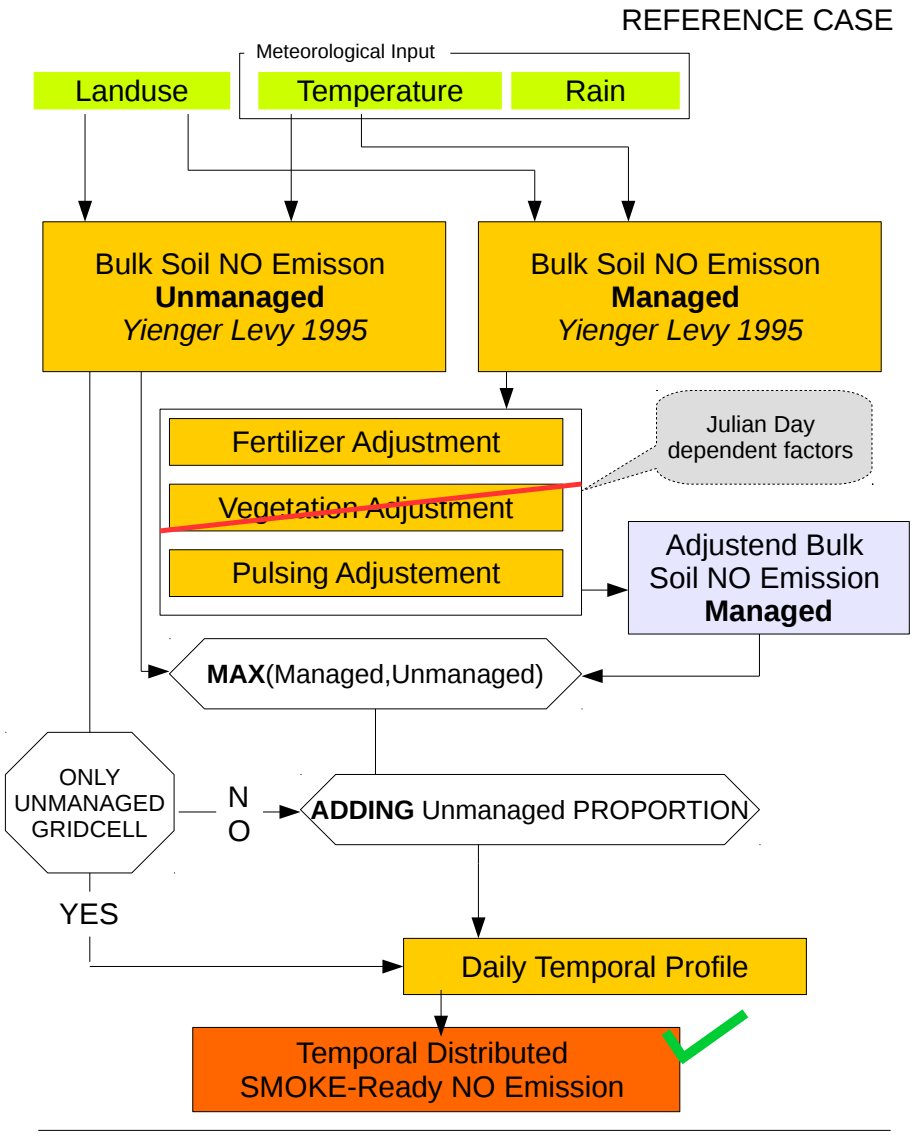

Suppl. Flowchart 1

Figure A.1: From the supplement of publication „Implementation of different big-leaf canopy reduction functions in the Biogenic Emission Inventory System (BEIS) and their impact on concentrations of oxidized nitrogen species in northern Europe “: Flowchart describing the model procedure to create biogenic NO emissions in BEIS in the REFERENCE CASE

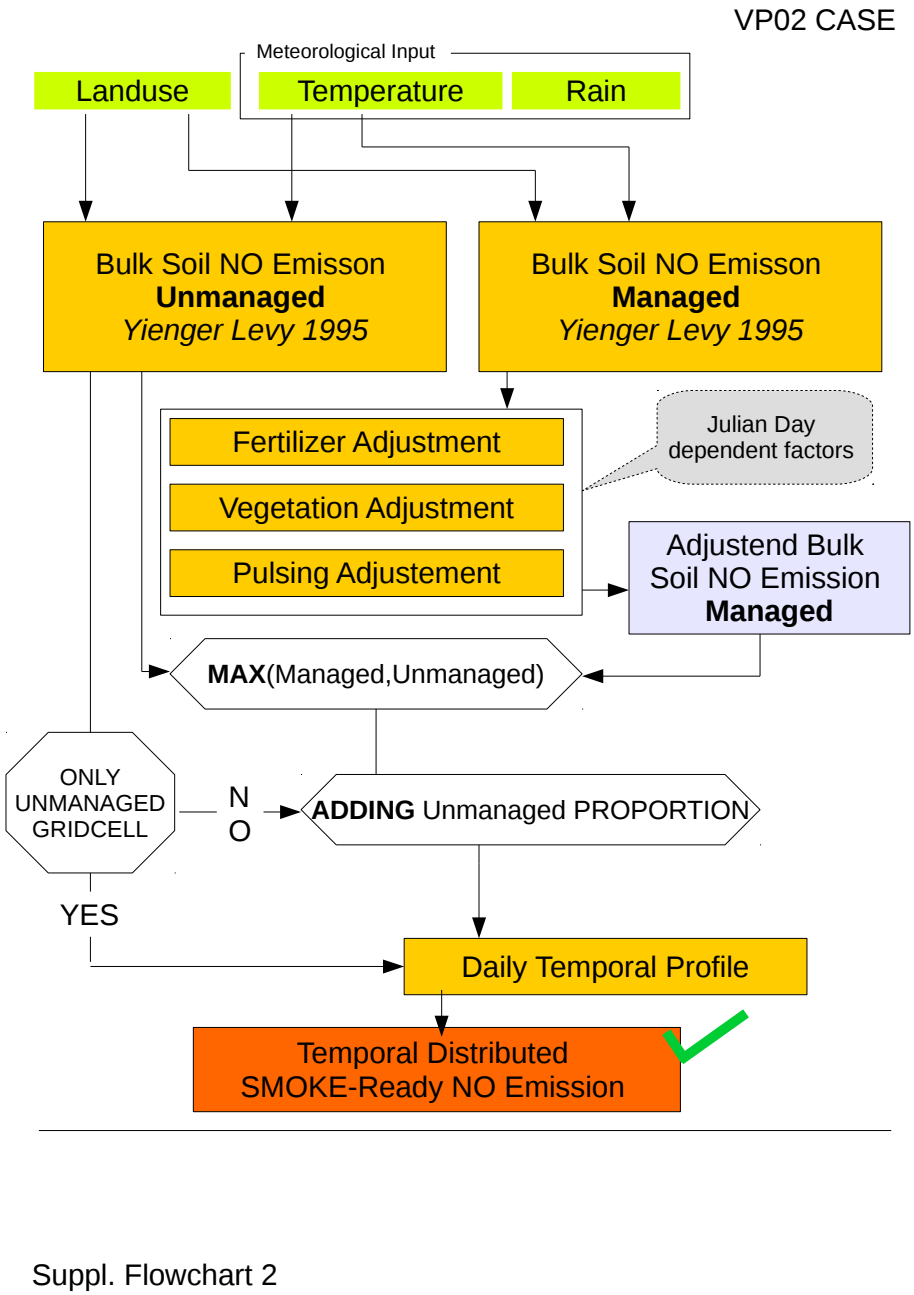

Suppl. Flowchart 2

Figure A.2: From the supplement of publication „Implementation of different big-leaf canopy reduction functions in the Biogenic Emission Inventory System (BEIS) and their impact on concentrations of oxidized nitrogen species in northern Europe “: Flowchart describing the model procedure to create biogenic NO emissions in BEIS with canopy reduction in the in the VP02 CASE

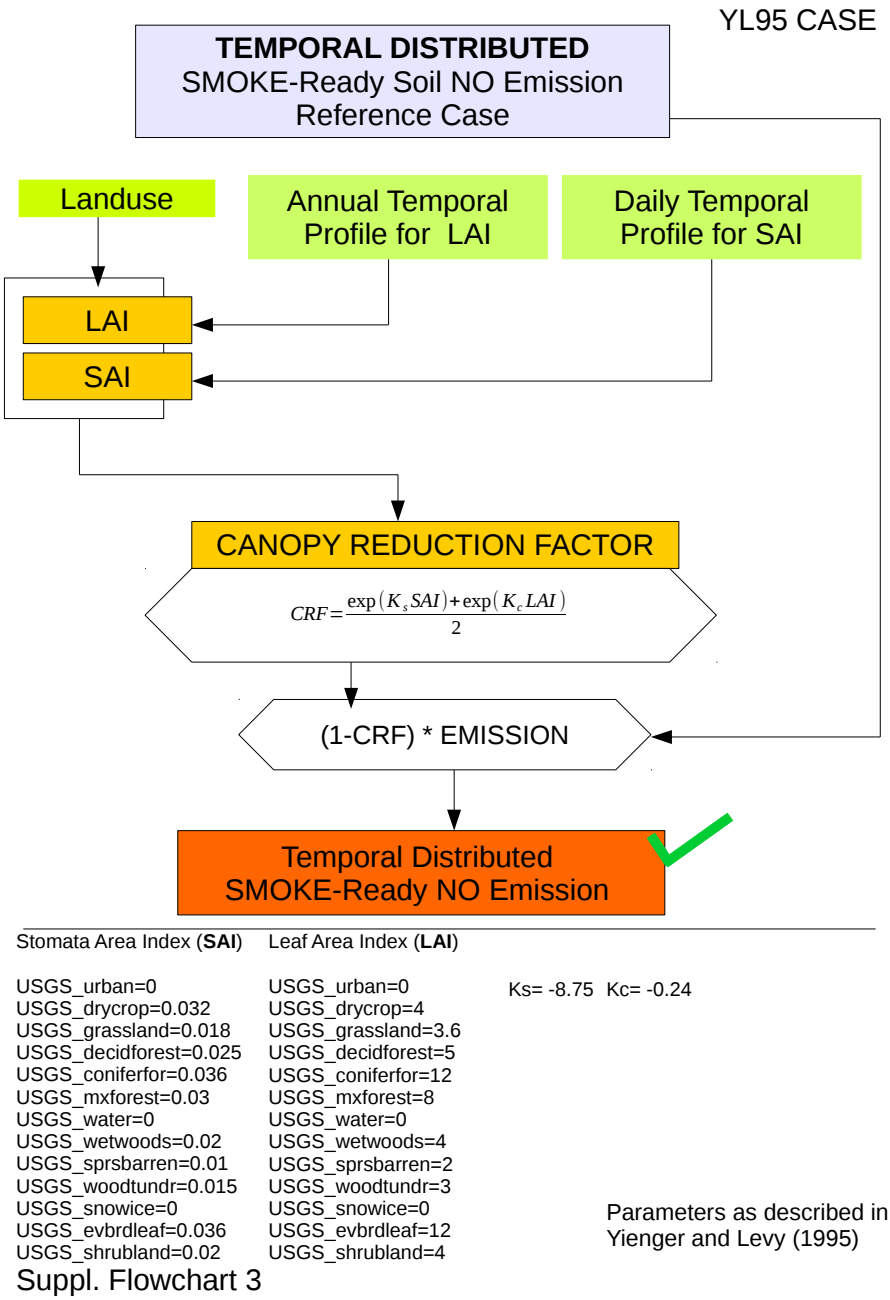

Figure A.3: From the supplement of publication „Implementation of different big-leaf canopy reduction functions in the Biogenic Emission Inventory System (BEIS) and their impact on concentrations of oxidized nitrogen species in northern Europe “: Flowchart describing the model procedure to create biogenic NO emissions in BEIS with canopy reduction in the in the YL95 CASE

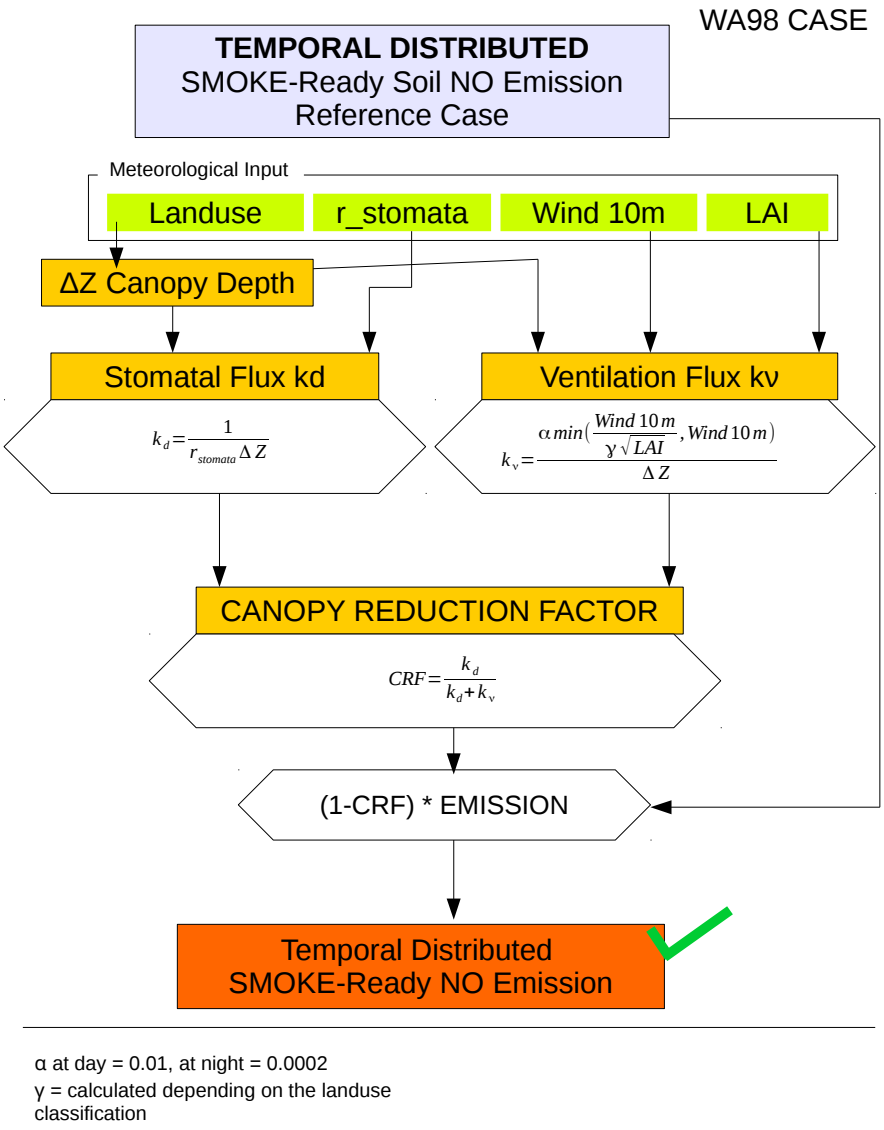

Figure A.4: From the supplement of publication „Implementation of different big-leaf canopy reduction functions in the Biogenic Emission Inventory System (BEIS) and their impact on concentrations of oxidized nitrogen species in northern Europe “: Flowchart describing the model procedure to create biogenic NO emissions in BEIS with canopy reduction in the in the WA98 CASE

A.2 Addendum to manuscript 3

Quantification of lightning-induced nitrogen oxide emissions over Europe

In this appendix chapter the supplement with the publication of manuscript 3 is presented. Table A.3 shows the original acronyms list used in the published version of the manuscript.

Table A.3: The original acronyms list used in the published version of the manuscript „Quantification of lightning-induced nitrogen oxide emissions over Europe“.

CBo5tucl AE6	carbon bond 5 chemistry mechanism with ISORROPIA AE6 aerosol mechanism
CMAQ	Community Multi-scale Air Quality Model
corr	linear Correlation coefficient
COSMO-CLM	Consortium for small scale modeling - Climate limited-area modelling-community
CTH	Cloud top height
DWD	Deutscher Wetterdienst
ECMWF	European Centre for Medium-Range Weather Forecasts
EMEP	European Monitoring and Evaluation program
EULINOX	The European Lightning Nitrogen Oxides Project
GEOS-CHEM	Goddard Earth Observing System Chemistry transport model
HRMC	High-Resolution Monthly Climatology
HTAP	Hemispheric Transport of Air Pollution
LIS/OTD	Lightning Imaging Sensor / Optical transient detector
MCIP	Meteorological Preprocessor for CMAQ
mol/fl.	Emission factor in mole N per flash
NASA	National Aeronautics and Space Administration
nm	Nanometer
NMB	Normalized mean bias
NO	Nitrogen oxide
NO2	Nitrogen dioxide
NO_y	NO + NO_2 + HONO + PAN + N_2O_5 + HNO_3 + NO_3
NH_x	NH_3 + NH_4^+
OMI	Ozone Measurement Instrument
PBL	Planetary boundary layer
RMSEP	Root mean square error of prediction
SMOKE-EU	Sparse Matrix Operator Kernel Emissions for Europe
STEAM	Ship Traffic Emission Assessment Model
TEMIS	Tropospheric Emission Monitoring Internet Service
Tg N	Teragram with respect to the mol weight of nitrogen
TRMM	Tropical Rainfall Measuring Mission
UTC	Universal Time Code
VHF	Very High Frequency

A.3 Addendum to manuscript 4

Natural oxidized reactive nitrogen air concentrations under largely reduced anthropogenic emissions in Europe

In this appendix chapter the supplement with the publication of manuscript 4 is presented. The supplement includes the full reduction factor table A.4 which is the full version of the chapter 6 table 6.2.

Table A.4: All Reduction factors for 2040 emissions as factors of 2010 emissions as calculated from the IIASA ECLIPSE V5a MTFR Scenario from the manuscript „Natural oxidized reactive nitrogen air concentrations under largely reduced anthropogenic emissions in Europe “.

Land	SO_X	NO_X	NH_3	VOC	$PM_{2.5}$
Albania	1.05	0.92	0.20	0.46	0.50
Austria	0.68	0.29	0.20	0.46	0.31
Belarus	0.93	0.95	0.20	0.46	0.74
Belgium	0.72	0.45	0.17	0.60	0.40
Bosnia and Herzegovina	0.30	0.67	0.25	0.39	0.46
Bulgaria	0.14	0.29	0.10	0.27	0.35
Croatia	0.38	0.48	0.27	0.46	0.33
Cyprus	0.09	0.28	0.19	0.50	0.31
Czech Republic	0.26	0.36	0.17	0.34	0.42
Denmark	0.49	0.35	0.17	0.32	0.19
Estonia	0.25	0.43	0.18	0.40	0.23
Finland	0.37	0.37	0.20	0.24	0.28
France	0.44	0.32	0.18	0.43	0.27
Germany	0.32	0.35	0.17	0.47	0.31
Greece	0.14	0.33	0.17	0.36	0.31
Hungary	0.33	0.36	0.18	0.35	0.32
Iceland	2.68	0.90	0.19	0.49	0.35
Ireland	0.47	0.32	0.20	0.52	0.20
Italy	0.60	0.37	0.19	0.40	0.32
Latvia	0.89	0.46	0.25	0.31	0.29
Lithuania	0.50	0.34	0.15	0.38	0.27
Luxembourg	0.56	0.15	0.14	0.55	0.36
Malta	0.06	0.20	0.23	0.52	0.14
Moldova	0.82	0.75	0.23	0.50	0.77
Netherlands	0.60	0.38	0.16	0.49	0.52
Norway	1.29	0.77	0.32	0.45	0.48
Poland	0.29	0.33	0.18	0.42	0.55
Portugal	0.71	0.42	0.16	0.50	0.38
Romania	0.20	0.47	0.21	0.28	0.32
Russian Federation	1.26	0.74	0.16	0.49	0.50
Serbia	0.25	0.56	0.15	0.38	0.60
Slovakia	0.24	0.51	0.20	0.49	0.39
Slovenia	0.33	0.27	0.17	0.49	0.42
Spain	0.45	0.42	0.20	0.51	0.76
Sweden	0.71	0.32	0.19	0.54	0.55
Switzerland	0.39	0.30	0.16	0.44	0.33
Turkey	1.11	1.16	0.24	0.50	0.48
Ukraine	0.44	0.87	0.22	0.43	0.60
United Kingdom	0.19	0.29	0.20	0.51	0.39
Shipping Emissions	0.12	0.29	0.85	0.92	0.49
Area weighted average	0.42	0.42	0.52	0.68	0.47

Danksagung

Meine Dissertation, und mein gesamtes Dissertationsvorhaben wären nicht möglich gewesen ohne die Hilfe und Unterstützung vieler, die mich finanziell, organisatorisch, wissenschaftlich fachlich wie moralisch in den letzten Jahren begeleitet und gestützt haben.

Ich danke der Helmholtz-Gemeinschaft Deutscher Forschungszentren e. V., ganz besonders dem Helmholtz-Zentrum Geesthacht für Material- und Küstenforschung für die finanzielle und materielle Ausstattung die nötig war, um meiner Forschung nachzugehen. Weiterhin danke ich der Universität Hamburg für die Beheimatung meines Dissertationsvorhabens und dem Zentrum für Erdsystemforschung und Nachhaltigkeit mit den daran beteiligten Institutionen wie dem Deutschen Klimarechenzentrum und der CliSAP Graduiertenschule SICSS für die Bereitstellung von Infratstrktur, wissenschaftlicher und organisatorischer Betreuung.

Ich danke meinen Betreuern und regelmäßigen Mitgliedern meines Panels, Prof. Dr. Kay-Christian Emeis, Dr. Volker Matthias, Prof. Dr. Lars Kutzbach, Dr. Andreas Richter und Prof. Dr. Markus Quante für die intensive Begleitung während der Panels, während der regelmäßigen Treffen und der ganzen Arbeitszeit meiner Arbeit und der mir zu Teil gewordenen Hilfe zur Umsetzung meiner Forschung. Ein ganz besonderer Dank geht an Dr. Armin Aulinger, für seine Unterstützung als Co-Autor, Wissenschaftler, Programmierer, Statistiker, Arbeitskollege, Korrektor und Freund, der mit unglaublicher Geduld meine Hochs und Tiefs im Laufe der Arbeit fachlich und menschlich mit durchlebt hat und viel wertvollen Input geben konnte.

Ich danke auch allen anderen Mitarbeitern im Institut für Küstenforschung für ihre Hilfe und Unterstützung meiner Arbeit. Den Mitarbeiterinnen und Mitarbeitern der Arbeitsgruppe KSR, allen voran Dr. Beate Geyer möchte ich für die Bereitstellung von meteorologischen Daten, einem offenen Ohr für meine wissenschaftlichen anliegen und den vielen unterhaltsamen und lustigen Stunden am Mittagstisch danken. Das gilt auch für die anderen Kolleginnen und Kollegen aus dem Institutsteil KS, hier vor allem Dr. Johannes Bieser für die Aufbereitung der anthropogenen Emissionen und der Einrichtung des BEIS Modells auf unserem HPC-Cluster. Nicht zuletzt danke ich auch den anderen Kolleginnen und Kollegen meiner Arbeitsgruppe Dr. Matthias Karl, Martin Ramacher, sowie Dr. Jens Meywerk von KIO und den Abschlussstudenten, die ich in meiner Zeit als Doktorand kennenlernen und betreuen durfte für die gute Zeit, die wir gemeinsam, vorallem in den morgentlichen Kaffeerunden, auf Retreats und gemeinsamen Unternehmungen verbracht haben und

das Arbeiten in Geesthacht zu einer schönen Zeit gemacht haben.

Ganz besonders möchte ich auch meinem guten Freund Ole Struck danken, der nicht nur immer ein offenes Ohr für mich hatte, sondern auch mit wissenschaftlichem Sachverstand in unzähligen Diskussionen und mit Gegenlegesen und Korrektur meiner Arbeit einen großen Beitrag geleistet hat. Ich danke für die die moralische Unterstützung, das auffangen in schweren Zeiten und dem ganz anderen, fordernden und gleichzeitig entspannenden Freizeitausgleich ganz, ganz herzlich meinen Freunden und Kameraden Patrick Reichard, Ron Schudde und Sönke Regelin sowie meinem guten Freund Paul Dontenwill. Für die zweite wissenschaftliche Heimat, den Austausch und den anderen Blickwinkel auf das Geschehen in dieser Welt möchte ich mich auch bei Dr. Wilhelm Ruhe und Oberst Dr. Frank Müller sowie den Kolleginnen und Kollegen und Kameradinnen und Kameraden in den Dezernaten Atmosphärenphysik und MNMSG vom Geoinformationsdienst der Bundeswehr für die gute wissenschaftliche Betreuung, erörterung meiner Arbeit und fachlichen Hinweise danken.
Für die bedingungslose Unterstützung, die Liebe, die tolle Kindheit und Jugend, Geborgenheit, die Möglichkeit mich zu entwickeln und meinen Hobbys, meinen Interesse und meinen Neigungen nachzugehen und mich nie fürchten zu müssen, ohne Netz und doppelten Boden im Leben darstehen zu müssen was es erst ermöglicht hat, diese Arbeit anfertigen zu können, danke ich mit tiefst empfundener Dankbarkeit meinen Eltern, Veronika und Dietrich, von ganzem Herzen.

Schließlich, aber nicht zuletzt, danke ich dem Menschen, den ich liebe, es mit mir und meinen Marotten, meiner guten wie schlechten Laune, meinem Engagement, meinen verrückten Hobbys, Freunden und den guten und schlechten Zeiten im Leben ausgehalten hat, mich unterstützt und gestützt hat, meiner Freundin Annika.

Ich möchte diese Dissertation mit Worten schließen, die mich seit über 10 Jahren begleiten. Sie sind kein Lebensmotto, keine Leitlinie, aber stehen für mich symbolisch dafür, für eine bessere Welt einzustehen, in der ein Kinderglaube erwachsen und Realität werden kann. Ich glaube dies täte uns allen und unserer Welt sehr gut. Auch wenn dies bedeutet, sich und seine Belange hinter das Interesse einer besseren Zukunft zu stellen.

> Wer seinen Kinderglauben sich bewahrt, in einer reinen, unbefleckten Brust - und gegen das Gelächter einer Welt zu leben wagt, - wie er als Kind geträumt - bis auf den letzten Tag, das ist ein Mann!
>
> *(Nach Henning Hermann Robert Karl von Tresckow*
> *Generalmajor und Teil des militärischen Widerstands gegen den Nationalsozialismus*
> *vom 20. Juli 1944, 1901–1944)*

Versicherung an Eides statt

Affirmation on oath

Hiermit versichere ich an Eides statt, dass ich die vorliegende Dissertation mit dem Titel: „On the effect of reactive oxidized nitrogen emissions from natural sources on air concentrations and deposition of nitrogen compounds in European coastal areas“ selbstständig verfasst und keine anderen als die angegebenen Hilfsmittel – insbesondere keine im Quellenverzeichnis nicht benannten Internet-Quellen – benutzt habe. Alle Stellen, die wörtlich oder sinngemäß aus Veröffentlichungen entnommen wurden, sind als solche kenntlich gemacht. Ich versichere weiterhin, dass ich die Dissertation oder Teile davon vorher weder im In- noch im Ausland in einem anderen Prüfungsverfahren eingereicht habe und die eingereichte schriftliche Fassung der auf dem elektronischen Speichermedium entspricht.

_____

Jan Alexander Arndt